Laser Ablation Inductively Coupled Plasma Mass Spectrometry (LA-ICP-MS) as a Biomonitoring Tool

Brianne Duncan

A dissertation

submitted in partial fulfillment of the

requirements for the degree of

Doctor of Philosophy

University of Washington

2019

Reading Committee:

Chris Simpson, Chair

Julia Yue Cui

Timothy Larson

Program Authorized to Offer Degree:

Department of Environmental and Occupational Health Sciences

University of Washington

Abstract

Laser Ablation Inductively Coupled Plasma Mass Spectrometry (LA-ICP-MS) as a Biomonitoring Tool

Brianne Duncan

Chair of the Supervisory Committee:

Chris Simpson

Department of Environmental and Occupational Health Sciences

Using laser ablation inductively coupled plasma mass spectrometry (LA-ICP-MS) this research analyzed human cadaver hair for gadolinium and mice hair samples for cadmium. This project combined fundamental bench science (analytical chemistry and animal studies), and insight into exposures to an emerging contaminant. This study demonstrated the feasibility of LA-ICP-MS to measure time resolved exposure profiles in hair samples, potentially opening up a transformative new exposure analysis method for investigators conducting both bench toxicology and human epidemiology studies. Consecutive autopsy cases that presented at the University of Washington's medical department, who had received a gadolinium-based contrasting agent (GBCA) to enhance magnetic resonance imaging procedures constituted the human population component of this research. Multiple hairs from numerous subjects were analyzed using LA-ICP-MS along with calibration gels (bovine-skin based) and a standard reference material glass disc with trace metals. Overall analytical method accuracy and precision was acceptable. There was moderate correlation between gadolinium dose and area under the curve as well as gadolinium peak position and GBCA injection day. Hair concentrations were also compared to the other tissue (brain, bone, and skin) concentrations using linear regression. This analysis showed good correlation between hair gadolinium concentrations and brain and skin gadolinium concentrations. These results suggest that hair may serve as a safe and effective biomonitoring tissue for patients who receive GBCA injections. A mouse animal model was used to evaluate LA-ICP-MS as a biomonitoring tool in assessing cadmium exposure. Hair samples from mice that were part of a mechanistic toxicology study at the University of Washington were opportunistically obtained for inclusion in this analytical methods-focused element of the research. The mice were dosed with cadmium-spiked water at three levels (0, 0.6, and 3 mg/L) for 14 weeks before they were sacrificed. Hairs from seven mice were analyzed using LA-ICP-MS. This research showed that there were increasing concentrations of cadmium in hair shafts with increasing doses of cadmium in drinking water among mice.

TABLE OF CONTENTS

LIST OF FIGURES

LIST OF TABLES

ACKNOWLEDGEMENTS

Funding for this project was supplied in part by the National Institute of Environmental Health Sciences (grant number P30ES007033) and in part by a grant from Guerbet, LLC.

Research of gadolinium in autopsy cases was conducted in collaboration with, and samples were provided by, Ken Maravilla, Makoto Hasegawa, Masahiro Kobayashi, Desiree A. Marshall, and Luis Gonzalez-Cuyar at the University of Washington (UW) School of Medicine. Cadmium research in the mouse model was made possible through the opportunistic samples provided by Zhengui Xia and Liang Zhang in the UW DEOHS Toxicology Program. Michael Paulsen (UW Simpson Laboratory) also provided years of invaluable support for methodological development and sample analysis. Thanks to my wonderful committee members (Tania Busch Isaksen, Julia Yue Cui, Chris Simpson, and Timothy Larson) and graduate student representative (Gregory Korshin), who helped me to focus on my objectives and asked all the hard questions. An extra thanks to my advisor, Chris Simpson, who provided guidance, support, and motivation in all the right proportions.

The support and patience of my boyfriend, family, and friends was essential, and immensely appreciated.

Chapter 1. Introduction

The over-arching goal of this research was to evaluate the potential of LA-ICP-MS analysis of hair samples as a tool for retrospectively biomonitoring time-varying exposures in humans. In this chapter, Sections 1.1 through 1.3 present general background information supporting research efforts, and Section 1.4 summarizes the subsequent chapters, which present study results.

1.1 Hair Background

Hair is a unique feature of mammals and can be present on most bodily surfaces (Buffoli et al. 2014; Robbins 2012a). Hair is derived from epidermal cells and has two structurally distinct features: the follicle (the portion within the skin) and the shaft (the external hair fiber; Buffoli et al. 2014; Robbins 2012a). The general anatomy of the hair and follicle are shown in Figure 1. The follicle is the growth structure for the hair fiber and at the base of the follicle is the bulb, which produces the hair (Buffoli et al. 2014). At the base of the bulb is an opening/indentation that houses the dermal papilla. Melanocytes (melanin/pigment-forming cells) are located within the bulb near the delineation with the dermal papilla. The dermal papilla is thought to be an important component in directing the formation of the pigmented hair shaft (Buffoli et al. 2014). The vascular structures providing blood and nutrients are a series of arterioles, which are more concentrated around the lower portion of the follicle (Buffoli et al. 2014).

Hair fibers are fully keratinized, proteinaceous fibers with an outer cuticle, inner cortex, and sometimes a central medulla (Buffoli et al. 2014). The cuticle is chemically resistant and is comprised of flat, overlapping cells or “scales” (Robbins 2012a). The scales are arranged like overlapping shingles on a roof or scales on a fish, and are attached at the proximal/root end (Robbins 2012a). The cortex is the thickest layer of the hair shaft and is largely composed of keratin, which contains sulfhydryl groups of amino acids (Pozebon et al. 2017;Robbins 2012a). The cortex composition is macrofibrils, comprised of intermediate filaments, which are in turn comprised of filament protein chains (Robbins 2012a). The medulla, which is not present in all hairs, is a porous space that tends to be present in coarser/larger diameter hairs (Robbins 2012a). This porous space may be found throughout the length of the hair fiber, or discontinuously at random places along the hair (Robbins 2012a). Keratin proteins have been identified in the generally hollow medulla structures (Robbins 2012a). As the hair is formed in the follicle, it is exposed to blood, lymph, and extracellular fluid (Combs et al. 1982).

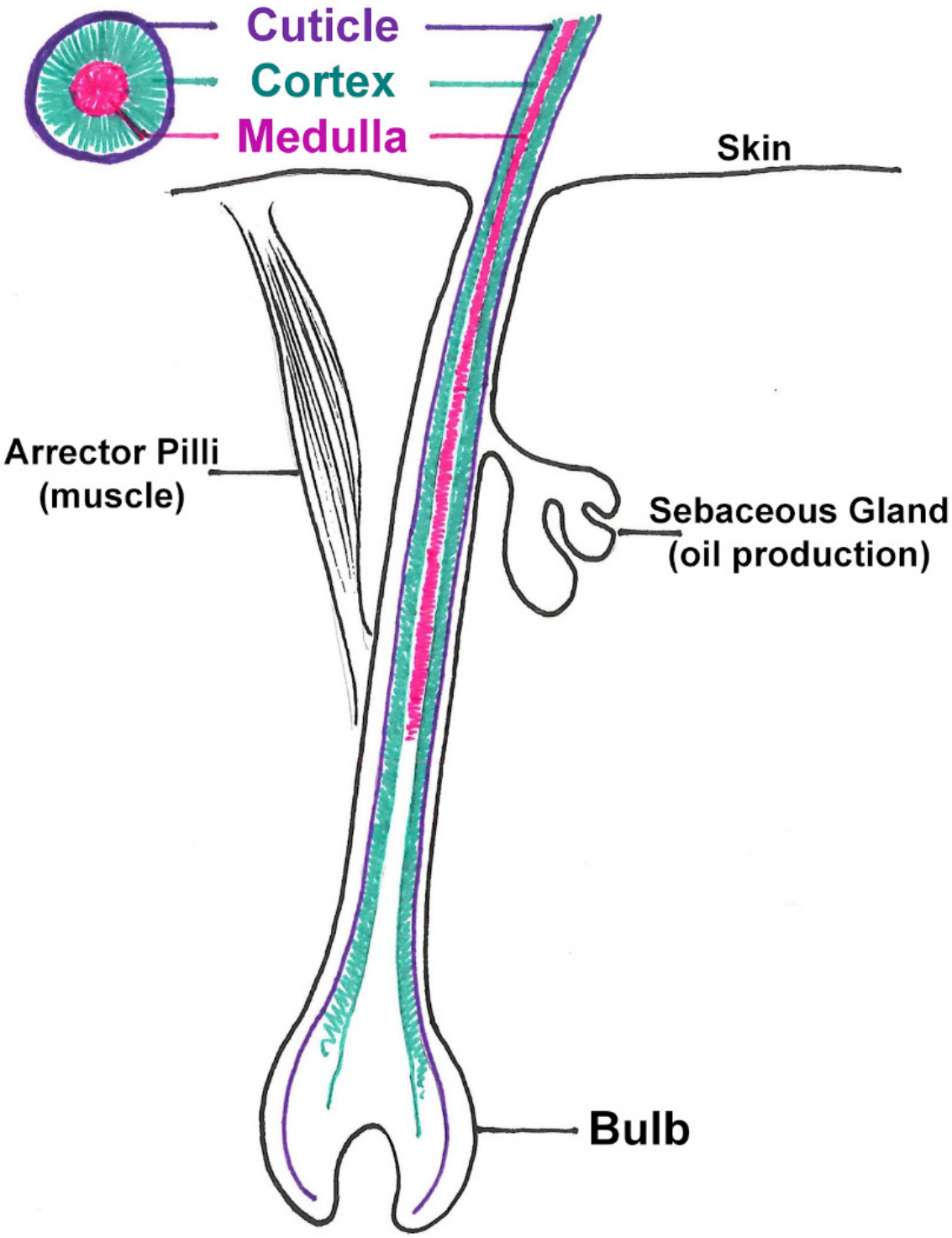

Figure 1. General anatomy of a hair follicle (sub-dermal) and fiber

The growth cycle for hair is comprised of four distinct phases: anagen (growth), catagen (apoptosis), telogen (resting), and exogen (falling out/shedding; Alonso and Fuchs 2006; Buffoli et al. 2014). For human hair, there is no spatial patterning for the distribution of hairs in various phases (Robbins 2012a). This means that a localized area may have a random assortment of hairs in one or more phases (Robbins 2012a). In humans, 80–90% of scalp hair is in anagen phase, 1–3% is in catagen phase, and 4–20% are in telogen phase (Lebeau et al. 2011; Robertson 1999). Anagen phase is the longest in humans and on average lasts 2–6 years, though some people exhibit longer anagen phase time periods (Robbins 2012a). Studies have observed increased vascularization around the follicle during the anagen phase (Buffoli et al. 2014). Catagen and telogen phases generally last a few weeks apiece, but sometimes longer (Robbins 2012a). A network of nerve fibers also surrounds the hair follicle and the proximity of this nerve tissue to the follicle suggests that neurotransitters/neuropeptides may influence hair growth (Buffoli et al. 2014). Other molecular species direct or modulate hair follicle cycling and hair growth, such as proteins and hormones (Robbins 2012a; Tobin 2012). Further, the sebaceous gland is known to affect hair growth rates (Lee et al. 2012). Each follicle can function independently depending on localized tissue responses to chemical signaling (Robbins 2012a; Tobin 2012).

Scalp hair generally grows at the rate of 1 cm/month (Robbins 2002; Tobin 2012). However, average growth rates can range from 0.6 to 1.5 cm/month (Tobin 2012). Age and gender affect the rate of hair growth, with men ages 15–30 years and women ages 16–24 observing the greatest rates (Tobin 2012). Individual subjects may also have inconsistent growth rates between hairs (i.e., intra-subject variability), or during different periods of time (Tobin 2012). Research has demonstrated that ethnicity may influence hair growth rates. One study of Chinese, Japanese, and Caucasian subjects with straight hair noted that the Asian participants had a faster growth rate (average of 1.3 cm/month) compared to the Caucasian subjects (average of 1.0 cm/month; Saint Olive Baque et al. 2012). Another study reported that hair growth rate from each follicle begins to slow as it moves toward the end of the anagen phase (Saitoh et al. 1970).

The sulfhydryl groups present in the cortex show high affinity for metals, which can facilitate deposition of metals into the hair shaft (Pozebon et al. 2017). Carboxylic acid groups show high affinity for di- and trivalent metals and all three hair layers contain regions with large amounts of these groups (Robbins 2012b). However, the mechanism by which metals are incorporated into the hair during fiber synthesis is still not well defined (Pozebon et al. 2017). The kinetics of metals distribution in the hair is dependent upon the form of the metallic compound, and the element of interest (Tobin 2012). Trace element concentrations in hair can be dependent upon blood concentrations, but other bodily processes and disturbances may affect these concentrations including diet and metabolic irregularities (Kempson et al. 2007; Robbins 2012b). The content of the hair shaft is generally considered to be the result of hair formation within the follicle, but some metals can make their way from the surface of the hair into the hair matrix

(Kempson et al. 2007). Sources of metals in hair include blood, interstitial fluid, sweat, air pollution, water, soap, and other hair products (Robbins 2012a, b; Tobin 2012).

1.2 Biomonitoring and Metals in Hair

Humans are exposed to metal contaminants through numerous personal and work-related scenarios. Metals are found in the earth's crust and people can be exposed to them through air (suspended particles and vapors), water, and soil that is inhaled or ingested (ATSDR 2012a). Commercial products may utilize certain metals such as: arsenic in pesticides and treated wood (ATSDR 2007); cadmium in batteries or pigments (ATSDR 2012a); gadolinium in magnetic resonance imaging (MRI) dyes (EMA 2017); manganese in steel materials and fireworks (ATSDR 2012b); and zinc in dietary supplements and anti-dandruff shampoos (ATSDR 2005). The workers involved in manufacturing those products may be at elevated risk of exposure and the people who use the products are also at risk of exposure.

Since the Occupational Safety and Health Administration (OSHA) was established in 1971, the United States (US) has continued to strengthen worker safety requirements (OSHA 2010). OSHA issued updated guidance in 2016 to further support reduction of worker exposures to metals in smelting and refinery settings where workers continue to face serious risks (OSHA 2016). An important part of the framework for protecting human health from the consequences of exposure to contaminants is biomonitoring.

Biomonitoring utilizes biomarkers (i.e., compounds or their metabolites) present in the body (Goyer et al. 2004; NRC 2006). There are three primary groups of biomarkers:

1. Biomarkers of Exposure—Compound, metabolite, or product of an interaction quantified within a bodily compartment.
2. Biomarkers of Effect—Biochemical, physiological, behavioral, or other recognizable alteration associated with an adverse effect or disease.
3. Biomarkers of Susceptibility—Indicator for the ability of an organism to respond – in either a beneficial or adverse way - to a compound (NRC 2006).

The National Research Council (NRC) states, "the ultimate objective of biomonitoring is to link information on exposures, susceptibility, and effects to understand the public health implications of exposure to environmental chemicals" (NRC 2006). The NRC also notes that biomonitoring has several applications, but of primary interest for this study we will consider biomonitoring for exposure assessment purposes (NRC 2006).

Biomarkers are quantified in a variety of bodily tissues including blood, bone, feces, hair, liver, nails, plasma, skin, sweat, and urine. One major limitation in biomonitoring is that the concentration in the tissue is often quantified without knowing when an exposure occurred (NRC

2006). Research conducted at the University of Washington, and other institutions, is attempting to fill that gap. For example, a study on manganese exposures in welders sought to elucidate the time course of manganese exposure and uptake in blood (Baker et al. 2016). These researchers found that blood manganese may be a useful biomarker for longer exposures to airborne manganese.

Sampling of tissues for exposure biomonitoring can be constrained by a number of serious practical limitations. Some tissues are physically inaccessible in live subjects (e.g., brain), sampling methods are invasive (e.g., bone), or tissues can be representative of recent exposures only (e.g., urine, blood). In contrast to the tissue samples mentioned above, hair sample collection poses no known physical risk to subjects and offers the potential for metal-specific, time-resolved exposure data. Additionally, hair analysis can be very informative for xenobiotic metals exposures (e.g., gadolinium in magnetic resonance imaging (MRI) contrast agents; Tobin 2012). Hair sample storage and transport are considerably simpler than other tissue samples and the non-invasiveness of sampling is very attractive (Pozebon et al. 2017).

Since the 1960s, hair has gained traction in assessing exposures to metals (Kintz and Villain 2005). Early attempts to use hair as a biomarker of exposure suffered from significant methodological shortcomings in sampling, washing, instrumentation, and data analysis (ATSDR 2003; ERG 2001). A number of studies have been published that aimed to address the limitations listed above including data on reference/background ranges (Goulle et al. 2005; Mikulewicz et al. 2013), washing methods (Eastman et al. 2013; Reiss 2016), and correlations between hair and other tissues (Ferré-Huguet et al. 2009; Zota et al. 2016). Traditional bulk methods for measuring metals in hair involve cutting a tuft of hair from the occipital region of the head. The book, *Hair in Toxicology*, noted that the best sample collection region on the head is the *vertex posterior* because it has less variability in hair growth rates (Kintz and Villain 2005). The hair is typically washed, sonicated, and rinsed to remove exogenous contamination, then dissolved in concentrated mineral acid and analyzed for various metals by atomic absorbance spectroscopy (AAS) or ICP-MS (Bader et al. 1999; Goulle et al. 2005; Pozebon et al. 2017).

1.3 Laser Ablation Inductively Coupled Plasma Mass Spectrometry

In the last 25 years, laser ablation (LA) ICP-MS has slowly emerged as a technique for analysis of biological material that offers the potential for high-resolution quantification of chemical elements in one, two, or three dimensions. The laser can be programmed to ablate a single point, a line or raster pattern, or applied to biological cross-sections for three-dimensional reconstruction of metals distributions within tissues, organs, or organisms. When a hair is analyzed using a line scan technique, the result is that numerous data points are continuously compiled as the hair is ablated and material is sent to the ICP-MS. Depending on the optimized

instrument parameters (e.g. laser pulse rate, spot size, and energy) and the length of the hair, each hair may have hundreds to thousands of discrete data points.

The earliest publication found that applied LA-ICP-MS to the analysis of hair was from the Department of Chemistry at the University of Surrey in England (Durrant and Ward 1994). At that time, the study found that LA-ICP-MS suffered from inferior accuracy and precision compared to traditional solution ICP-MS. The researchers reported that the lowered precision and accuracy were due to both laser and sample characteristics. A study published about 10 years later noted that concentration-based detection limits for LA were only slightly less sensitive than for traditional solution ICP-MS (Rodushkin and Axelsson 2003). At this point in the method development, the authors noted that the variation in elemental concentrations from a single sample were largely due to the heterogeneity within the sample matrix, though laser parameters also played a part. Since then, studies researching technical aspects of LA-ICP-MS analyses of biological samples included the use of different washing techniques (Eastman et al. 2013), instrument calibration, accuracy, and precision (Hare et al. 2012), ablation optimization for isotopic ratios (Santamaria-Fernandez et al. 2009), and varying quantification approaches (Limbeck et al. 2015).

Numerous studies have demonstrated that LA-ICP-MS can detect metals in hair that show patterns consistent with exposure history. For example, one study detected a decrease in uranium concentrations in the hair shaft after the subject changed their drinking water from a high-uranium source to a low-uranium source (Sela et al. 2007). Another detected increased mercury and platinum in human hair after dosing events (Stadlbauer et al. 2005). More recently, a research group in Canada used time-resolved LA-ICP-MS on grizzly bear hairs to estimate dietary intake of metals indicative of fish consumption. This study reported strong correlations between results with LA-ICP-MS and regular solution ICP-MS. Additionally, the data showed coinciding temporal relationships for metal quantitation and fish consumption (Noel et al. 2015). Another recent study, published in 2016, assessed the use of LA-ICP-MS to quantify deposition and elimination of metallo-drugs in a mouse model using the whiskers of mice dosed with gadolinium and vanadium-based complexes (Lum et al. 2016). The researchers found that mice with higher gadolinium doses showed higher gadolinium levels in their whiskers compared to the mice that received lower gadolinium doses. They concluded that LA-ICP-MS analysis of hair showed excellent potential for therapeutic drug monitoring.

1.4 Summary of Subsequent Chapters

Chapter 2 presents the results of a study that investigated intra-subject variability in gadolinium deposition within the hair shaft. The study population included consecutive autopsy cases that presented at the University of Washington’s medical department, who had received a gadolinium contrasting agent to enhance magnetic resonance imaging procedures. Multiple hairs from

numerous subjects were analyzed using LA-ICP-MS along with calibration gels (bovine-skin based) and a standard reference material glass disc with trace metals. Overall analytical method accuracy and precision was investigated. Factors contributing to intra-subject variability of peak positioning and magnitude were considered. Peak gadolinium concentrations as well as area under the curve were assessed to determine if either measure was correlated with the dose of gadolinium received in the injection.

Chapter 3 utilized the same subject population and samples from the preceding chapter, but included brain, skin, and bone tissues, in addition to the hair samples. Subjects received a gadolinium-based contrasting agent (GBCA) injection within one year before death, and if a subject received more than one injection, all injections were with the same type of GBCA. Hair concentrations were compared to the other tissue concentrations using linear regression to assess for possible correlation.

Chapter 4 uses a mouse animal model to evaluate LA-ICP-MS as a biomonitoring tool in assessing cadmium exposure. Hair samples from mice that were part of a mechanistic toxicology study at the University of Washington were opportunistically obtained for inclusion in this analytical methods focused research study. The mice were dosed with cadmium-spiked water at three levels (0, 0.6, and 3 mg/L) for 14 weeks before they were sacrificed. Hairs from seven mice were analyzed using LA-ICP-MS. Hair concentrations were evaluated and compared to the received dose to determine if there was a correlation. Intra-specimen variability was also assessed through analysis of a larger number of hairs (N=25) from two different specimens.

Chapter 2. Intra-Subject Variability in Hair Gadolinium Concentrations Among Patients who Received Gadolinium-based Contrast Agents

2.1 Abstract

Objectives:

This study utilized laser ablation inductively coupled plasma mass spectrometry (LA-ICP-MS) to quantify gadolinium in the hair of autopsy cases that had received an injection of gadolinium based contrast agent (GBCA) before death. We correlated hair concentrations with gadolinium dose and assessed inter- and intra-subject variability to determine whether this biomonitoring method may be appropriate for retrospective determination of exposures to GBCAs.

Materials and Methods:

Consecutive autopsy reports were reviewed for GBCA injections and subjects who received a single type of GBCA in the last year were included. Hair samples from 16 cases and two controls were identified for inclusion. Hair samples were analyzed using LA-ICP-MS as a line scan technique along the hair shaft. Instrument sensitivity and accuracy were reviewed, and sulfur was assessed for use as an internal standard. Average peak concentrations and average area under the curve were calculated for each subject. Linear regression analysis between hair measures and gadolinium dose was executed to explore potential correlation.

Results:

Using sulfur as an internal standard introduced additional variability into the quantification of gadolinium in the hair shaft. The position of the peak maxima was a good estimate for the day GBCA injection occurred ($R^2 = 0.46$; $p = 0.0022$), and average area under the curve was a better predictor of gadolinium dose ($R^2 = 0.41$; $p = 0.0046$) compared to average of peak maxima concentrations.

Conclusions:

Correlation between hair gadolinium area under the curve and gadolinium dose suggests that LA-ICP-MS analysis of hair may be an effective method to evaluate subjects in vivo after exposure to GBCAs.

2.2 Introduction

For decades, health care providers considered gadolinium-based contrast agents (GBCAs), used for magnetic resonance imaging (MRI) safe and with limited risk of adverse reactions. Risks were primarily restricted to individuals with compromised kidney function (Rogosnitzky and Branch 2016). Initially, GBCAs were thought to be completely excreted from the body after injection (Rogosnitzky and Branch 2016). However, recent research revealed that gadolinium deposition occurs in the brain, bone, and other tissues (EMA 2017; FDA 2017b; Rogosnitzky and Branch 2016). Beginning in 2014, studies showed that there was evidence of elevated gadolinium levels within different regions of the brain, including the globus pallidus (GP) and dentate nucleus (DN). The Kanda et al. (2014) study was the first to evaluate the relationship between imaging signal intensity (using MRI T1-weighted imaging [WI]) and GBCA injections. The authors found that there was a correlation between signal intensity in the GP and DN and the number of GBCA injections a patient had received.

As a follow-up, the same research group conducted chemical analyses of the GP and DN tissues collected postmortem from patients injected with GBCAs to quantify gadolinium concentrations (Kanda et al. 2015). The tissues were analyzed using inductively coupled plasma mass spectrometry (ICP-MS). This research concluded that patients who received GBCAs had significantly higher gadolinium concentrations in the GP and DN tissues than controls. McDonald et al. (2015) reported similar findings of elevated gadolinium in brain tissues (GP, DN, thalamus, and pons) of patients who received GBCA injections compared to controls.

Based on the expanding research supporting gadolinium deposition within the human body, in 2017 and 2018 the U.S. Food and Drug Administration (FDA) issued notifications that GBCAs would require additional communications from providers to patients (FDA 2017b). The FDA did not find evidence that GBCAs were linked directly to adverse health effects but indicated that its review continues (FDA 2017b). Also in 2017, the European Medicines Agency (EMA) restricted the use of some linear GBCAs (open ring around gadolinium in compound structure), but did not restrict any macrocyclic GBCAs (closed ring around gadolinium) (McDonald et al. 2018). The macrocyclic configuration imparts greater stability to the compound, making them less likely to liberate the gadolinium atom compared to the linear compounds (EMA 2017).

Monitoring patients who receive GBCA injections is difficult because the tissues apparently at risk of gadolinium accumulation can be difficult to access. Generally, these tissues are physically inaccessible (e.g., brain), sampling is invasive (e.g., bone), or the tissues are representative of recent exposures only (e.g., urine, blood). Though T1-WI MRI techniques can be indicative of elevated gadolinium in brain tissues, other metals (e.g., iron and copper) contribute to the signal intensity (Ginat and Meyers 2012). This precludes the use of T1-WI to quantitatively assess gadolinium-specific exposures. In contrast to the tissue samples mentioned above, hair sample

collection poses no known physical risk to participants and offers the potential for gadolinium-specific, time-resolved exposure data.

Since the 1960s, hair has gained traction in assessing exposures to metals (Kintz and Villain 2005). Early attempts to use hair as a biomarker of exposure suffered from significant methodological shortcomings in sampling, washing, instrumentation, and data analysis (ATSDR 2003; ERG 2001). A number of studies have been published that aimed to address the limitations listed above including data on reference/background ranges (Goulle et al. 2005; Mikulewicz et al. 2013), washing methods (Eastman et al. 2013; Reiss 2016), and correlations between hair and other tissues (Ferré-Huguet et al. 2009; Zota et al. 2016). Traditional bulk methods for measuring metals in hair involve cutting a tuft of hair from the occipital region of the head. The book, *Hair in Toxicology*, noted that the best sample collection region on the head is the *vertex posterior* because it has less variability in hair growth rates (Kintz and Villain 2005). The hair is typically washed, sonicated, and rinsed to remove exogenous contamination, then dissolved in concentrated mineral acid and analyzed for various metals by atomic absorbance spectroscopy (AAS) or ICP-MS (Bader et al. 1999; Goulle et al. 2005; Pozebon et al. 2017).

Numerous studies have been published showing that LA-ICP-MS can detect metals in hair that show patterns consistent with exposure history. For example, one study detected a decrease in uranium concentrations in the hair shaft after the individual changed their drinking water from a high-uranium source to a low-uranium source (Sela et al. 2007). Another detected increased mercury and platinum in human hair after dosing events (Stadlbauer et al. 2005). A more recent study, published in 2016, assessed the use of LA-ICP-MS to quantify deposition and elimination of metallo-drugs in a mouse model using the whiskers of mice dosed with gadolinium and vanadium-based complexes (Lum et al. 2016). The researchers found that mice with higher gadolinium doses showed higher gadolinium levels in their whiskers compared to the mice that received lower gadolinium doses. They concluded that LA-ICP-MS analysis of hair showed excellent potential for therapeutic drug monitoring.

Scalp hair generally grows at the rate of 1 cm/month (Robbins 2002; Tobin 2012). However, average growth rates can range from 0.6 to 1.5 cm/month (Tobin 2012). Age and gender affect the rate of hair growth, with men ages 15–30 years and women ages 16–24 observing the greatest rates (Tobin 2012). Individual subjects may also have inconsistent growth rates between hairs, or during different periods of time (Tobin 2012). Research has demonstrated that ethnicity may influence hair growth rates. One study of Chinese, Japanese, and Caucasian subjects with straight hair noted that the Asian participants had a faster growth rate (average of 1.3 cm/month) compared to the Caucasian subjects (average of 1.0 cm/month; Saint Olive Baque et al. 2012).

The sulfydryl groups present in the cortex show high affinity for metals, which can facilitate deposition of metals into the hair shaft (Pozebon et al. 2017). Carboxylic acid groups show high

affinity for di- and tri-valent metals and all three hair layers contain regions with large amounts of these groups (Robbins 2012b). However, the mechanism by which metals are incorporated into hair during fiber synthesis is still not well defined (Pozebon et al. 2017). The kinetics of metals distribution in the hair is dependent upon the form of the metallic compound, and the metallic element of interest (Tobin 2012). Trace element concentrations in hair can be dependent upon blood concentrations, but other bodily processes and disturbances may affect these concentrations including diet and metabolic irregularities (Kempson et al. 2007; Robbins 2012b). The content of the hair shaft is generally considered to be the result of hair formation within the follicle, but some metals can make their way from the surface of the hair into the hair matrix (Kempson et al. 2007). Sources of metals in hair include blood, interstitial fluid, sweat, air pollution, water, soap, and other hair products (Robbins 2012a, b; Tobin 2012).

Studies using LA-ICP-MS on hair have generally limited data, focusing on one or a few subjects or one or a few hairs per subject. The purpose of this pilot study is two-fold: 1) to assess the temporal relationship between peak hair concentration positions along the hair shaft and the time a dosing event occurred; and 2) to understand intra-subject variability of hair concentrations of gadolinium quantified using LA-ICP-MS and identify the most appropriate metric for representing the association between these hair concentrations and the gadolinium dose. Hair samples were obtained from human autopsy subjects who had received injections of GBCA for medical imaging purposes.

2.3 Methods

Subjects:

This study was approved by the University of Washington Human Subjects Review Board for retrospective review of medical records and was Health Insurance Portability and Accountability Act compliant. Autopsy consent from each subject granted authorization for use of tissues for research purposes.

Consecutive autopsy reports were reviewed as they presented at our institution's medical department from December 2017 to May 2019. Study inclusion criteria were accessible, complete medical records with full history of GBCA injections (e.g., date, type, and dose). Subjects were excluded if medical records were not accessible or were incomplete. Forty-two cases and two controls were identified in the records review. Cases who received their last GBCA injection over a year before their death, who had hair length too short to capture the exposure period (days between last GBCA injection and death), assuming a scalp hair growth rate of approximately 1 cm/month (Robbins 2002), or that received more than one type of GBCA were excluded. This resulted in inclusion of 16 cases and the two aforementioned controls. Cases received one of four GBCAs: gadoxetate, gadobenate, gadobutrol, or gadoteriodol.

A summary of the subject characteristics is provided in Table 1, including estimated glomerular filtration rate (eGFR), which is an indicator of kidney function. eGFR values below 60 mL/min/1.73 m^2 are clinically significant and indicative of moderate or more serious kidney dysfunction (NKF 2019).

Table 1. Study population characteristics

Characteristic (Units)	Controls	Cases
Subjects (N)	2	16
Male (N)	0	8
Female (N)	2	8
Age (Years, min–max [average])	70–79 (75)	19–79 (57)
eGFR <60 mL/min/1.73 m^2 (N)	1	4
eGFR >60 mL/min/1.73 m^2 (N)	1	12
Linear agent (N)	Not applicable	5
Macrocyclic agent (N)	Not applicable	11
Time between last injection and death (days, min–max [average])	Not applicable	2–69 (22)
Hairs analyzed per subject (N, min–max [average])	2	4–18 (10)

Table 2 shows the GBCA and gadolinium molarity and concentrations, as well as the number of cases that received each agent. Gadolinium ion concentrations were calculated using the molarity of the GBCA solution used for imaging, and the molecular weight of gadolinium (0.15725 g/mmol). Agent injection volumes were from 10 to 40 mL (average 17 mL).

Table 2. GBCA molarity and concentrations

GBCA Type	GBCA	Formula	Molarity (mmol/mL)	GBCA Concentration (g/mL)	Gd Concentration (g/mL)	Cases (N)
Macrocyclic	Gadobutrol	$C_{18}H_{31}GdN_4O_9$	1	0.60	0.157	1
	Gadoteridol	$C_{17}H_{29}GdN_4O_7$	0.5	0.28	0.079	10
Linear	Gadobenate	$C_{22}H_{28}GdN_3O_{11}$	0.5	0.53	0.079	4
	Gadoxetate	$C_{23}H_{28}GdN_3O_{11}$	0.25	0.18	0.039	1

Sample Analysis:

Scalp samples with hair were collected from the subjects at the time of the autopsy. Further details of sample processing are provided in Appendix A. Generally, the hair was sonicated in acetone (to remove exogenous contamination), dried, and mounted onto slides with double stick tape. Samples were analyzed along with gelatin standards (bovine skin-based; 0–2,000 µg/g) and a glass pellet standard reference material (SRM; National Institute of Standards and Technology [NIST] 612) with trace metals.

The laser ablation tool has a two-volume sample cell to prevent signal broadening and lost material during ablation. Helium was the carrier gas from the laser and argon was T-ed in between the laser and the ICP-MS. Table 3 summarizes the laser parameters for each material (hair, SRM, calibrant). Hairs were ablated using a continuous laser path (i.e., line scan) along the length of the hair from root to tip, and ablation paths were traced in the laser software (Agilent NWR ESI ActiveView). Calibration gels and the SRM were incorporated into the sample sequence throughout analysis and facilitated assessment of instrument stability. Results were exported from the ICP-MS software (MassHunter) as counts per second (cps).

Table 3. Laser and ICP-MS parameters,

Instrument and Parameter (Units)	Hair	Calibrants	SRM
Laser: Elemental Scientific, Inc. (ESI) New Wave Research (NWR) 213 (Nd:YAG [neodymium: yttrium aluminum garnet])			
Wavelength (nm)	213		
Helium flow (L/min)	0.8		
Argon makeup flow (L/min)	1.07		
Isotopes	^{34}S, ^{157}Gd	^{157}Gd	^{157}Gd
Spot size (µm)	30	30	100
Firing rate (Hz)	20	20	20
Scan speed (µm/sec)	100	100	20
Energy (%)	60	60	50
ICP-MS: Agilent 7900			
Sampling period (sec)	0.515		
Radiofrequency (watts)	1,550		
Mode	Helium		
Collision cell gas	Not used		

Data Processing and Analysis:

Gadolinium dose(s) (in grams) for each case was calculated from the GBCA-specific gadolinium concentration in the imaging solution and the volumetric dose (in mL) of the injection.

The raw cps results for the *m/*z34 (sulfur) intensities for the hair samples was used to assess ^{34}S as an internal standard. Previous studies have used sulfur (^{32}S and ^{34}S) and carbon (^{13}C) as internal standards since they are part of the keratinized hair matrix (Bartkus et al. 2011; Dressler et al. 2010; Luo et al. 2017; Rodushkin and Axelsson 2003). The use of an internal standard is reported to help adjust for variability in ablation of the sample by the laser or drift in the response of the ICP-MS over time (Kumtabtim et al. 2011).

The same raw ^{34}S hair results and the *m/z*157 (gadolinium) intensities for the SRM samples were reviewed to determine instrument stability. For calibrants, the average of the raw cps results was used to generate the calibration curves. Similar to other studies (Noel et al. 2015; Sanborn and Telmer 2003; Sinclair et al. 1998), the raw cps results for ^{157}Gd were processed with a rolling mean centered on five values before calculating a weight-based concentration for the hair line scan from a calibration curve. Using the scan speed of the laser (100 µm/sec) and the acquisition time, the distance from the hair root was calculated in millimeters (mm). That distance was used to estimate the numbers of days before death using the reported average hair growth rate of 1.06 cm/month (Robbins 2002).

Each hair line scan was reviewed to determine whether a ^{157}Gd peak was present. This review considered both the overall shape of the scan and the apparent zero-level baseline of each hair. If the scan showed an elevated ^{157}Gd response, with a peak-like shape to the line, the hair was designated as having a peak. The peak window was also manually identified; the high variability in shape, peak positioning, and cps magnitude precluded use of an automated algorithm to define the peak window.

For a hair with an identified peak, the maximum concentration within the peak and the area under the curve (using Simpson's Rule to integrate the area; Stanford No Date) were calculated. If the calculated concentrations included a baseline with values below zero, the baseline was adjusted by adding the minimum (negative) concentration to all values in the hair's line scan. All concentrations along a hair line scan correspond to a point in the subject's past, or days before death. The number of days before death that the peak maxima corresponded to was also compiled so that these "estimated" days before death could be compared to the known days between the last GBCA injection and death.

Statistical Analysis:

Using the 'lm()' function in RStudio (version 3.4.0), a linear regression analysis was conducted to evaluate three relationships: 1) actual v. estimated days from injection to death; 2) gadolinium dose v. peak maximum; and 3) gadolinium dose v. area under the curve. Significance was

determined as $p < 0.05$. No study to date has evaluated gadolinium dose and hair concentrations in humans. The peak maximum concentrations and area under the curve will be compared to determine which measure correlates more strongly with gadolinium dose.

2.4 Results

This pilot study included 16 cases that received one type of GBCA with the last injection occurring within one year of their death, as well as two controls who received no GBCAs at any time. There were 155 hairs analyzed from the cases and four hairs analyzed from the controls. A summary of the subjects, GBCA, and hairs are included in Table 4. Subject 8 only had one hair with a peak (out of four analyzed), so there are no statistics in Table 4 other than a single value for estimated days, peak maxima, and area under the curve. The low number of hairs analyzed for subject 8 was due to very sparse hair on the scalp sample. Subject 16 had a low proportion of hairs with peaks present, and those results may be due to the fact that the hair length was shorter than the estimated length needed to capture the exposure period in six of the hairs analyzed (i.e., too short).

Gadolinium dose (in grams) was calculated from the GBCA-specific gadolinium concentration (see Table 2) and injected GBCA volume (mL). Results for peak concentrations and area under the curve are presented in Section 2.4.3.

Table 4. GBCA and hair statistics summary by subject

Subject No.	GBCA Name (Last Dose [mL])	Gd Dose (g)	Days From Last Injection to Death	Hairs without Peaks (N)	Hairs with Peaks (N)	Estimated Days from Last Injection to Death avg ± SD (range)	^{157}Gd Peak Maxima (µg/g); avg ± SD (range)	^{157}Gd Peak Area Under the Curve (µg/g*mm); avg ± SD (range)
1	Gadobutrol (10)	1.6	29	0	11	35 ± 13 (5.9–51)	0.4 ± 0.17 (0.16–0.67)	16 ± 9.2 (5.2–32)
2	Gadoteridol (20)	1.6	25	0	11	20 ± 9.6 (4.9–30)	2.4 ± 1.2 (0.25–4.6)	58 ± 26 (4.5–100)
3	Gadoteridol (20)	1.6	51	1	10	36 ± 25 (4–68)	0.39 ± 0.22 (0.1–0.82)	19 ± 15 (6.2–48)
4	Gadoteridol (15)	1.2	5	1	9	5 ± 2.1 (2.7–8.7)	0.27 ± 0.21 (0.045–0.61)	6.5 ± 4.9 (0.66–13)
5	Gadoteridol (17)	1.3	4	0	10	8.3 ± 3.5 (4.5–15)	3.3 ± 1.3 (2.1–6.7)	128 ± 23 (109–167)
6	Gadoteridol (15)	1.2	5	0	10	5.8 ± 3.5 (0.54–10)	0.95 ± 0.39 (0.39–1.5)	29 ± 14 (7.5–47)
7	Gadoteridol (16)	1.3	9	0	10	10 ± 0.89 (8.7–11)	1.4 ± 0.39 (1–2.1)	46 ± 12 (30–69)
8	Gadoteridol (18)	1.4	69	3	1	15	0.69	16
9	Gadoteridol (40)	3.2	2	0	10	3.9 ± 1.4 (0.73–5.6)	5.35 ± 1.46 (1.88–7.44)	201 ± 79 (66–310)
10	Gadoteridol (12)	0.95	7	0	9	12 ± 6 (5.4–23)	4.4 ± 2.5 (1.8–8.5)	95 ± 33 (47–151)
11	Gadoteridol (20)	1.6	16	2	8	14 ± 12 (2.7–34)	0.4 ± 0.24 (0.036–0.71)	9.2 ± 5.5 (2.1–15)
12	Gadobenate (16)	1.3	19	1	5	10 ± 5 (3.7–16)	2.1 ± 0.32 (1.7–2.5)	26 ± 5.1 (21–34)
13	Gadobenate (17)	1.3	17	1	4	17 ± 5.8 (9.5–22)	1.8 ± 0.58 (1–2.4)	29 ± 9.7 (16–38)
14	Gadobenate (14)	1.1	7	0	18	7.2 ± 0.4 (6.7–8)	2.9 ± 0.66 (1.2–3.5)	39 ± 7.4 (19–48)
15	Gadobenate (13)	1.0	52	3	7	49 ± 31 (6.9–84)	0.68 ± 0.41 (0.088–1.2)	13 ± 7.3 (1.4–19)
16	Gadoxetate (10)	0.39	30	8	2	20 ± 16 (8.7–32)	0.27 ± 0.072 (0.22–0.32)	4.5 ± 0.19 (4.3–4.6)

2.4.1 Internal Standard Assessment, Accuracy, and Precision

In a review of LA-ICP-MS state-of-the-science in 2015, it was noted that an internal standard and analyte of interest must be homogenously distributed within the sample material (Limbeck et al. 2015). While sulfur is incorporated throughout the hair shaft matrix, gadolinium is not. Additionally, the mass analyzer used for the current study is a quadrupole ICP-MS and measures isotopes sequentially rather than simultaneously. Although each 0.515 sec interval reports cps data for all selected isotopes, the results are not necessarily obtained from the same section of the ablated hair.

The variability between the ^{157}Gd raw signal (cps), sulfur-normalized (^{34}S) signal, and rolling average (centered on five values, cps) was compared to assess which method effectively reduced

data variability. Thirty-five hairs from six subjects analyzed in September 2018 and January 2019 were included in this analysis. A section of each hair scan was identified that was outside of any elevated gadolinium peak concentrations and included in the comparison. Overall, the rolling average results showed the smallest CV values in 34/35 (97%) hairs (see Table 5 for overall summary and Figure 22 for results for individual hairs).

Table 5. CV comparison for ^{157}Gd results

Measure	Individual Hair CVs avg ± SD (range)
Raw ^{157}Gd	0.95 ± 0.70 (0.26–3.3)
^{34}S normalized (^{157}Gd/^{34}S)	1.0 ± 0.73 (0.25–3.4)
Rolling average ^{157}Gd	0.67 ± 0.47 (0.13–1.8)

In 71% of hairs (25/35), normalizing to ^{34}S introduced additional variability compared to the raw ^{157}Gd results (i.e., higher CVs). Based on the available guidance, the instrument limitations, and the CV assessment, the ^{157}Gd results were not normalized to any internal standard. For additional details on this assessment, see Appendix D.

To assess instrument drift, ^{34}S results from the hair samples, and ^{157}Gd results from the SRM were reviewed. The ^{34}S results for all hair samples (N=159) ranged from 1,259,000 to 7,624,000 cps (average 5,294,000 cps). The CVs for each hair fell between 0.051 and 0.35 (average 0.16). Using linear regression for each line scan, the slope of the ^{34}S line was assessed to determine whether the instrument showed any drift pattern over the course of the line scan. The hair with the largest ^{34}S slope (subject 5 hair 9) only observed an increase in 1.5% over the average cps value. The SRM analysis (N=37) for ^{157}Gd was similarly reviewed for drift and revealed a comparable pattern of minimal change in slope (max slope was an increase of 0.62% over the average cps value). These findings demonstrate that there was minimal within-sample change in instrument response that would adversely affect the accuracy and precision of each measurement. For a more comprehensive discussion of these analyses, see Appendix E.

2.4.2 Distance Along Hair Shaft as Time of Dose Estimate

The peak maxima location was used to derive the estimated number of days before death. Comparing these numbers to the known days before death (when injection occurred) the estimates both over- and under-estimated the number of days. In 53% of hairs, the day on which injection occurred was over estimated (72/135; meaning the peak was farther from the root than expected), and in 47% of hairs the injection day was under estimated (63/135; peak closer to root than expected).

Subject 14 had the most consistent estimate of injection day as evidenced by the low CV value (0.05) for estimated days and subject 11 had the most variable estimate of injection day (CV = 0.88; see Table 4). Example line scan plots for the low variability (subject 14) and high variability (subject 11) examples are provided in Figure 2a and b respectively. Variability in the peak positioning can be due to variability in the growth rates or growth cycle phase for individual hairs. Figure 3 shows the distribution of the difference between actual and estimated days for all subjects, with a good exponential shape favoring the difference of fewer days. A linear regression between the actual and average estimated days for a subject showed moderate linearity ($R^2 = 0.46$) with a relationship that was statistically significant ($p < 0.05$). The slope of the line was 0.45, suggesting that the model underestimates the day on which injection occurred. Figure 4 shows the plot and linear regression results.

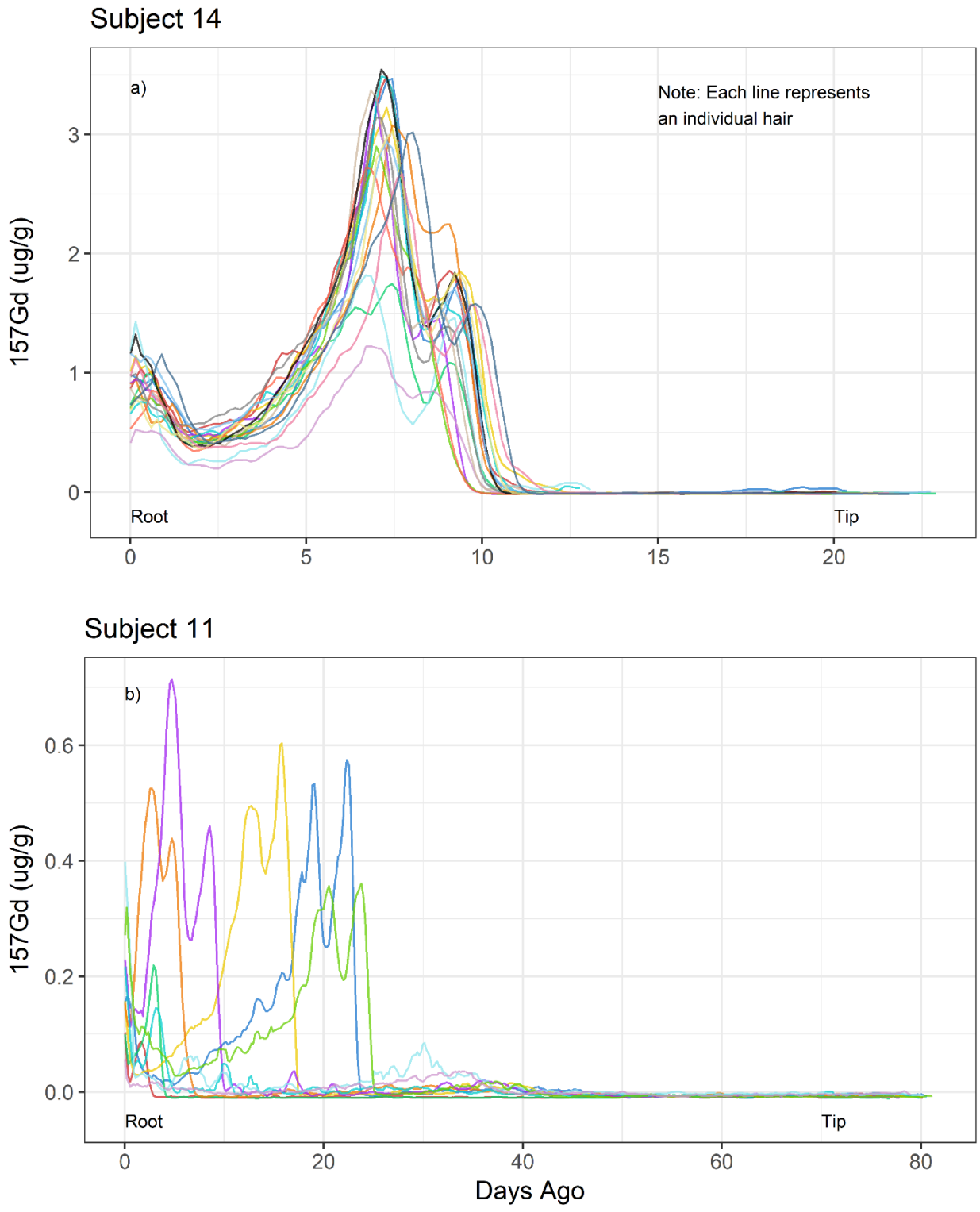

Figure 2. Hair line scan results with a) low variability in the estimated days, and b) high variability in the estimated days

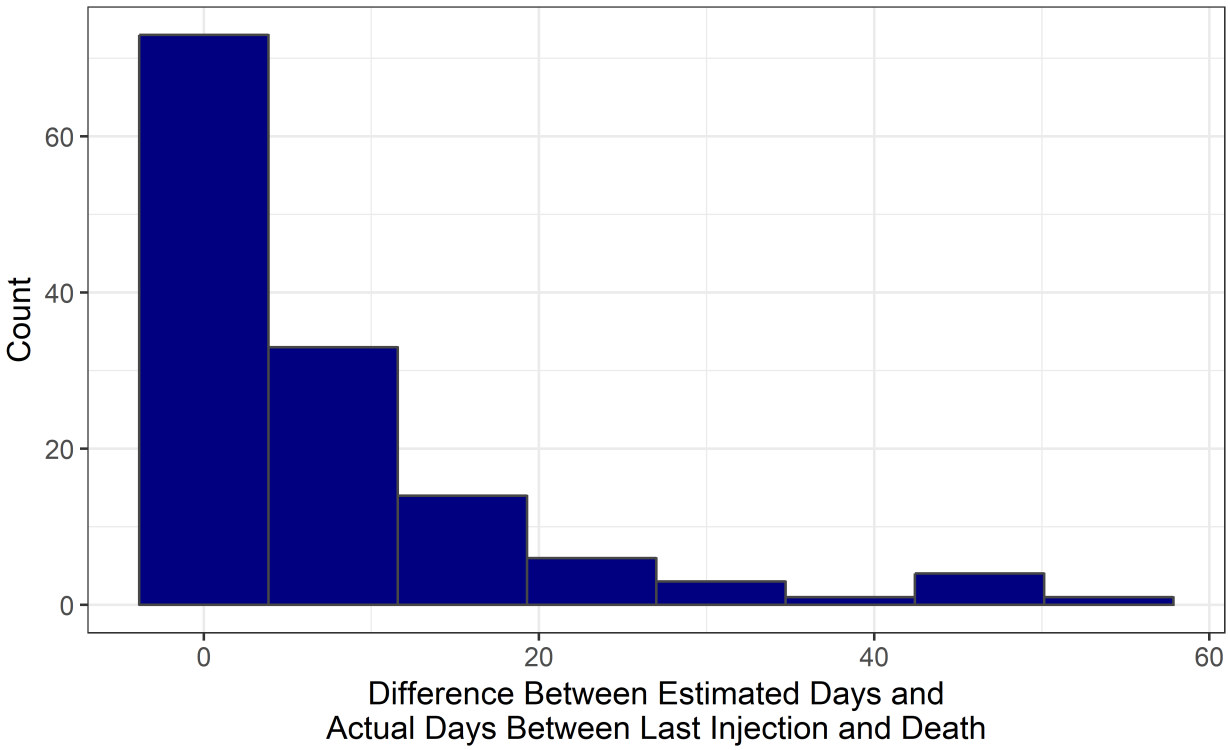

Figure 3. Distribution of difference between estimated and actual days

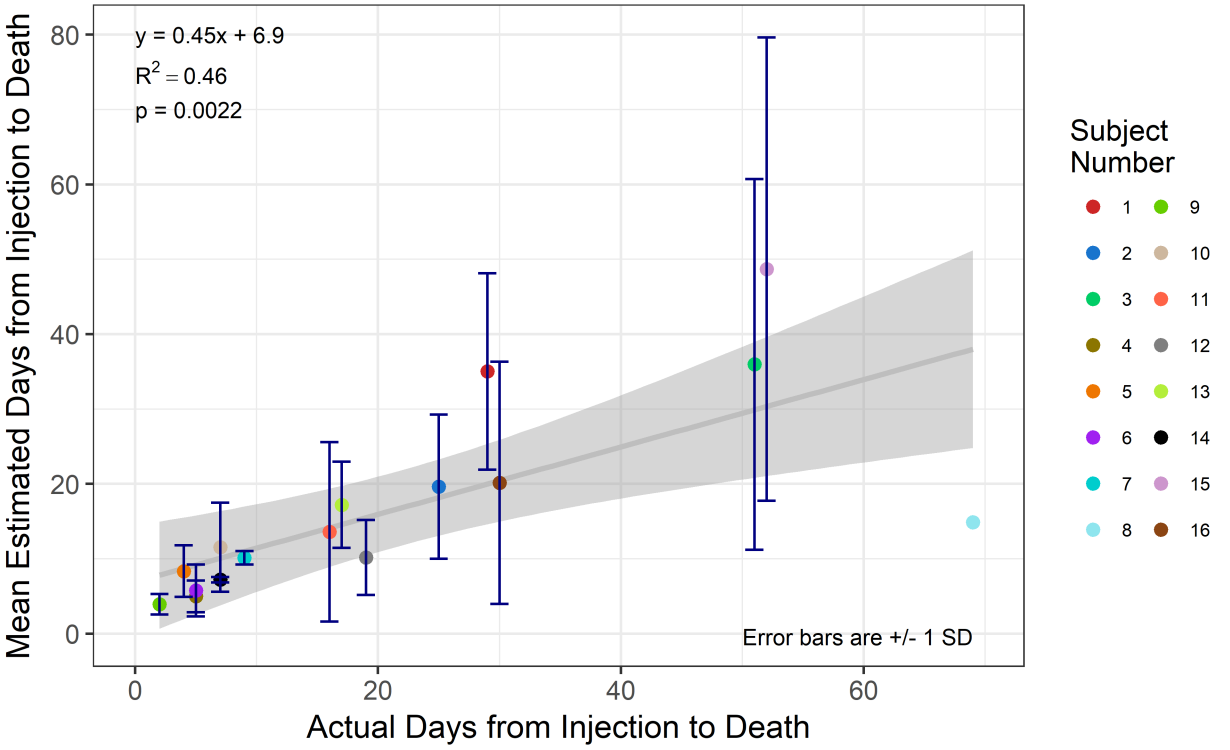

Figure 4. Linear regression of estimated and actual days

2.4.3 Gadolinium Dose Compared to Hair Concentrations and Integrals

Of the hairs analyzed from the cases, 87% had a ^{157}Gd peak (135/155). Peak maximum values ranged from 0.045 to 8.5 µg/g with a median of 1.5 µg/g. None of the hairs analyzed from the control subjects had a ^{157}Gd peak and these samples showed a generally flat line for ^{157}Gd. For the controls, the two hairs analyzed for subject 17 both had an average concentration of 0.067 µg/g, and the two hairs analyzed for subject 18 had average concentrations below the detection limit (0.05 µg/g).

Subject 10 had the highest peak maxima concentration (8.5 µg/g) of any hair analyzed but received a relatively smaller dose of gadolinium (0.948 g). Subject 10 also had the greatest variability (i.e., largest spread) of peak maxima concentrations for hairs analyzed. Subject 9 received the largest gadolinium dose (3.2 g) and had the highest average peak maxima concentration at 5.35 µg/g. Due to the small sample size, quantitative evaluation of ^{157}Gd peak maxima among GBCA types was not possible. Figure 5 shows the distribution of peak maxima concentrations by ascending dose for each subject.

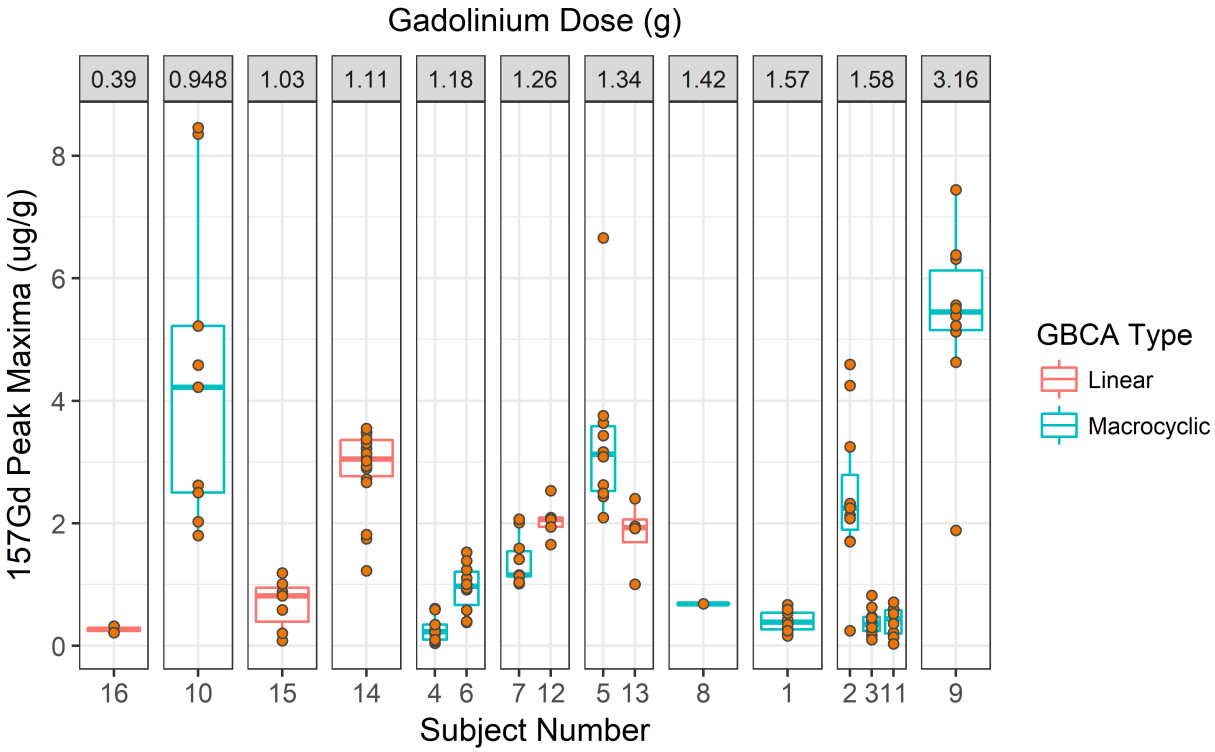

Figure 5. ^{157}Gd peak maxima by gadolinium dose, subject, and GBCA type

Area under curve values were between 0.66 and 310 µg/g*mm, with a median of 37 µg/g*mm. Subject 9 received the largest dose (3.16 g) of gadolinium among the subjects included and had the largest area under the curve value (310 µg/g*mm). This subject also had the greatest spread in the area under the curve values for the hairs analyzed (see Figure 6).

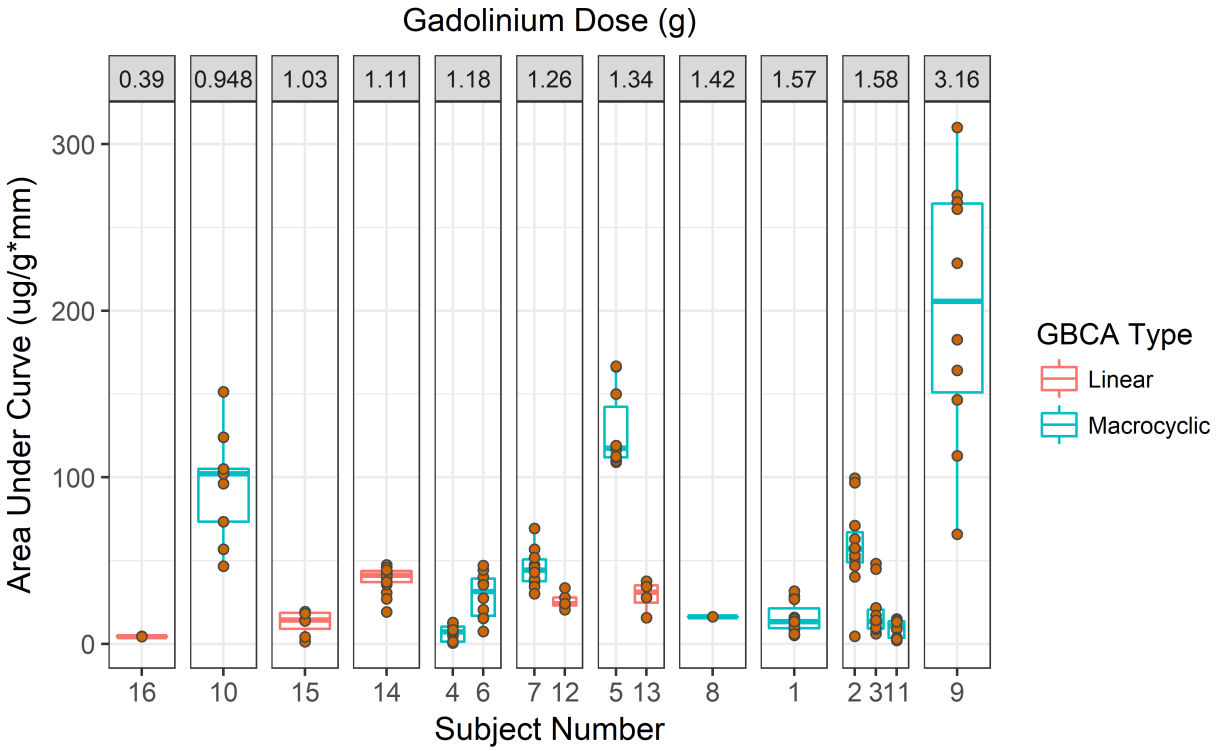

Figure 6. Area under the curve by gadolinium dose, subject, and GBCA type

Linear regression of the average peak maxima concentration and gadolinium dose did not show good linearity ($R^2 = 0.18$) and was not statistically significant ($p = 0.06$). Regression for area under the curve and gadolinium dose revealed a moderate relationship ($R^2 = 0.41$) that was statistically significant ($p = 0.0046$). The regressions for dose versus average peak maxima and area under the curve are shown in Figure 7a and b respectively. The area under the curve regression was a statistically significant, more linear correlation with dose compared to the peak maxima concentrations.

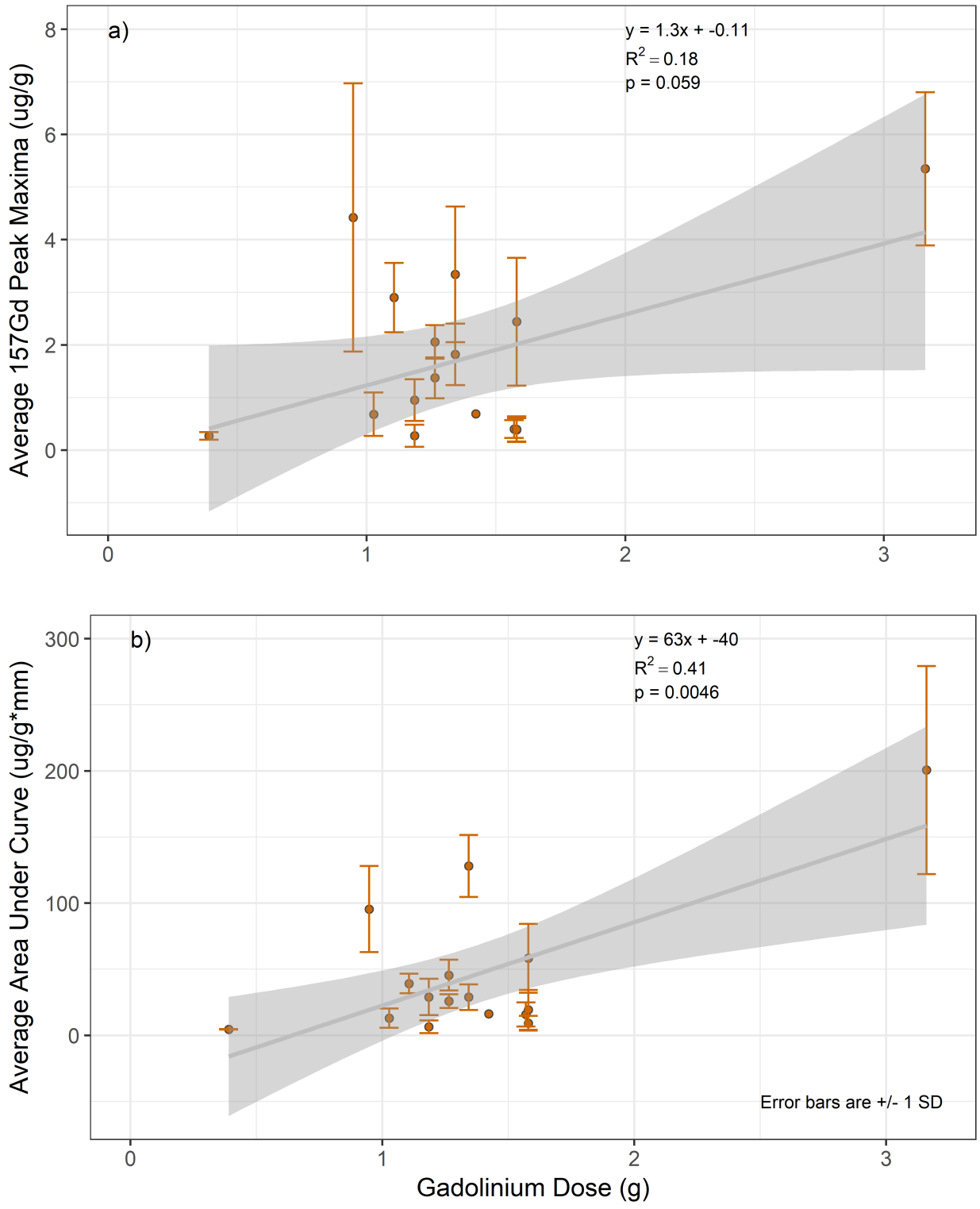

Figure 7. Linear regression of gadolinium dose and average a) ^{157}Gd peak maxima concentration; and b) area under the curve

2.5 Conclusions/Discussion

The samples analyzed for this study revealed good accuracy and precision and line scan variability that was consistent with other published studies. The CVs for each hair's ^{34}S cps results were between 0.051 and 0.35 (average 0.16) and other studies showed similar CV values, 0.012 to 1.2 (average reported CVs ranged from 0.13 to 0.5), for numerous elements (Bartkus et al. 2011; Cheajesadagul et al. 2011; Dressler et al. 2010; Durrant and Ward 1994; Legrand et al. 2004; Legrand et al. 2007; Luo et al. 2017; Pozebon et al. 2008; Rodushkin and Axelsson 2003; Sela et al. 2007; Stadlbauer et al. 2005).

Human scalp hair undergoes a cycle comprised of four phases: anagen (growth), catagen (apoptosis), telogen (resting), and exogen (falling out/shedding; Alonso and Fuchs 2006;Buffoli et al. 2014). In humans, 80–90% of scalp hair is in anagen phase, 1–3% is in catagen phase, and 4–20% are in telogen phase (Lebeau et al. 2011; Robertson 1999). Based on these distributions, we would expect to observe gadolinium peaks in approximately 85% of the hairs from cases that received a GBCA injection. In fact 87% of the hairs analyzed (135/155) showed the expected gadolinium peak, very close to the expected detection frequency. Based on these results, deposition of gadolinium is occurring in the hair shaft of people who receive GBCA injections, and gadolinium is detectable in hair using LA-ICP-MS.

Generally, the methods utilized in this study resulted in high quality data and could be used in other applications. The limit of detection achieved was sufficient to quantify ^{157}Gd concentrations in subjects dosed with GBCAs. Analytical variability in ^{34}S cps results (average of 16%) was good, and in some cases better than other studies reported.

The average peak maxima location proved to be a good predictor of the GBCA injection day in these samples. However, there was high intra-subject variability for estimated day among some subjects. A physiological reason for the differences, could be the length of the shaft within the follicle during different hair cycle phases. During the anagen phase, the root extends farther into the skin, compared to catagen or telogen, when it moves closer to the skin surface in preparation for shedding (Pozebon et al. 2017; Tobin 2012).

The intra-subject variability may also be due to variability in individual hair growth rates. Subject 8 had the greatest difference between actual and estimated days (underestimated by 54 days), but this subject only had one hair with a ^{157}Gd peak out of four analyzed due to sparse hair on the scalp sample. It is possible that this particular subject had other hair growth abnormalities, such as alopecia. Two other subjects with relatively high variability (subject 3 and 15) received injections that were farther in the past (51 and 52 days, respectively) than the other subjects. This suggests that certain hair follicles may consistently have slower growth rates. Over longer periods, the cumulative effect of these small differences can represent larger differences in

overall hair growth. Quantitative assessment of this relationship was not conducted because of the small sample size, as well as the skewed distribution of actual days with more subjects experiencing a smaller number of days between injection and death.

The large intra-subject variability of scalp hair growth has been documented in previous studies. Wilkins et al. (2003) used an antibiotic (ofloxacin) as a reference marker in male and female subjects between 18 and 40 years old and observed "considerable" intra-subject variability in the antibiotic positioning along the hair shaft. That study calculated estimated hair growth rates for six individuals with ranges from 0.49–0.61 cm/month (the smallest range) to 0.49–0.98 cm/month (the largest range).

Other potential causes of the intra-subject variability observed in our study include factors that influence the follicle itself. A network of nerve fibers surrounds the hair follicle and the proximity of this nerve tissue to the follicle suggests that neurotransitters/neuropeptides may influence hair growth (Buffoli et al. 2014). Other molecular species direct or modulate hair follicle cycling and hair growth, such as proteins and hormones (Robbins 2012a; Tobin 2012). Further, the sebaceous gland is known to affect hair growth rates (Lee et al. 2012). Each follicle can function independently depending on localized tissue responses to chemical signaling (Robbins 2012a; Tobin 2012). The individualized nature of each hair follicle may account for differences in apparent individual hair growth rates.

To determine a more precise estimate of hair growth rates, a dosing study (using a reference marker) is recommended that includes a larger number of live subjects and hairs, sampled across regular time intervals, extending multiple months. The study should include only hairs in anagen phase to ensure the assessment considers actively growing hairs. This could be accomplished by pluck hairs from a section of the scalp to initiate anagen phase simultaneously in numerous follicles. The high spatial resolution afforded by LA-ICP-MS analysis will facilitate quantitation of growth rates to a high degree of accuracy. Appendix G describes plans for a zinc supplementation study of this sort.

The measure of the individual hair peak maximum and average ^{157}Gd peak maxima for a subject offers a snapshot of the highest depositional period for hair. However, because the gadolinium from the GBCA is not instantly excreted, the peak maximum is not inclusive of the metabolism and excretion periods. The area under the curve measure integrates the time course of gadolinium during deposition within the hair, and is a cumulative measure of exposure (Urso et al. 2002). The integrated measure is a more accurate estimate of the overall exposure to a substance (Scheff et al. 2011).

There was a moderate and statistically significant correlation between gadolinium dose and the area under the curve. This suggests that the integrated area under the curve may be related to the

gadolinium dose in the injection. However, the r-squared value of this regression (0.41) still indicates a substantial source of variability, for reasons we currently do not understand. In Section 3, a comparison of hair gadolinium concentrations and concentrations in other tissues, for the subjects included in this study, revealed stronger linear relationships (particularly with brain tissue). Thus, the area under the curve may accurately reflect the deposited dose, but not necessarily the administered dose. The dose was not adjusted for a subject's height or weight (this information was not available), which may be an additional source of variability.

The high intra-subject variability of ^{157}Gd peak concentrations (average of 43%) may preclude the use of this measure to predict delivered dose in smaller sample sizes. To account for variations in hair growth and the magnitude of concentrations, we recommend a minimum of 10 hairs per subject, but ideally 20 or more hairs per subject for future analysis.

Several studies have reported that exposure to linear GBCAs results in higher tissue concentrations than macrocyclic GBCAs (McDonald et al. 2017; Murata et al. 2016). However, we did not observe a difference (after a qualitative review of the plots in Figure 5 and Figure 6) between the two GBCA types and the magnitude of the average ^{157}Gd peak concentration or the average area under the curve.

Although this study included numerous subjects with up to 18 hairs analyzed per subject, a larger dataset will supply more comprehensive data on inter- and intra-subject variability. Increasing the study size would potentially permit inclusion of controlling variables (e.g., age, gender, ethnicity) that may reveal other patterns of distribution and elimination. This technique can also be applied on live subjects, since only the hair shaft is needed for analysis and can easily be plucked. Hair, particularly in humans, offers an interesting potential to serve as a timeline of exposure preserving temporal integrity within the matrix.

Study Limitations:

Collecting autopsy cases is difficult and recruitment methods employed by other studies cannot be utilized. Due to limited knowledge on the pharmacokinetics of gadolinium in numerous tissues, patients that received more than one GBCA were not eligible to avoid introducing additional variability into the results that could not be adequately understood. The small sample size prevented inclusion of controlling variables (e.g., gender, age, eGFR) in the regression analysis. High intra-subject variability for the position and magnitude of the gadolinium peak within the hair shaft suggest that larger sample sizes (both subjects and hairs) may be more appropriate.

Conclusions:

There was moderate correlation between gadolinium dose and area under the curve as well as gadolinium peak position and GBCA injection day. Monitoring methods employing LA-ICP-MS analysis of hair can be applied to live patients to assess gadolinium exposures.

Chapter 3. Human Hair as a Possible Surrogate Marker of Retained Tissue Gadolinium

3.1 Abstract

Objectives:

We employed laser ablation inductively coupled plasma mass spectrometry (LA-ICP-MS) to quantify gadolinium in hair samples from autopsy cases with gadolinium based contrast agent (GBCA) exposure, to correlate those measurements with gadolinium concentrations in brain, skin, and bone tissues from the same case to investigate a potential non-invasive method to quantify and monitor gadolinium.

Materials and Methods:

Medical records from autopsy cases at our institution were screened for history of exposure to GBCAs. Cases with exposure to a single type of GBCA with the most recent injection occurring within one year were identified and included in the study. Tissue and hair samples from 18 autopsies (16 cases with exposure to GBCA, 2 controls) were included in the study. The concentration of gadolinium in hair samples was analyzed by LA-ICP-MS, and brain (globus pallidus, dentate nucleus, white matter), bone and skin tissues were analyzed by bulk ICP-MS. The average of the maximum value in the hair samples were used to generate a representative measure of the hair gadolinium concentration for each case. A linear regression analysis between each tissue type and hair was conducted to assess for possible correlation.

Results:

Comparing the different tissues revealed good correlation between some tissue types. The best model fit occurred between white matter and hair ($R^2 = 0.83$; p-value < 0.0001) followed by the comparison between dentate nucleus and hair ($R^2 = 0.72$;
p-value < 0.0001) and dentate nucleus and skin ($R^2 = 0.70$; p-value < 0.0001).

Conclusions:

A good correlation in this study between hair gadolinium concentrations and brain and skin gadolinium concentrations suggests that hair may serve as a safe and effective biomonitoring tissue for patients who receive GBCA injections.

3.2 Introduction

Gadolinium based contrast agents (GBCAs) are used in magnetic resonance imaging (MRI) to increase diagnostic performance. Gadolinium in its elemental form is toxic to humans since the ionic radius of gadolinium is close to that of calcium and, thus, it may block calcium channels (Rogosnitzky and Branch 2016). To prevent this, gadolinium in contrast agents is administered in a chelated form (i.e., incorporated into a ligand) and in this form it was considered safe (FDA 2017a; Layne et al. 2018). The first indication that there was an issue with GBCAs came in 2006 with the discovery of nephrogenic systemic fibrosis (NSF). NSF is a rare debilitating condition that occurs in patients with renal failure and has been associated with the use of GBCAs (FDA 2017a).

To further underscore concerns of potential adverse effects from gadolinium use, Kanda et al. (2014) reported an increasing T1-weighted image (WI) hyperintensity within the brain in the globus pallidus and dentate nucleus related to cumulative doses of GBCA, even in patients with normal renal function. This observed hyperintense T1 was confirmed to be associated with retention of small amounts of gadolinium from an autopsy study by McDonald et al. (2015). A subsequent autopsy study by Murata et al. (2016) demonstrated the variability in retained gadolinium among different contrast agents. Significance of these small amounts of retained gadolinium in human tissue is not fully understood, however the potential for toxicity remains of great concern. Although several observational studies have failed to show a toxic effect from these small amounts of retained gadolinium, there is a small group of patients who reportedly suffer from various maladies including pain and debilitation, which they attribute to GBCA exposure. Although controversial and, as yet, unproven, these patients have been referred to as having “gadolinium deposition disease” by Semelka et al. (2016) who is currently studying this patient group and continuing to evaluate them.

A major impediment to evaluating patients with possible gadolinium toxicity is that a reliable method to non-invasively sample, quantify, and monitor gadolinium in humans in vivo is needed. One possible biological material that is known to concentrate heavy metals, is readily accessible, and can be obtained non-invasively is hair. The purpose of this study is to use laser ablation (LA) ICP-MS to evaluate gadolinium levels in hair obtained from decedents that were exposed to GBCA during life and to determine if there is a possible correlation with concentrations in other body tissues obtained at autopsy including brain, bone and skin.

3.3 Methods

Subjects:

This study was approved by the University of Washington Human Subjects Review Board for retrospective review of medical records and was Health Insurance Portability and Accountability Act compliant. Additionally, autopsy consent from each case granted authorization for use of tissues for research purposes.

Cases were identified and their electronic medical records (EMR) screened when they presented for autopsy between December 2017 and May 2019 at the pathology department at our institution. If they met inclusion criteria, brain, bone, skin, and hair samples were collected. Inclusion criteria included having complete and accessible medical records, a history of one or more GBCA injection(s), exposure to a single type of GBCA, and most recent exposure within one year before death. Exclusion criteria included inaccessible or incomplete medical records, and exposure to multiple GBCA types. Initially, a total of 42 cases with gadolinium exposure and two controls were identified from the consecutive autopsy review.

EMRs were subsequently more thoroughly searched for exposure to GBCA. The type of GBCA administered, dose, and date of injection for all recorded injections were compiled for all cases with exposure. Subjects documented without exposure to GBCAs were included as controls. Age, sex, and estimated glomerular filtration rate (eGFR) were recorded for all subjects. For subjects with eGFR values above 60, autopsy records report “> 60.” For subjects with eGFR values below 60, the actual numeric value is reported.

A tiered screening methodology was employed to identify cases that did not meet inclusion criteria. Nine subjects received injections of more than one GBCA type, 12 received injections more than a year before their death, 1 had very short hair that was too short to capture the exposure period, 1 did not have a hair sample, and 1 more was missing required information in the EMR. In total, 24 potential cases were excluded from this initial study group. Eighteen cases with a history of exposure to a single type of GBCA with the most recent injection occurring within one year were identified for inclusion. Two of those cases did not have hair long enough to capture the exposure period (e.g., hair length representative of one month of growth, but exposure period was six months prior) and were excluded. Human scalp hair, on average, grows at the rate of 1 cm/month (Robbins 2002). Final inclusion was 16 cases and two controls in this study. Table 6 summarizes subject characteristics for the subset included here.

Table 6. Study population characteristics

Characteristic (Units)	Controls	Cases
Subjects (N)	2	16
Male (N)	0	8
Female (N)	2	8
Age (Years, min–max [average])	70–79 (75)	19–79 (57)
eGFR <60 mL/min/1.73 m^2 (N)	1	4
eGFR >60 mL/min/1.73 m^2 (N)	1	12
Linear agent (N)	Not applicable	5
Macrocyclic agent (N)	Not applicable	11
Time between last injection and death (Days, min–max [average])	Not applicable	2–69 (22)

Sample Analysis:

Scalp samples with hair and brain sections including the globus pallidus (GP), dentate nucleus (DN), and white matter (WM) were collected for all subjects. Skin and bone (rib) samples were also collected at the time of autopsy for most subjects. Brain, bone and skin tissue samples were stored in a 10% formalin solution. All tissue samples were cut using stainless steel surgical scissors which were cleaned between each sample to prevent cross contamination of gadolinium. Brain, bone and skin tissue samples were cut, then weighed using an analytical balance (AG104; Mettler Toledo, Greifensee, Switzerland). Samples underwent microwave assisted nitric acid digestion before inductively coupled plasma mass spectrometry (ICP-MS) analysis following a modified version of the U.S. Environmental Protection Agency (EPA) method 6020a (revision 1, 2007).

Hairs from the scalp samples were plucked, including the root when possible, using carbon fiber (non-metal) tweezers and placed in microfuge tubes (one per subject); these tubes were filled with acetone and the caps closed. Tweezers were cleaned with methanol between subjects to prevent cross contamination. The microfuge tubes with hairs and acetone were sonicated for 30 minutes in water at room temperature. The hairs were then removed from the acetone and placed in Kim Wipe pouches to be dried in an incubator at 37°C for one hour. This washing process has been used previously (Reiss et al. 2016) and removes exogenous contamination from the hair shaft. The cleaned hairs are then mounted onto glass slides covered in double stick tape, which adheres the hair to the slide without damaging the shaft. The slides were placed on the laser stage along with calibration gels and a glass pellet standard reference material (SRM; National

Institute of Standards and Technology [NIST] 612) with trace metals. The calibration gels were bovine skin-based gelatin amended with selected isotope concentrations between 0 and 2,000 µg/g.

For LA analysis, the laser path along each hair was traced as a single line scan from root to tip in the instrument software (Agilent NWR ESI ActiveView). After the material was ablated it was transported through a teflon tube to the ICP-MS via a stream of He for analysis. Between four and 18 hairs were analyzed from cases and two hairs were analyzed from the controls. Calibration gels and SRM were included in each batch run to assess instrument stability over time. After samples were analyzed, counts per second (cps) data was output from the ICP-MS software (MassHunter).

Instrument Parameters:

The instrumentation used for analysis of the hairs included an Elemental Scientific, Inc. (ESI) New Wave Research (NWR) 213 (Nd:YAG [neodymium: yttrium aluminum garnet]) laser ablation tool interfaced to an Agilent 7900 ICP-MS. The laser operates at a 213 nanometer (nm) wavelength (ESI No Date). The laser is outfitted with a two volume sample cell which minimizes material lost during ablation as well as signal broadening. The helium flow through the laser was 800 mL/min with 1.07 L/min of argon makeup gas T-ed in between the laser and ICP-MS. The sampling period for all isotopes and materials was 0.515 seconds and integration time for gadolinium-157 (^{157}Gd) was 0.4 seconds. The ICP-MS was set to helium mode without collision cell gas and a radiofrequency power of 1550 watts. Laser parameters for the hair and gel analysis were as follows: spot size of 30 µm; firing rate of 20 Hz; scan speed of 100 µm/sec; and energy of 60%. Brain, skin, and bone tissue were analyzed using the same ICP-MS instrument listed above, except that argon carrier gas flow was 1.03 L/min with no makeup gas.

Data Processing and Analysis:

Laboratory-reported Gd concentrations were used for the brain (globus pallidus, dentate nucleus, and white matter), skin, and bone samples. The time series of *m/z*157 intensities for each hair profile was processed using a rolling mean centered on five values. Similar data reduction techniques (i.e., rolling average and/or median) have been employed by previous LA-ICP-MS analysis of hair (Noel et al. 2015), corals (Sinclair et al. 1998), and otoliths (Sanborn and Telmer 2003). Mass-based concentrations (i.e., µg/g) of ^{157}Gd in each hair line scan were calculated using a linear regression calibration curve derived from the gels. The distance along the hair shaft (in millimeters [mm]) was derived from the scan speed of the laser (100 µm/sec for hair) and the acquisition time of each data point. An example plotted line scan for an individual hair showing a ^{157}Gd peak is provided in Figure 8a; an example of a hair from one of the control subjects with no peak is shown in Figure 8b.

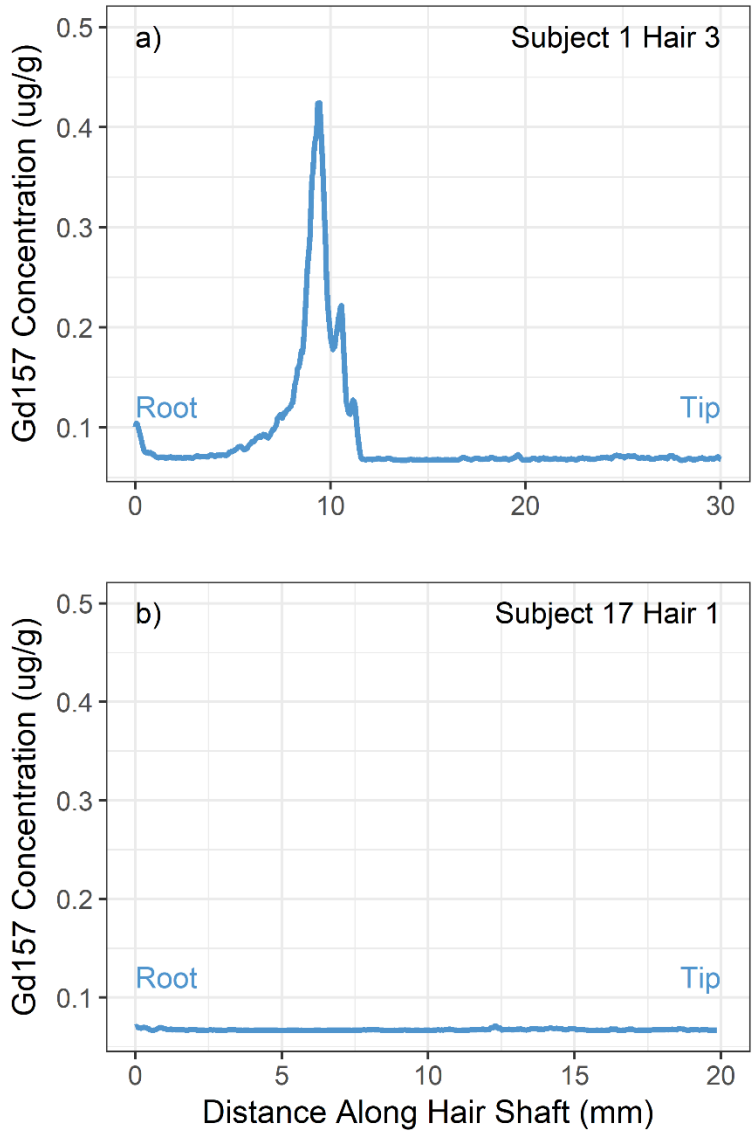

Figure 8. Example hair plots showing: a) hair profile with a ^{157}Gd peak; and b) hair profile without ^{157}Gd peak

For each hair line scan with an identified peak, the portion along the shaft (excluding the root) that included a ^{157}Gd peak was isolated and the maximum concentration was selected as the representative measure for the individual hair. These maximum values were averaged for all hairs analyzed for a specific subject to generate a representative measure of the hair gadolinium concentration for that subject. Hair from control subjects showed no ^{157}Gd peaks and the average of the hair line scan was used as the representative concentration for each hair; an average of all hairs analyzed was used as the representative concentration for a control. Concentrations below the LA-ICP-MS method detection limit (0.05 µg/g) were set to 0.05 µg/g.

Statistical Analysis:

Using the ‘lm()’ function in RStudio (version 3.4.0), a linear regression between each tissue type was conducted to assess the relationship between tissue concentrations. Significance was determined as $p < 0.05$. Due to the small sample size, no adjustments were made (i.e., did not use controlling variables).

3.4 Results

There were 16 cases with exposure to GBCAs and two controls included in this study. Approximately a quarter of the cases received linear GBCAs (gadoxetate or gadobenate) and the remaining three quarters received macrocyclic GBCAs (gadobutrol or gadoteridol). There is some variability in the concentration of injectable gadolinium agents. Thus, gadoxetate contains 0.25 mmol/mL, gadobenate and gadoteridol contain 0.5 mmol/mL, and gadobutrol contains 1.0 mmol/mL. Total GBCA dose for each case was calculated as the total number of mL injected multiplied by the GBCA molarity of the agent received. Two cases (subjects 3 and 6) received three injections and the other 14 cases received only one injection. For the two cases that received multiple GBCA injections, subject 3 received injections at 51, 70 and 75 days before death, and subject 6 received injections at 5, 6 and 106 days before death. Days between the last injection and death were between two and 69. For two subjects (2 and 3), brain and hair samples were received for analysis, but no skin or bone samples.

Cases had higher ^{157}Gd concentrations than controls by at least a factor of five (conservative estimate due to detection limit) and up to a factor of 100. Among the brain tissue samples, the GP results were generally the highest with an average concentration of 0.11 µg/g compared to the DN and WM, which had average concentrations of 0.046 and 0.027 µg/g respectively. Skin concentrations ranged from 0.0154 to 0.21 µg/g (average 0.07 µg/g) and bone concentrations ranged from 0.11 to 2.3 µg/g (average 0.88 µg/g). Hair was the tissue with the highest ^{157}Gd concentrations (average 1.73 µg/g) with the highest value being 5.4 µg/g for subject 9. This was consistent with previously published articles (IAEA 1993; Pozebon et al. 2017) noting that metals concentrations in hair can be one to two orders of magnitude higher compared to other tissues. Summaries of the subjects and tissue concentrations are in Table 7.

Table 7. GBCA summary and tissue concentrations for cases and controls

Subject No.	GBCA Type	GBCA Name (Dose [mL])	GBCA Dose (mmol)	Days From Injection to Death	Brain-GP (µg/g)	Brain-DN (µg/g)	Brain-WM (µg/g)	Skin (µg/g)	Bone (µg/g)	Hair (µg/g)
1	Macrocyclic	Gadobutrol (10)		29	0.050	0.030	0.0084	0.017	0.41	0.4
2	Macrocyclic	Gadoteridol (20)	10	25	0.036	0.029	0.029	No data	No data	2.4
3	Macrocyclic	Gadoteridol (20)	10	51	0.12	0.024	0.0044	No data	No data	0.39
			10							
			10							
4	Macrocyclic	Gadoteridol (15)	10	5	0.015	0.016	0.013	0.018	0.2	0.27
5	Macrocyclic	Gadoteridol (17)	7.5	4	0.060	0.047	0.043	0.065	1.1	3.3
6	Macrocyclic	Gadoteridol (15)	8.5	5	0.018	0.017	0.018	0.022	0.13	0.95
			7.5							
			7							
7	Macrocyclic	Gadoteridol (16)	5.5	9	0.519	0.056	0.053	0.035	0.59	1.4
8	Macrocyclic	Gadoteridol (18)	8	69	0.012	0.0050	0.0031	0.015	0.41	0.69
9	Macrocyclic	Gadoteridol (40)	9	2	0.11	0.10	0.099	0.18	0.45	5.4
10	Macrocyclic	Gadoteridol (12)	20	7	0.31	0.15	0.070	0.187	2.34	4.4
11	Macrocyclic	Gadoteridol (20)	6	16	0.0075	0.0056	0.0043	0.017	0.11	0.4
12	Linear	Gadobenate (16)	10	19	0.128	0.0615	0.019	0.21	2.0	2.1
13	Linear	Gadobenate (17)	8	17	0.30	0.080	0.025	0.11	2.1	1.8
14	Linear	Gadobenate (14)	8.5	7	0.055	0.065	0.031	0.097	1.4	2.9
15	Linear	Gadobenate (13)	7	52	0.048	0.035	0.0062	0.042	0.50	0.68
16	Linear	Gadoxetate (10)	6.5	30	0.063	0.013	0.0057	0.017	0.54	0.27
		Average		22	0.11	0.046	0.027	0.073	0.88	1.73
		SD		20	0.14	0.039	0.027	0.070	0.77	1.58
17	NA	NA		NA	0.0012	0.0030	0.0011	0.0080	0.0040	0.067
18	NA	NA		NA	0.0006 U	0.0008	0.0003	0.0004	0.0016	0.05 U

Comparison of the different tissues using linear regression revealed good agreement (i.e., correlation) between some tissue types. The best model fit was the comparison between WM and hair concentrations (R^2 = 0.83; p-value < 0.0001) followed by the comparison between DN and hair (R^2 = 0.72; p-value < 0.0001) and DN and skin (R^2 = 0.70; p-value < 0.0001). The correlation between DN and hair is shown in Figure 9. The dentate nucleus is of particular interest as it plays an important role in planning and initiation of voluntary movement, and is also a known location of high gadolinium deposition in the brain (McDonald et al. 2015; Murata et al. 2016).

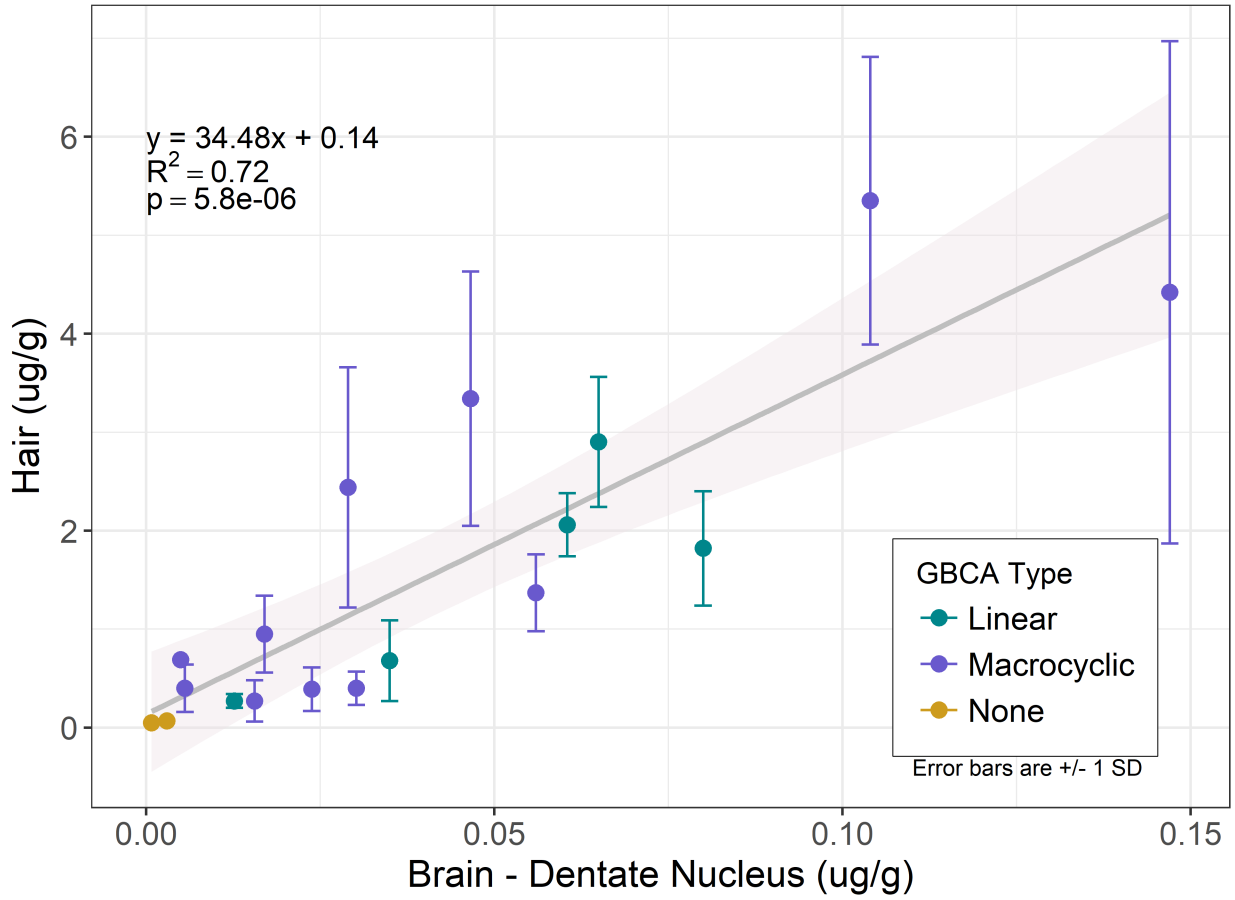

Figure 9. Linear regression between dentate nucleus and hair

Increasing hair concentrations of ^{157}Gd correlated significantly with increasing concentrations in DN, WM, and skin tissues. Though the linearity between hair and bone was low ($R^2 = 0.30$), this relationship was still statistically significant at an alpha of 0.05. Figure 10 displays the linear regression results' R^2 values and associated p-values for all tests.

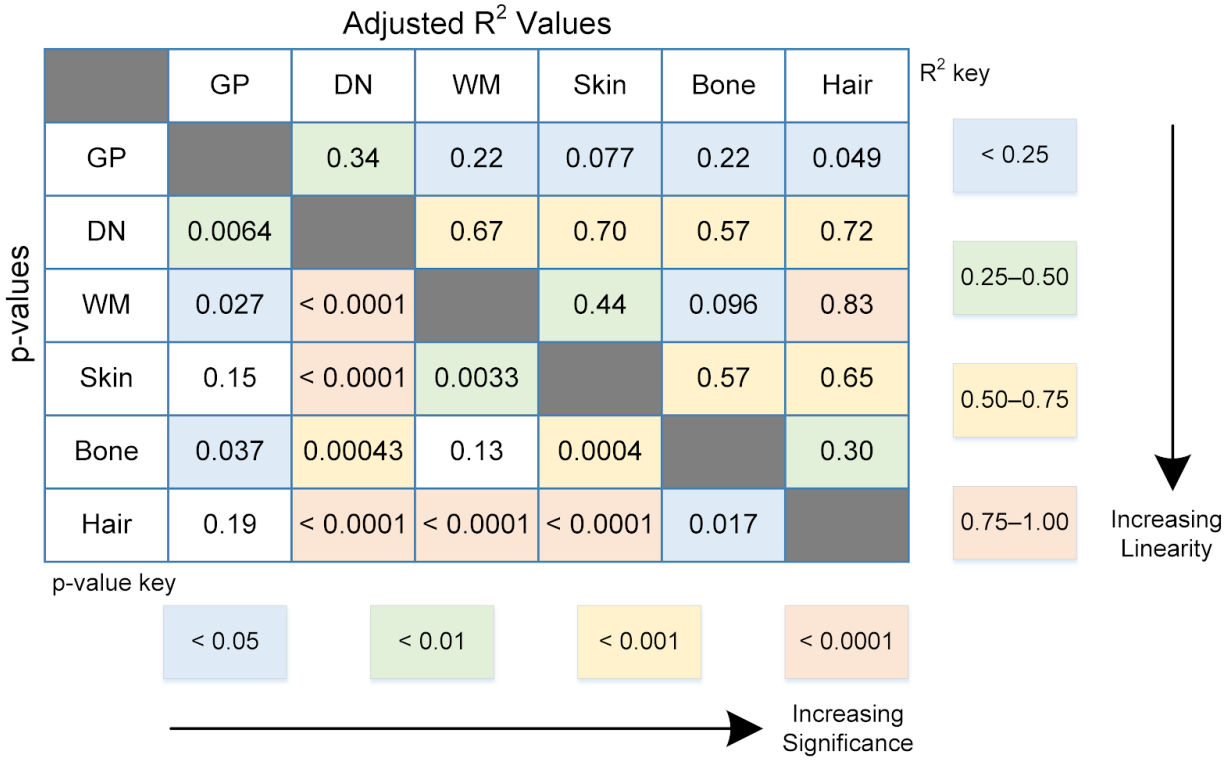

Figure 10. Summary of linear regression results comparing tissue concentrations

All regressions that included GP results were generally not linearly related (i.e., low R^2 values) indicating negligible or weak associations between GP concentrations and other tissue concentrations. The GP results for subject 7 were almost twice as high as the next highest GP concentration. The other tissue concentrations for this subject did not reflect the same degree of elevated gadolinium concentrations. This result was considered an outlier in the GP results and if it is excluded from the regression analysis the linearity of the relationship between GP and hair is improved from an R^2 of 0.049 (p-value = 0.19) to 0.22 (p-value <0.05). Figure 11 shows the comparison between GP and hair with the outlier.

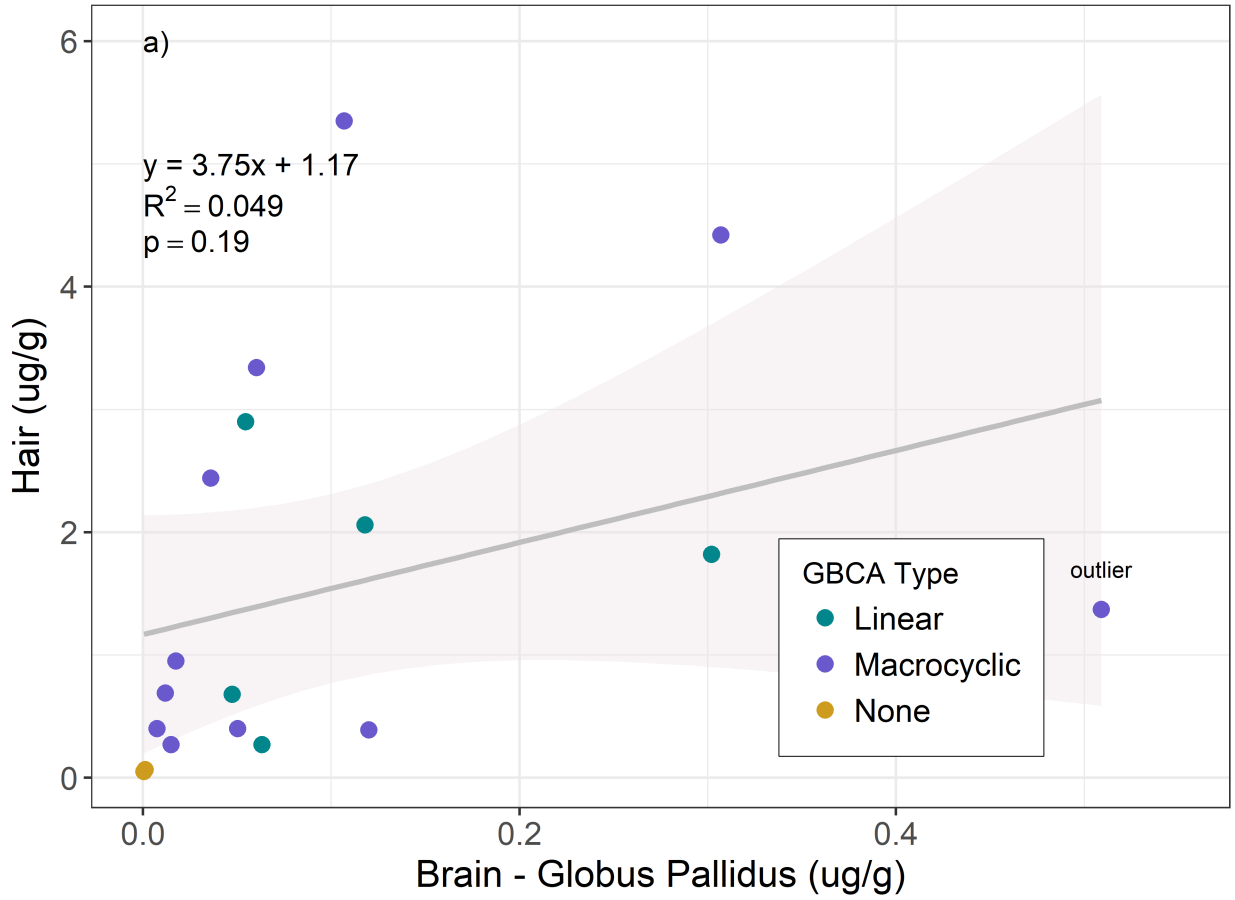

Figure 11. Linear regression between globus pallidus and hair, including the outlier (subject 7)

3.5 Conclusions/Discussion

GBCAs are administered intravenously and most are excreted in urine (Layne et al. 2018). There are two general types of GBCAs, the first is linear in which the structure of the ligand includes an open chain linked to the gadolinium atom. The second is macrocyclic, where the gadolinium atom is enclosed within a cyclic ligand (FDA 2017a). Linear agents are less stable than macrocyclic agents and thus are more likely to release the gadolinium into the body (EMA 2017). Multiple studies have demonstrated higher levels of retained tissue gadolinium associated with linear compared to macrocyclic agents (McDonald et al. 2017; Murata et al. 2016).

Using T1 hyperintensity in the globus pallidus and dentate nucleus to quantify gadolinium can be unreliable because other metals (e.g., iron and copper) can accumulate in these tissues and contribute to T1 hyperintensity (Ginat and Meyers 2012). The method used to quantify gadolinium in most studies using human autopsy tissue is ICP-MS, which is a destructive process (Kanda et al. 2015; McDonald et al. 2015; Murata et al. 2016). These studies have found that compared to cases without exposure to GBCAs, brain specimens including globus pallidus and dentate nucleus with history of GBCA use have statistically significant increased concentrations of gadolinium. The highest levels of retained gadolinium in the brain are found in deep grey nuclei including the GP and DN although lesser amounts can also be found in other brain structures including WM. It should also be noted that control subjects without exposure to GBCA may still show trace levels of gadolinium but at much lower levels (usually one to two orders of magnitude lower) compared with exposed patients. This presumably represents accumulation from exogenous background contamination in water or other sources of gadolinium.

As patients continue to receive GBCAs for diagnostic imaging procedures, development of appropriate monitoring strategies is crucial to better understand the natural history and to assess possible toxic effects of the small amounts retained in human tissue. The recent revelation that gadolinium deposition occurs in various tissues and the limited research on relationships between gadolinium deposition and adverse outcomes underscore this need for effective, noninvasive monitoring. The analyses presented here were chosen to include tissues with presumed different gadolinium kinetics (i.e. deposition and washout/elimination).

Hair fibers are proteinaceous fibers with an outer cuticle, inner cortex, and sometimes a central medulla (Buffoli et al. 2014). Figure 1 (see Chapter 1) shows the general anatomy of the two primary hair components: the hair shaft (i.e., the fiber) and the hair follicle (i.e., the structure embedded within the skin). The cortex is the thickest layer of the hair shaft and is largely composed of keratin, which contains sulfhydryl groups of amino acids (Pozebon et al. 2017; Robbins 2012a). The sulfhydryl groups show high affinity for metals, which can facilitate their deposition into the hair shaft (Pozebon et al. 2017). However, the mechanism by which metals are incorporated into hair during fiber synthesis is still not well defined (Pozebon et al. 2017).

Concentrations of metals in hair are generally higher (by an order of magnitude or more) than concentrations in blood and urine (IAEA 1993; Pozebon et al. 2017). Hair samples are stable and thus, make storage and transport considerably simpler than other tissue samples. Additionally, the non-invasiveness of sample collection is very attractive (Pozebon et al. 2017).

Recently, techniques linking LA with ICP-MS analysis have been developed to produce highly spatially resolved data of trace metals in biological samples. When a hair is analyzed using LA, the result is that numerous data points are continuously compiling as the hair is ablated and material is sent to the ICP-MS. Depending on the optimized instrument parameters (e.g. laser pulse rate) and the length of the hair, each hair may have hundreds to thousands of discrete data points.

High resolution quantitative elemental distributions with LA-ICP-MS have been produced in brain tissues (Becker et al. 2010), *D. magna* (planktonic crustaceans) and *D. rerio* (zebrafish) embryos (Bohme et al. 2015), skin tissues (Berry 2015), and at our own University of Washington laboratory in mouse brain tissue (Engstrom et al. 2017) and nasal rosettes from Coho salmon (Williams et al. 2016). Application of this micro-destructive technique (Agilent Technologies 2004) has also been used to quantify metals content in hair. This includes animal and human research on single point and time-resolved temporal frames (Bartkus et al. 2011; Byrne et al. 2010; Dressler et al. 2010; Noel et al. 2015; Reiss 2016; Stadlbauer et al. 2005; Steely et al. 2007).

Previous studies have used ICP-MS to quantify gadolinium in hair for target subject populations including cancer patients (Cihan et al. 2011), patients receiving GBCAs (Saussereau et al. 2008), and residents living near rare earth mining areas (Wang et al. 2017). Measurement of gadolinium using LA-ICP-MS on the whiskers of mice exposed to GBCAs was recently reported (Lum et al. 2016). This study employed line scan analysis techniques that showed higher doses of GBCA resulted in higher gadolinium concentrations within the whiskers.

LA-ICP-MS has been established as a powerful and sensitive analytical technique for trace metals quantification and distribution at micrometer resolution. Unfortunately, this method is destructive, and is difficult to employ on live tissue. Using this technique on hair strands has allowed monitoring of toxic metals and drugs, and has the potential to monitor gadolinium in patients after administration of GBCAs. However, this technique has not been fully investigated for gadolinium, and no study to date has correlated gadolinium concentrations in hair with other tissues such as brain, bone, and skin.

The measure used for the hair concentration in this study is representative of a maximum signal from a single dose, whereas the brain, skin, and bone concentrations may reflect accumulation from multiple doses for some subjects. Although two of our cases were exposed to more than

one dose of GBCA, there was still a very good correlation between the hair concentration and other tissue concentrations, especially in brain WM and DN. However, this was not adequately tested with our small pilot study sample size. In addition, this study tested one method of hair concentration quantification using a single maximum signal measure. There are other methods such as analyzing low levels of steady-state hair gadolinium concentration that may be useful but were not tested in this initial study. Independent of the hair measure, other tissue concentrations will presumably be attenuated over time, differentially for each tissue, and based on the tissue-specific excretion kinetics for gadolinium and/or the gadolinium chelates. The effect this will have on the relationship between hair and other tissues remains to be determined.

Other papers (Boyken et al. 2018; McDonald et al. 2017; Young et al. 2018) have reported higher tissue gadolinium concentrations (either through T1-WI or ICP-MS) in humans and animals who received linear GBCAs, compared to macrocyclic GBCAs. However, the data derived from this study did not show a difference in linear regression between these two types of GBCA. Although the case study group included roughly two thirds macrocyclic agents and one third linear agents, they defined a single continuous regression line. This likely reflects the fact that, although the two different types of GBCA retain gadolinium at different rates, the mechanism of tissue retention or, at least of hair accumulation, is similar for both GBCA types. In a way, this supports the potential for hair analysis since it further suggests the ability to measure gadolinium retention independent of GBCA type or types (in the case of multiple exposures) the patient may have been exposed to.

Study Limitations:

There are many limitations to this initial pilot study. Gathering relevant autopsy cases is difficult and precludes typical recruitment methods. One is subject to the limitations of which cases come to autopsy and what their past history of GBCA exposure is. Thus a small sample size was analyzed. In addition, the GBCA agents studied were limited for similar reasons.

Despite this we were able to study a reasonable distribution of linear and macrocyclic agents that included two cases with multiple exposures. Although we employed our best efforts to thoroughly review each subject’s medical records this study was a retrospective one and, thus, there is the potential that some pertinent information was not available. Only one LA-ICP-MS hair analysis method was tested in this study and future work with alternative analysis types are being pursued.

Conclusions:

This research study shows good correlation between hair gadolinium concentrations and brain and skin gadolinium concentrations suggesting that hair may serve as a safe and effective

biomonitoring tissue for patients who receive GBCA injections. This was an initial pilot study with a small sample size from a non-ideal study population. Nevertheless, the results are promising and should prompt further research.

Chapter 4. Assessment of Cadmium Dosing in a Mouse Model using LA-ICP-MS Analytical Techniques on Hair Samples

4.1 Abstract

Objectives:

Laser ablation inductively coupled plasma mass spectrometry (LA-ICP-MS) was used to analyze the hair of mice that were dosed with cadmium in their drinking water. Primary objectives of this study were to assess inter- and intra-specimen variability, as well as correlate the cadmium dose to the cadmium present in the hair shafts analyzed.

Materials and Methods:

Mice received cadmium in their drinking water at one of three concentrations (0, 0.6, or 3 mg/L) for 14 weeks. Skin samples with hair were collected after the mice were euthanized and hair was analyzed from seven difference mice. Cadmium was quantified in the hair using LA-ICP-MS as a line scan along the hair shaft. The average of the maximum concentration and the average area under the curve were calculated in all hairs from a specimen. Hair measures were compared to the dose received.

Results:

Elevated cadmium concentrations were observed in the mice who received cadmium at 0.6 and 3 mg/L concentrations. Variability within and between specimens may be attributable to differential hair growth cycle timing for individual follicles and spatial patterning within the mouse model. Metallothionein-related detoxification mechanisms may influence the deposition of cadmium into hair shafts.

Conclusions:

LA-ICP-MS sensitivity was sufficient to quantify cadmium in the hairs of mice dosed with cadmium at lower concentrations, and higher cadmium concentrations in hairs were associated with higher doses of cadmium.

4.2 Introduction

Humans are exposed to metal contaminants through numerous personal and work-related scenarios. Metals are found in the earth's crust and people can be exposed to them through air (suspended particles and vapors), water, and soil that is inhaled or ingested (ATSDR 2012a). Commercial products may utilize certain metals such as: arsenic in pesticides and treated wood (ATSDR 2007); cadmium in batteries or pigments (ATSDR 2012a); gadolinium in magnetic resonance imaging (MRI) dyes (EMA 2017); manganese in steel materials and fireworks (ATSDR12C); and zinc in dietary supplements and anti-dandruff shampoos (ATSDR 2005). The workers involved in manufacturing those products may be at elevated risk of exposure and the people who use the products are also at risk of exposure.

Since the Occupational Safety and Health Administration (OSHA) was established in 1971, the United States (US) has continued to strengthen worker safety requirements (OSHA 2010). OSHA issued updated guidance in 2016 to further support reduction of worker exposures to metals in smelting and refinery settings where workers continue to face serious risks (OSHA 2016). An important part of the framework for protecting human health from the consequences of exposure to contaminants is biomonitoring.

Biomonitoring utilizes biomarkers (i.e., compounds or their metabolites) present in the body (Goyer et al. 2004; NRC 2006). There are three primary groups of biomarkers:

1. Biomarkers of Exposure—Compound, metabolite, or product of an interaction measured within a bodily compartment.
2. Biomarkers of Effect—Biochemical, physiological, behavioral, or other recognizable alteration associated with an adverse effect or disease.
3. Biomarkers of Susceptibility—Indicator for the ability of an organism to respond – in either a beneficial or adverse way - to a compound (NRC 2006).

The National Research Council (NRC) states, "the ultimate objective of biomonitoring is to link information on exposures, susceptibility, and effects to understand the public health implications of exposure to environmental chemicals" (NRC 2006). The NRC also notes that biomonitoring has several applications, but of primary interest for this study we will consider biomonitoring for exposure assessment purposes (NRC 2006).

Biomarkers are measured in a variety of bodily tissues including blood, bone, feces, hair, liver, nails, plasma, skin, sweat, and urine. One major limitation in biomonitoring is that the concentration in the tissue is often measured without knowing when an exposure occurred (NRC 2006). Research conducted at the University of Washington, and other institutions, is attempting to fill in that gap. For example, a study on manganese exposures in welders sought to elucidate the time course of manganese exposure and uptake in blood (Baker et al. 2016). These

researchers found that blood manganese may be a useful biomarker for longer term manganese exposures.

While hair is an appealing medium for biomonitoring, due to the low risk to study subjects during sampling and ease of transport and storage, there are concerns over exogenous contamination and limited information on the mechanisms influencing deposition within the hair shaft. Kempson et al. (2007) noted that trace element concentrations in hair are dependent upon blood concentrations, but other bodily processes and disturbances can affect these concentrations. Though the outer layer of the hair shaft (the cuticle) may generally deter incorporation of exogenous material, some metals can make their way from the surface into the hair matrix (Kempson et al. 2007).

Mouse hair, unlike human hair, is primarily in a state of non-growth (i.e., telogen phase) as evidenced by the uniform hair length accomplished without continual trimming (Geyfman et al. 2015). Additionally, in the mouse, hair follicle cycling is patterned so that hair in spatially nearby areas enters into the same phase. Shedding (i.e., the exogen phase) begins near the top of the head and moves out and down towards the stomach and tail (Alonso and Fuchs 2006). One publication estimated the hair growth rate for mice at 0.25 cm/16 days (Tzung et al. 2009).

Early on in the mouse life, hair cycles are short and as the mouse ages the cycles become longer. When mice are born, their follicles are in an anagen phase, which lasts for only about two weeks (Plikus and Chuong 2008). The first post-natal catagen phase lasts three to four days, and a short one- or two-day first post-natal telogen phase occurs (Alonso and Fuchs 2006; Plikus and Chuong 2008; Plikus et al. 2008). At this point, the mouse is about three weeks old and hair follicles begin the second cycle. Second anagen lasts for about two weeks, second catagen is another three to four days, and second telogen lasts for three weeks (Plikus et al. 2008). Based on the growth rate reported by Tzung et al. (2009) and the approximate length of a guard hair (1 cm) the anagen phase may last around 64 days (after the second cycle). One study found that telogen phases (after the second cycle) could last up to 88 days (Plikus et al. 2008).

Mice have four different body hair types: guard, awl, zigzag, and auchene (Duverger and Morasso 2009). The guard hairs comprise 1–3% of the hairs on the body, are approximately 1 cm in length, and fairly straight in orientation. Awl hairs are also relatively straight but shorter in length (0.33–0.67 cm) and are 30% of the body hairs. Zigzag hairs exhibit three to four bends (in a zigzag-type configuration) and are a similar length to the awl hairs but are 65–70% of body hairs. Finally, auchene hairs have a single bend about a third of way down the length of the hair and are a small proportion of the hairs at 0.1% (Duverger and Morasso 2009).

Using a mouse model from a controlled laboratory cadmium dosing trial, this study sought to delineate spatially resolved concentrations of cadmium in hair using laser ablation inductively

coupled plasma mass spectrometry (LA-ICP-MS). The primary purpose of the research was to determine whether mice dosed with cadmium at different levels showed hair peak concentrations that were proportional to the dose received. Secondarily, large number of hairs analyzed from two of the mice facilitated review of intra-specimen variability.

4.3 Methods

Specimens:

Hair samples were obtained from a mechanistic toxicology study conducted at the University of Washington in which mice were treated with cadmium via their drinking water. The mice were raised for 8 weeks prior to dosing, dosed for 14 weeks (weeks 9 through 22), and sacrificed at week 22. The study included three dosing levels: 0 mg/L (control), 0.6 mg/L, and 3 mg/L. The mice study population included females and males from two genotypes: APOE3 (14 females and 15 males) and APOE4 (15 females and 15 males). After the mice were sacrificed, a section of the skin with hair attached was cut and transferred to one plastic tube per specimen for storage at approximately -28 °C.

For this pilot study, three specimens at the high and medium dose levels (3 and 0.6 mg/L respectively) and one specimen at the zero dose level were randomly selected for analysis. Specimens from one genotype (APOE4) and one gender (male) were included in this study. Twenty-five hairs from one specimen in the high and medium dose levels were analyzed, and ten hairs were analyzed from the other four specimens in the high and medium dose levels. Five hairs were analyzed from the zero dose level specimen. Guard hairs from the most posterior-dorsal section of the skin samples were targeted to maximize the likelihood that the area from which we collected our samples had not undergone the exogen phase. By choosing hairs that were in place when dosing began that have not shed we are more likely to observe the exposure peak within the hair. Based on the above details regarding hair phase cycling, an estimated timing for growth, dosing, and exogen are presented in Figure 12. Under this timeline, the dosing is estimated to have occurred toward the end of the second cycle, and cadmium deposition would be expected in the hair shaft from the third cycle.

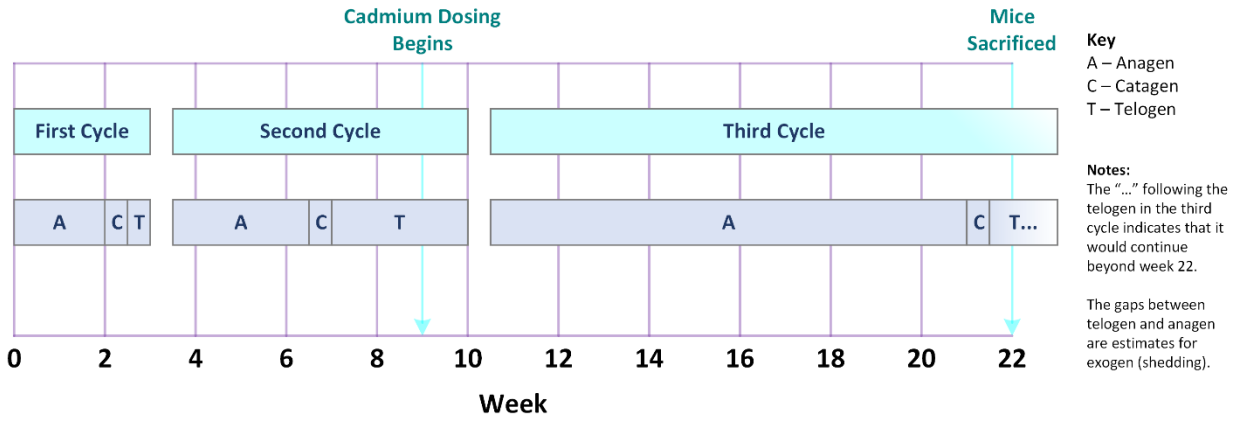

Figure 12. Estimated timing for hair phase cycle one through three

Sample Analysis:

Sample mounting and analysis methods are briefly summarized here, but for a more comprehensive description see Section 2.3, Section 3.3, and Appendix A. Samples were plucked similarly to the human cadaver samples (non-metallic tweezers), but did not undergo the acetone washing because background/environmental sources of cadmium were expected to be negligible. Samples were mounted onto glass slides with double stick tape and analyzed using a line scan technique with LA-ICP-MS. Instrument parameters are provided in Table 8. Calibration gels to facilitate calculation of cadmium concentrations and SRM (NIST 612) were included in batch analyses for instrument QC.

Table 8. Laser and ICP-MS parameters for mice hair and SRM

Instrument and Parameter (Units)	Value
Laser: Elemental Scientific, Inc. (ESI) New Wave Research (NWR) 213 (Nd:YAG [neodymium: yttrium aluminum garnet])	
Wavelength (nm)	213
Helium flow (L/min)	0.8
Argon makeup flow (L/min)	1.07
Isotopes	^{34}S, ^{111}Cd
Spot size (µm)	10
Firing rate (Hz)	20
Scan speed (µm/sec)	100
Energy (%)	60
ICP-MS: Agilent 7900	
Sampling period (sec)	0.515
Radiofrequency (watts)	1,550
Mode	Helium
Collision cell gas	Not used

Data Processing and Analysis:

Raw results (cps) for *m/z*111 (cadmium) intensities were smoothed with a rolling mean centered on five values. Mass-based concentrations were calculated using a calibration curve generated from the calibration gels with the range of 0–10 or 0–25 µg/g, depending on the magnitude of the scan results. Distance along the hair shaft (in millimeters[mm]) was calculated using the laser scan speed (100 µm/sec) and the acquisition time of each data point. Results for each hair were reviewed to determine whether a ^{111}Cd peak was observed and the maximum value within the peak was assigned as the measure for a hair with a peak. The area under the curve within the peak window was also calculated using Simpson's rule to integrate the curve (Stanford No Date). Hairs that did not have a peak were assigned an average value of the line scan. For each specimen, the following measures were averaged: peak concentrations, area under the curve values, and average of non-peak line scans. Concentrations below the LA-ICP-MS method detection limit (0.05 µg/g) were set to 0.05 µg/g.

4.4 Results

Ninety-four hairs from seven APOE4 male mouse specimens were analyzed using LA-ICP-MS on July 18 and 19, 2019. Although the mice were continually dosed for 14 weeks until they were sacrificed, the shape of the line scan did not show an elevated concentration that stabilized. For lines with full ^{111}Cd peaks, the line scan increases (nearer the distal/tip end) and then decreases back towards zero (nearer the proximal/root end). Some hairs showed partial peaks, meaning the decrease is present at the distal end near the tip, but the initial increase is not captured in the hair shaft. Other hairs showed no evidence of a peak, but did show consistently elevated levels of ^{111}Cd relative to hairs from the control group of animals. Examples of a hair with no peak, a partial peak, and a full peak are shown in Figure 13. Hairs with partial peaks were included in the analysis of hairs with peaks.

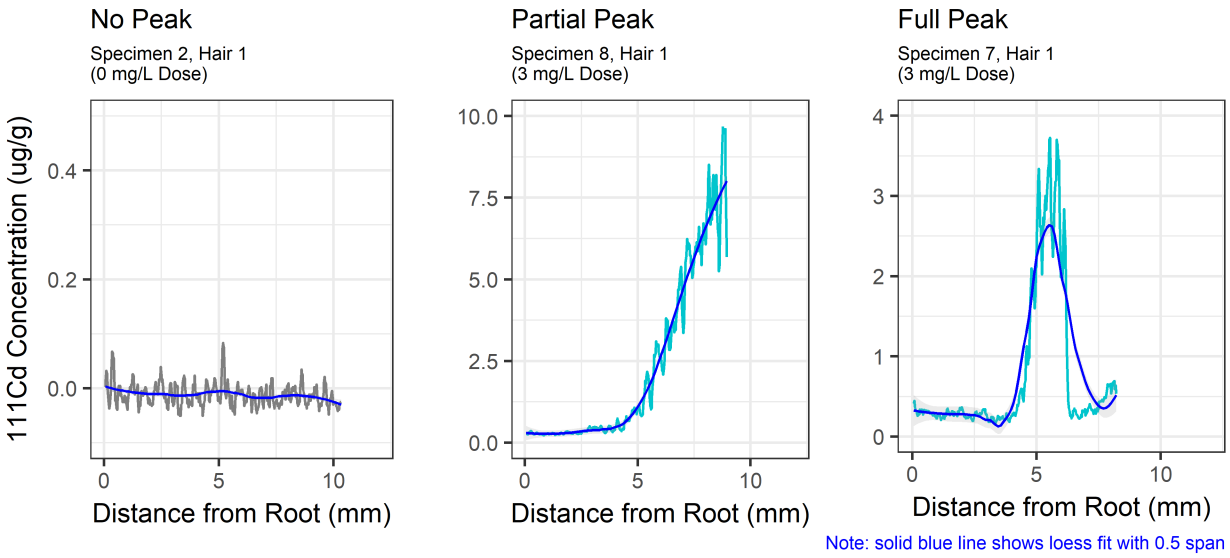

Figure 13. Example plots for different cadmium peak status

The zero-level specimen hairs did not show any cadmium peaks, and average values for these hair line scans were below the detection limit of 0.05 µg/g. There were 7/44 (16%) hairs in the medium dose level (0.6 mg/L) and 17/45 (38%) hairs in the high dose level (3 mg/L) that exhibited ^{111}Cd partial peaks. Twenty-four hairs exhibited full peaks, 17/44 (39%) in the medium dose level and 7/45 (16% in the high dose level). Specimen 6 in the medium dose level did not have any hairs with ^{111}Cd peaks (see Section 4.5 for discussion of specimen 6). Table 9 summarizes hairs from all specimens.

Table 9. Summary of cadmium concentrations

Specimen	Dose (mg/L)	Hairs without ^{111}Cd Peaks (N)	Hairs without ^{111}Cd Peaks Line Scan (µg/g) avg ± SD (range)	Hairs with ^{111}Cd Partial Peaks (N)	Hairs with ^{111}Cd Partial Peaks Peak Maxima (µg/g) avg ± SD (range)	Hairs with ^{111}Cd Peaks (N)	Hairs with ^{111}Cd Peaks Peak Maxima (µg/g) avg ± SD (range)
2	0	5	All hairs <0.05	0	NA	0	NA
4	0.6	5	All hairs <0.05	6	2.7 ± 1.7 (0.3–5.2)	13	1.5 ± 0.86 (0.37–3.2)
5		5	All hairs <0.05	1	0.32	4	0.64 ± 0.3 (0.32–1)
6		10	All hairs <0.05	0	NA	0	NA
7	3	8	0.16 ± 0.049 (0.095–0.24)	0	NA	2	2.5 ± 1.7 (1.3–3.7)
8		11	0.22 ± 0.11 (0.048–0.43)	10	7.4 ± 3 (1.3–11)	4	8.6 ± 5.1 (2.1–14)
9		2	1.2 ± 0.21 (1–1.3)	7	11 ± 3.7 (5.9–16)	1	19

For hairs without peaks, the zero and medium dose level specimen hairs had average concentrations below the detection limit (< 0.05 µg/g). Hairs without peaks from specimens dosed at the high level showed higher average concentrations within the hair shaft, ranging from just below the detection limit (0.048 µg/g) to 1.3 µg/g. Data for hairs without peaks is summarized in Table 9 and shown in Figure 14. Among hairs without peaks, the high dose level had the greatest spread in average hair concentrations for a single specimen (specimen 9).

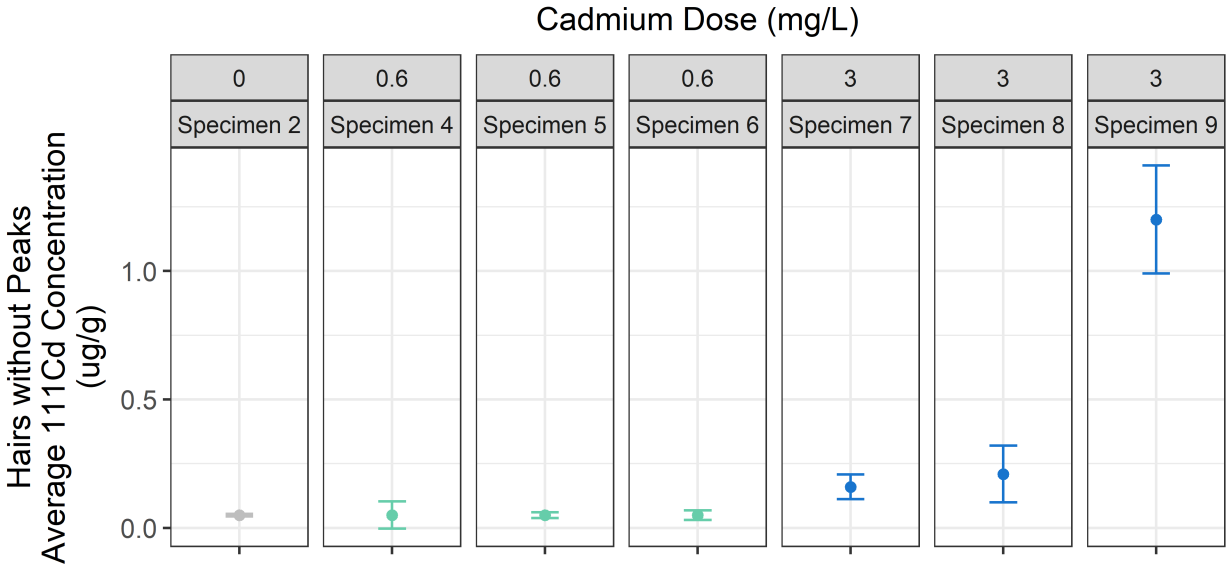

Figure 14. Average ^{111}Cd concentrations in hairs without peaks

Among hairs with partial ^{111}Cd peaks, the peak maxima concentrations for the medium and high dose levels ranged from 0.3 to 5.2 µg/g and 1.3 to 16 µg/g, respectively. Specimen CV values between hairs with partial peaks ranged from 0.34 to 0.63. The hairs with full peaks had average peak maxima concentrations of 0.32 to 3.2 µg/g and 1.3 to 19 µg/g for the medium and high dose levels respectively. CV values for full peak hairs from specimens were 0.47–0.68, generally in the same range as those with partial peaks. Figure 15 shows the distribution of ^{111}Cd peak concentrations for each specimen.

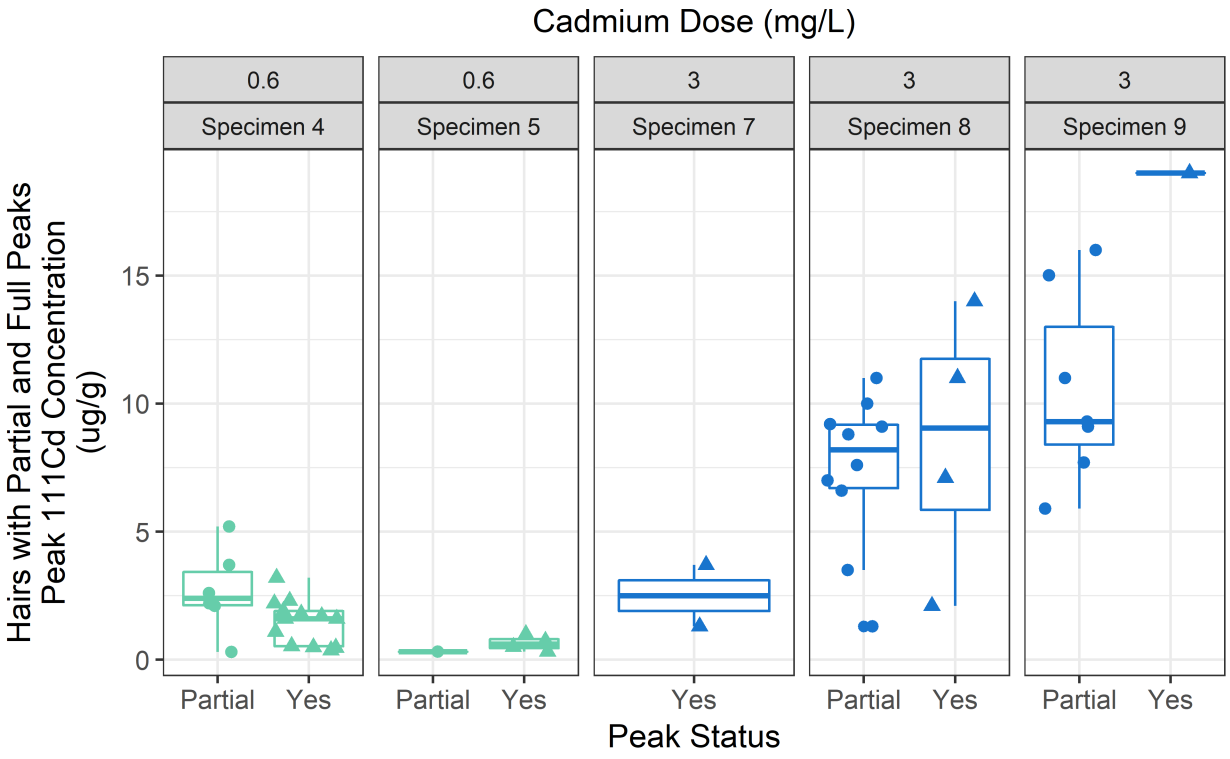

Figure 15. Partial and full peak ^{111}Cd concentrations for each specimen

Area under the curve for peak windows was calculated and results are presented in Table 10. The high dose level had higher area under the curve averages compared to the medium dose level. Using the area under the curve as the measure for the hair (for full and partial peaks) resulted in similar appearing distributions for most specimens (see Figure 16). Specimen 9 showed greater spread in AUC values compared to peak ^{111}Cd maximum concentrations for partial peaks. Whereas specimen 8 had less spread for AUC values compared to peak ^{111}Cd maximum concentrations for full peaks.

Table 10. Summary of area under the curve measures for partial and full peaks

Specimen	Dose (mg/L)	Hairs with ^{111}Cd Partial Peaks		Hairs with ^{111}Cd Peaks	
		(N)	Area Under Curve (µg/g*mm) avg ± SD (range)	(N)	Area Under Curve (µg/g*mm) avg ± SD (range)
2	0	0	NA	0	NA
4	0.6	6	47 ± 32 (4.6–93)	13	26 ± 16 (5.7–62)
5		1	2.6	4	5.1 ± 1.6 (3.2–7)
6		0	NA	0	NA
7	3	0	NA	2	29 ± 22 (14–44)
8		10	140 ± 67 (10–240)	4	160 ± 88 (39–240)
9		7	220 ± 110 (93–420)	1	260

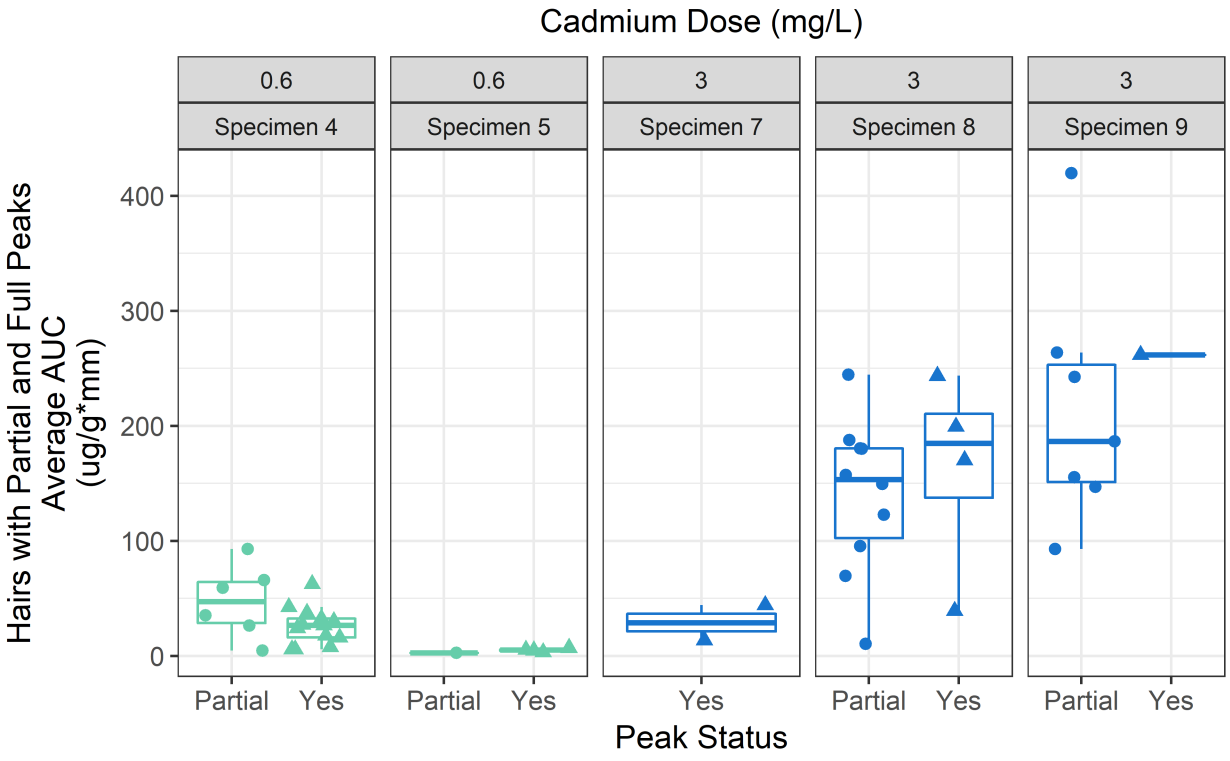

Figure 16. Partial and full peak area under the curve for each specimen

Average peak ^{111}Cd maxima for each specimen that received a cadmium dose > 0 mg/L and average concentrations of the zero-dose level were plotted against the cadmium dose in Figure 17. Although the sample size is small (N=6; no peaks for specimen 6), the dose-response appears to have a positive slope, with higher doses exhibiting higher ^{111}Cd concentrations.

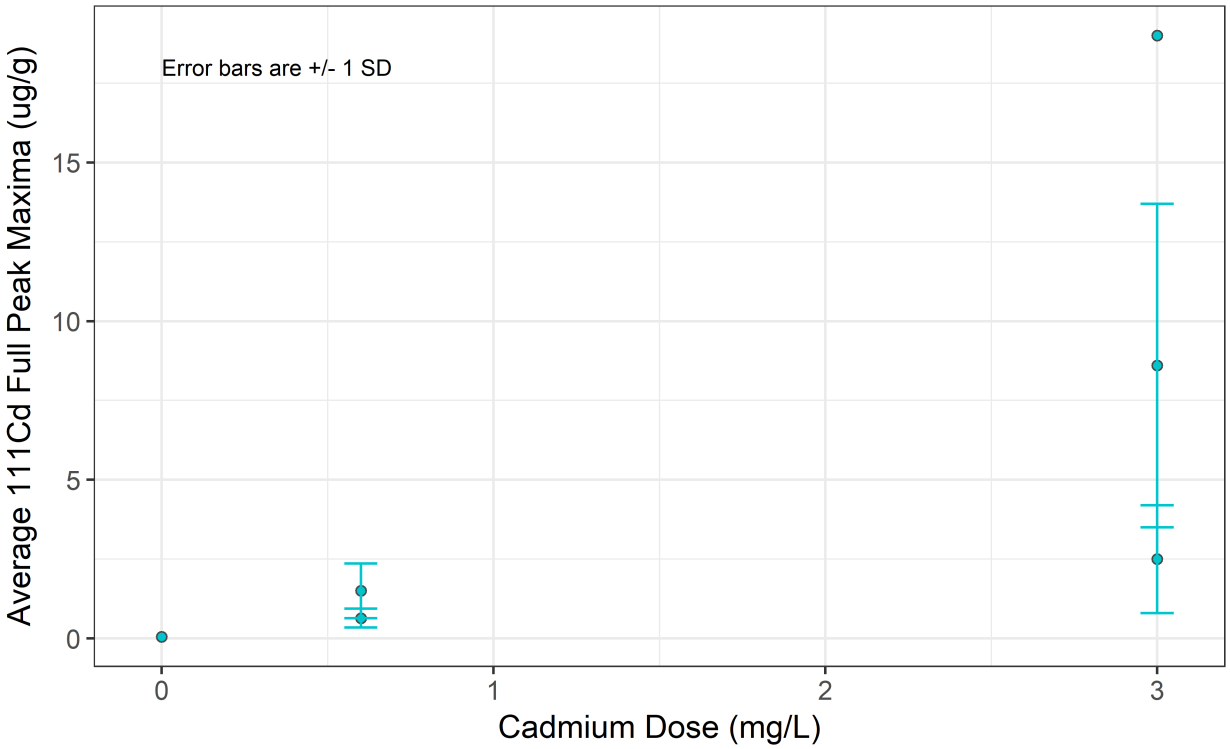

Figure 17. Cadmium dose and average ^{111}Cd peak maxima concentration

Overall, specimens from the high dose level had the highest peak ^{111}Cd concentrations and area under the curve values among hairs with or without ^{111Cd} peaks.

4.5 Conclusions/Discussion

Despite continual cadmium dosing between weeks 9 and 22, mice hair concentrations did not equilibrate at an elevated level, but rather exhibited an increase and subsequent decrease back to baseline. This depositional behavior suggests there is a removal mechanism that decreases cadmium concentrations in compartments contributing to hair concentrations. Metallothionein is a small protein that is induced in the presence of heavy metals (e.g., cadmium), hormones, other proteins, and a variety of metabolites (Glaven et al. 1991; Klaassen et al. 2009; Vallee 1991). Metallothionein binds cadmium after it is absorbed (usually in the gastrointestinal tract) into the body (Klaassen et al. 2009). Induction of this protein continues until 90% or more of the cadmium is bound (Brady 1991). The retention time of cadmium in various tissues is dependent

upon the presence of metallothionein, and cadmium primarily accumulates in the liver and kidneys (Klaassen et al. 2009). The cadmium-protein complex is generated largely in the liver, but is transported through the blood and to the kidneys (Klaassen et al. 2009). However, the distribution of cadmium to various tissues is not controlled by the presence of metallothionein (Klaassen et al. 2009). Metallothionein helps to protect the body against acute or chronic exposure to cadmium (and other heavy metals) by sequestering the free ions (Klaassen et al. 2009; Vallee 1991). Upregulation of this protein likely accounts for the shape of the line scan with concentrations increasing after dosing begins, and then decreasing again from the tip to the root.

An earlier study by Kollmer (1982) assessed cadmium concentrations in the hairs of rats dosed with cadmium in drinking water. Concentrations ranged from 3 to 600 mg/L and the rats were exposed for 198 days (a little over 28 weeks). These researchers induced anagen phase by plucking hairs so that hair shaft growth periods captured exposures of interest. This study found that the internal deposition of cadmium was proportional to the amount ingested through drinking water. Similar to our study, Kollmer (1982) also found that the amount of cadmium deposited into the hair shaft was proportional to the amount of cadmium absorbed. Consistent with the results observed in this study's line scans, Kollmer (1982) found that after prolonged exposure to the cadmium-dosed water, hair concentrations decreased to background levels after a few days.

Specimen 6 in the medium dose level did not show "peaks" but the shape of the scans were indicative that there was an increase in the concentration towards the tip of the hair. The overall shape of the line scan was visualized using a loess regression with a span of 0.5 and Figure 18 shows plots for all 10 hairs from specimen 6. Two possible explanations for this trend were identified. The first is that although we did not expect any background sources of cadmium, mice use saliva to clean their fur and cadmium may have been deposited onto the surface of the hair shaft near its distal end from this exogenous source. The second possibility is that dosing began before these hairs had begun their growth phase (i.e., anagen phase), and at the onset of the growth of these hairs cadmium removal efficiency via metallothionein was nearing maximization. As noted previously, hair growth in mice is spatially patterned, so it is likely that hairs collected in close proximity to each other, as was done in this study, would share similar growth characteristics.

Due to the presence of the partial peaks, the maximum signal or area under the curve of a partial peak may underrepresent the true ^{111}Cd peak maximum or area. This is because higher concentrations may have been present in the hair shaft that was shed during exogen, or the compartment from which the cadmium deposited (e.g., blood, intracellular fluid, etc.) into the hair had higher concentrations during the shedding phase and this timeframe was not captured in any hair shaft during the follicular transition back to anagen.

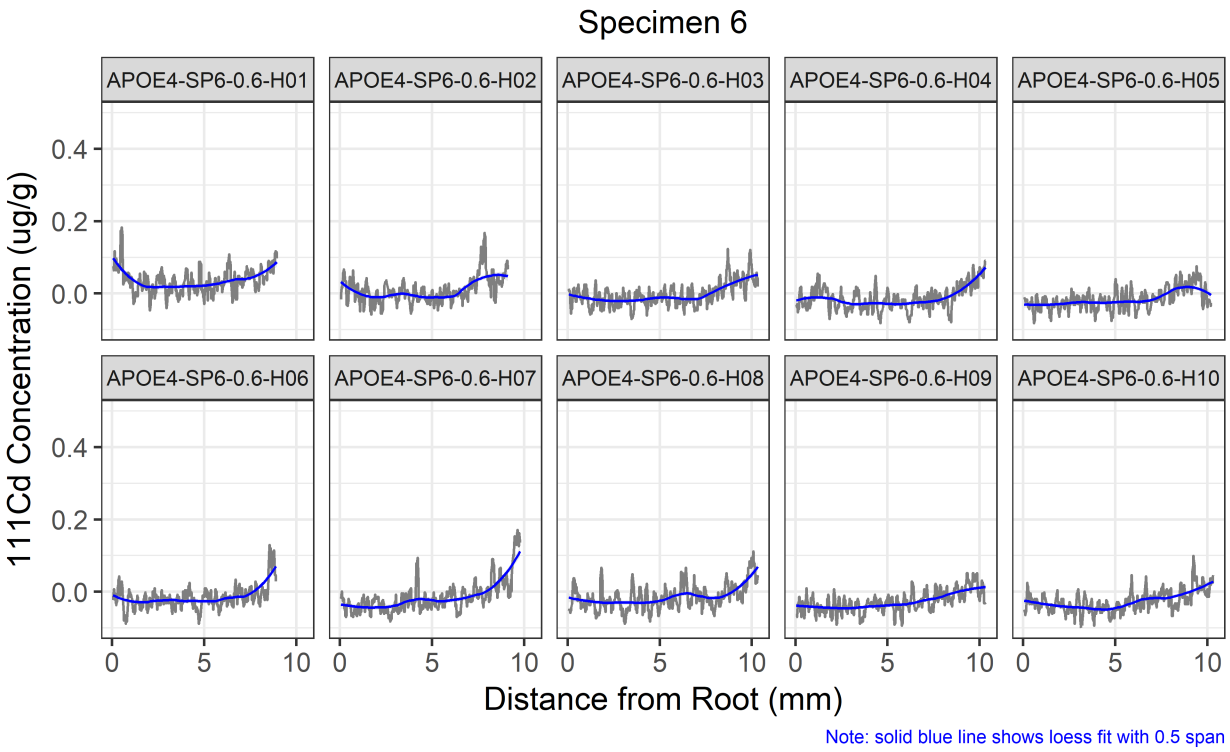

Figure 18. Specimen 6 line scans

Intra-specimen variability in the magnitude of peak ^{111}Cd concentrations and area under the curve may be due to numerous influences on hair shaft formation including localized cell signaling (Robbins 2012a; Tobin 2012). Although, these differences may also be due to the partial peaks mentioned above. Hairs were not collected from neighboring follicles on the skin, and spatial variability between samples is likely to contribute to variability in the timing of anagen phase initiation. This is particularly relevant in the mouse model given the spatial patterning of the hair cycle.

The spatial and temporal patterns of mouse hair growth likely contribute to inter-specimen variability. Variability between mice that received the same dose may also be due to the partial peak effect. Using LA-ICP-MS analysis of hair in natural hair cycling presents challenges in achieving coordinated cadmium deposition among multiple specimens during anagen phase. This source of variability may be minimized by inducing the anagen phase (by plucking dorsal hairs) right before, or at the outset of dosing. Another contributor to inter-specimen variability could be differential water drinking habits between mice. The toxicological study that dosed the mice did not directly control the ingested mass of cadmium. A mouse that consumed more of the cadmium-dosed water would be expected to show higher hair cadmium concentrations.

Study Limitations:

Issues with the timing of sampling considering hair phase cycling were observed in this study (i.e., partial and missing peaks). This could be resolved by sampling from live specimens at several time periods after dosing is initiated or inducing anagen phase to coordinate with dosing. Also, speculation on the metallothionein activity can be confirmed by sampling blood or hepatic tissues simultaneously. A 2016 study showed that repeated sampling of live rat and mice specimens to obtain hepatic biopsies was feasible using a laparoscopic technique (Garofalo et al. 2016). The small number of specimens included in this pilot study prevented quantitative comparison between dosing levels, such as regression or ANOVA. Hair samples from only one genotype and one gender were analyzed and do not capture variability that may exist between genotypes and gender.

Conclusions:

LA-ICP-MS methods were sensitive enough to effectively quantify cadmium in the hairs of mice dosed with cadmium at concentrations in the low mg/L range. This research showed that there were increasing concentrations of ^{111}Cd in hair shafts with increasing doses of cadmium in drinking water among mice. The specimens included in this study were small in number, but the results suggest that there is a relationship between hair cadmium concentrations and cadmium dose. Limitations including the brief anagen phase of mouse hair (compared to human hair) relative to the multi-month cadmium dosing period, and spatial patterning of mouse hair growth likely contributed to variability in these results. Further research can elucidate more specific relationships between cadmium in hair and the role that metallothionein may play in detoxification.

Appendices

Appendix A—LA-ICP-MS Standard Operating Procedure

The following describes the standard operating procedure (SOP) for analysis of hair with LA-ICP-MS.

Materials

1. Petrographic slides: Beta Diamond Products, Inc.
    a. 27 mm x 46 mm plain: Cat No. PS2746
    b. 2 in x 3 in plain: Cat No. PS2X3
2. Gold Seal Micro Slides: Cat. No. 3010
3. NIST glass 612
4. Gelatin, from bovine skin: Sigma G9391-100g; Lot 041M0052V
5. ICP-MS element standards in solution
    a. Fe (56, 57)
    b. Mn (55)
    c. Zn (66)
    d. Cd (115)
    e. Cr (52)
    f. Ag (107)
    g. Au(197)
    h. Pb (208)
    i. Gd (157)
    j. Tb (159)
    k. As (75) (polyatomics common)
    l. Se (78) (high in gas blank)
6. Tape for hair mounting
    a. Single-sided
        i. Scotch tape
        ii. Packing tape: Home Depot
    b. Double-sided
7. Tweezers: Ted Pella carbon fiber, carbon reinforced polyvinylidene fluoride (PVDF)
8. Ceramic scissors: Kyocera Cat No. CS-124
9. Light with magnifier
10. Acetone, HPLC grade
11. Microfuge tube(s): 1.7 mL, VWR Cat. No. 97003-294
12. Plastic pipette(s): 1.5 mL, VWR Cat. No. 16001-172

13. Polypropylene centrifuge tube(s): 50 mL, Corning CentriStar 430829
14. Plastic weigh boats: Fisher Scientific Cat No. 02-202-101
15. Kim Wipes
16. Sonicator
17. Incubator
18. Helium: Praxair, Ultra High Purity 5.0, T size
19. Argon

Personal Protective Equipment (PPE)

Use the following PPE during spike solution preparation, calibration gel preparation, sample preparation/washing, and sampling mounting:

- Gloves
- Goggles
- Lab coat

Standards

14-element standards in gelatin for LA-ICP-MS (see Table 11).

Table 11. Element standard stock solutions

Element	Concentration (mg/L or ppm)	Note
Ag	1000	Certified standard purchased by Simpson Lab
As	1000	Certified standard purchased by EHL
Au	1000	Certified standard purchased by Simpson Lab
Ca	1000	Certified standard purchased by Simpson Lab
Cd	1000	Certified standard purchased by EHL
Cr	1000	Certified standard purchased by EHL
Fe	1000	Certified standard purchased by EHL
Gd	1000	Certified standard purchased by Simpson Lab
Mn	1000	Certified standard purchased by Simpson Lab
P	1000	Certified standard purchased by Simpson Lab
Pb	1000	Certified standard purchased by EHL
Se	1000	Certified standard purchased by EHL
Tb	1000	Certified standard purchased by EHL. Expired, but OK for use as internal standard
Zn	1000	Certified standard purchased by EHL

Solutions

1. Spike solutions

   High (200 or 400 ppm) spike solution: Combine 200 uL of 1000 ppm stock for Ca, Fe, and Zn and 400 uL of 1000 ppm stock for P (1 mL total). Don't add Tb ISTD.

   76.92 ppm spike solution: Combine 200 uL of 1000 ppm stock for all elements (2.6 mL total). Don't add Tb ISTD.

   7.69 ppm spike solution: Dilute 76.92 spike 1:10 in water (50 uL 76.92 ppm spike solution + 450 uL water). Don't add Tb ISTD.

   0.769 ppm spike solution: Diluting 7.69 spike 1:10 in water (50 uL 7.69 ppm spike solution + 450 uL water). Don't add Tb ISTD.

2. Tb internal standard

   Dilute 1000 ppm stock 1:10 in water (150 uL 1000 ppm Tb stock + 1350 uL) and spike 100 uL into each gelatin sample (n=13) = 50 ppm

Gelatin Calibration Standards

The gel concentrations selected for the calibration curve are summarized in Table 12, along with the relevant spike solution and volume needed. Further instructions on preparing the gelatins is presented below the table. Spike solution volumes were calculated using the relationship in the following formula:

$$V_{spike\ solution}\ (uL) = \frac{C_{gelatin\ calibrant}\ \left(\frac{ug}{g}\right) \times M_{gelatin}\ (g)}{C_{spike\ solution}\ \left(\frac{ng}{uL}\right) \times \frac{ug}{1000\ ng}}$$

Where: $M_{gelatin} = 200\ mg\ or\ 0.2\ g$

Table 12. Calibrant concentrations and spike solutions

Gel Concentration (µg/g or ppm)	Spike Solution (ng/uL or ppm)	Spike Solution Volume (uL)	Note
1000 or 2000	High (200 or 400)	1000	1000 ppm for Ca, Fe, and Zn; 2000 ppm for P
500	76.92	1300	
250	76.92	650	
100	76.92	260	
50	76.92	130	
25	76.92	65	
10	76.92	26	
5	76.92	13	
1	7.69	26	
0.5	7.69	13	
0.1	0.769	26	
0.05	0.769	13	
0	NA	0	

Preparation

1. Label empty small plastic weigh boats (N=13) with standard concentration and date.
   a. Weigh and record empty weights.
2. Using a new plastic spatula, weigh 200 mg gelatin into weigh boats (N=13).
3. Add water to three 50 mL plastic centrifuge tubes and place caps on loosely.
4. Place tubes in a beaker of water and heat water to boiling on hot plate.
5. Add 6 mL hot water to plastic weigh boats, one at a time, starting with standard 0.
   a. Use 5 mL plastic pipet (add 3 mL two times).
6. Spike with 0 to 1000 uL of the appropriate spike solution as indicated in Table 12.
7. Add 100 uL of Tb internal standard
8. Mix with 1 mL pipet (plastic tip) to distribute standards and dissolve gelatin.
9. Put on shaker table for additional mixing.
10. For STD 1000/2000, 500 and 250, mix hot water and gelatin before and after spiking to avoid cooling the hot water too quickly
11. Dry in incubator two days at 37 °C with door ajar (use magnet to prop open door).

Slide Mounting

1. Place double sided tape on slide in two rows.
   a. Tape torn edge is parallel with short edge of slide.
   b. Tape to lined or grid paper with overhanging tape (prevents slide from shifting).
2. Place clear packing tape sticky side up on double stick tape
   a. Stickier than double stick tape so gels are less likely to shift or detach

3. Cut small squares (0.25 x 0.25 in.) from each dried gelatin calibration standard using ceramic scissors
    a. Use tweezers to manipulate to prevent breakage from using hands
    b. Work from low to high concentrations
4. Wipe tools with dry Kim Wipe between standards
5. Place cut square onto double stick tape and press gently into place
    a. Orient squares with “up side up” meaning keep the side facing the air up, and the side touching the weigh boat down
    b. The two sides have different textures
6. Label slide with Calibrant concentration for each square, “Gel calibrants” at the top, and the date mounted anywhere it fits
7. Place slide in closed container for storage and transportation.

QC Materials

Analysis of standard reference material (SRM) National Institute of Standards and Technology (NIST) trace elements in glass (NIST 612) is incorporated during sample analysis.

Hair Samples

Storage

Human gadolinium (Gd) study subjects—scalp and hair samples are stored in individual ziplock bags within a larger ziplock bag in the Simpson Lab Freezer FZ-S1. The freezer has a temperature of approximately -16 °C and is located on level -1 of the Health Sciences Building in the F-Wing, outside F-047.

Mouse cadmium (Cd) specimens—hide and hair samples are stored in separate closed plastic test tubes inside the Simpson Lab Freezer FZ-S4. The freezer has a temperature of approximately -25 °C and is located on level -1 of the Health Sciences Building in the F-Wing, outside F-047.

Inventory Incoming Samples

Human Hair—Upon receipt of human Gd samples, information on the subject is entered into the subject inventory spreadsheet (HairDatasheet from Makoto 012919 ver2.xlsx).

Preparation

Washing in acetone is only performed for human hair to remove potential exogenous contamination. This step was determined as unnecessary for the mouse specimens since

exposure to other anthropogenic sources of metals contamination from cadmium was not expected.

1. Remove sample from ziplock bag using tweezers and place on clean Kim Wipe in hood
2. Remove hairs from scalp using tweezers and place into a microfuge tube (1.5 mL)
    a. Effort to include the root will facilitate identification of the proximal/distal ends after mounting
3. Fill microfuge tube with acetone and close lid (ensure it is closed tightly)
4. Label microfuge tube with subject number
5. Sonicate microfuge tube for 30 minutes (do not heat the water, room temperature is OK)
6. Fold a Kim Wipe to make a small pocket and place on slanted polyethylene surface and place in the hood
7. Pour contents of the microfuge tube (acetone and hair) into the Kim Wipe pocket
    a. Pocket will trap the hair
    b. Slanted polyethylene surface will allow acetone to flow away from the hair
8. Place Kim Wipe pocket and polyethylene surface in incubator to dry at 37 °C for one hour.

Slide Mounting

1. Label slide (27 mm x 46 mm or 2 in x 3 in) with “Gd Hair” and the date samples were mounted
2. Place one strip of double sided tape on slide.
    a. Tape torn edge is parallel with short edge of slide.
    b. Tape to lined or grid paper with overhanging tape (prevents slide from shifting).
3. Place one strip of single sided Scotch tape sticky side up directly on top of the double sided tape
4. Grasp single hair strand with tweezers and place onto tape
    a. If possible, align root side on the left
    b. Make hair lay as straight as possible to minimize pivot points on laser path
5. Press down lightly with glove-covered finger to ensure hair is securely positioned on tape
6. Place a blue dot on the slide long edge near one of the hairs (positional marker for laser path tracing)
7. Take a picture of the slide and denote sample numbering within the picture
8. Hand draw copy of slide layout to assign sample numbers to each hair
9. Place slide in 50 mL centrifuge tube and close cap

a. Squeeze sides of tube to make slightly oblong, slides are just wider than the tube and need a little extra space to get them inside.

10. Label tube with subject number and place in metal rack for storage and transportation.

Track Sample Analysis

Human Hair—Once a sample is prepared for analysis, add information on the sample ID, elements for analysis, and instrument parameters to the sample tracking spreadsheet (LaserSampleTracking.csv). After samples are analyzed and data exported (see subsequent sections) enter the file path of the exported *.csv file and date of analysis into the sample tracking spreadsheet.

Also input the date of analysis of the first hair analyzed from a subject and the number of hairs currently analyzed for a subject into the subject inventory spreadsheet (HairDatasheet from Makoto 012919 ver2.xlsx).

Instruments

Equipment

- ICP-MS: Agilent 7900
- Laser Ablation: ESI NWR 213 (Nd:YAG neodymium: yttrium aluminum garnet)

Software

- ICP-MS: Agilent: User = admin; Password = 7890#fasT
- Laser:
  - Window 7 embedded. Account is “User” and has no password
  - NWR ESI ActiveView, Ver 4.1.2 Build:26, 10/21/2016, part 2040-1107
  - TeamViewer: used to allow ESI technical support to control the laser system remotely. Icon is on the desktop.
  - Plugin for laser to Agilent communication: Icon on laser desktop is named “Agilent Host”

IP Addresses (as of 10/28/19)

- PC with MassHunter: 192.168.254.12
- ICP-MS: 192.168.254.13
- HPLC: 192.168.254.11
- Laser: 192.168.254.14

Appendix B—Determination of Hair Peak Locations

Due to the high variability in data shape, peak positioning, and cps magnitude, it was more efficient to manually identify the section along the hair shaft that corresponded to a gadolinium peak. The plot of sulfur was included to confirm that the data presented was acquired from the hair shaft. For example, a low sulfur signal can indicate hair is not being ablated and analyzed because the data acquisition was part of the laser warmup or cool-down period, or because the laser path was not on the hair. Each hair was reviewed and the approximate data acquisition scan time for the start and end of a peak were tabulated in the sample tracking spreadsheet. These markers were included on the data plots and reviewed for accuracy. If the peak window identified did not properly capture the peak, the tracking spreadsheet was updated and the plot re-generated to confirm the accuracy. Figure 19 shows an example plot of a hair line scan (including the raw ^{157}Gd cps data, smoothed ^{157}Gd data with mass-based concentrations calculated, and raw ^{34}S data) in which the peak is defined by the dashed vertical lines in the middle plot.

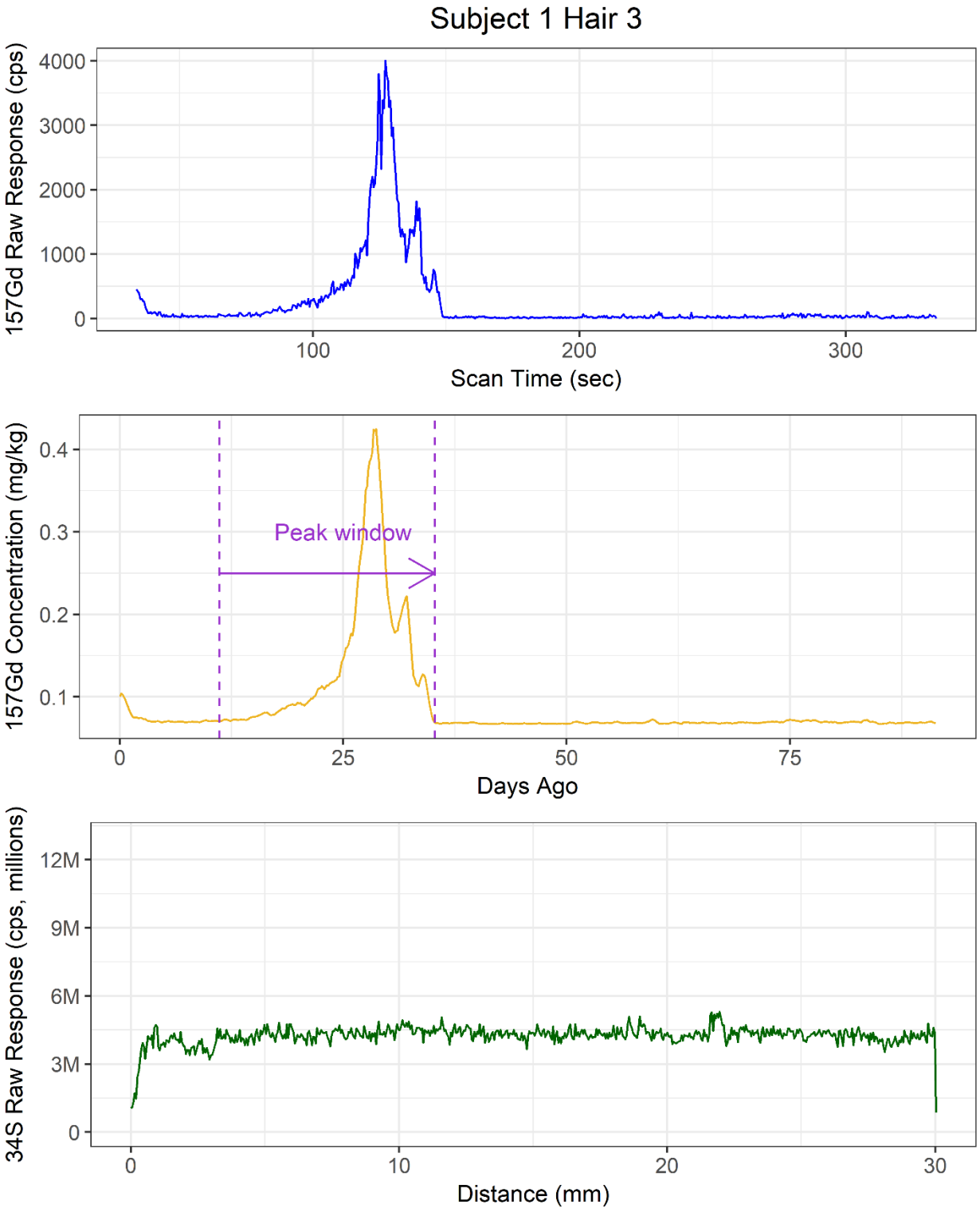

Figure 19. Example hair plot with identified peak interval

Appendix C—Hair Deposition Measures for a Subject

Gadolinium in Hair

There were four measures considered as a singular measure assigned to an individual subject that had received GBCAs:

1. Largest peak maximum concentration for a single hair among all hairs analyzed from a subject within the manually identified peak window.
2. Average of the peak maxima concentrations for all hairs analyzed from a subject within the manually identified peak windows.
3. Largest area under the curve for a single hair among all hairs analyzed from a subject within the manually identified peak window.
4. Average area under the curve for all peaks identified in all hairs from a subject within the manually identified peak window.

Using a measure derived from a single hair (i.e., measures 1 and 3 above) ignores the more robust dataset available from all hairs included in the analysis. Using an averaged value of peak maxima concentrations or area under the curve (measures 2 and 4 above respectively) leverages the full dataset. Due to the individualized nature of hair follicles, being inclusive of measures that consider intra-subject variability is more representative of the overall physiological response of the person (see Section 1.1 and Section 2.2 for additional details on intra-subject variability).

Estimated Injection Day

To determine the measure that was most appropriate to estimate injection day, the actual number of days between injection and death were compared to the estimated days between injection death under the following two scenarios:

1. Days before death corresponding to the single hair largest peak maximum concentration.
2. Days before death corresponding to an average of all peak maxima concentrations for a subject.

The comparison was conducted using linear regression. This analysis revealed that the strongest correlation and best linearity occurred between the actual days and the days estimated using the average of the maximum concentration for all hairs analyzed from a subject (measure number 2 in above list). Figure 20 shows the comparison of each regression. Note that the R^2 value for the selected measure is the highest at 0.47 and the relationship is significant at an alpha of 0.002.

To further visualize the selected method, Figure 21 below illustrates how the peak maxima from each hair are averaged to obtain the measure for a given subject. This illustration is theoretical and does not represent real data from a subject.

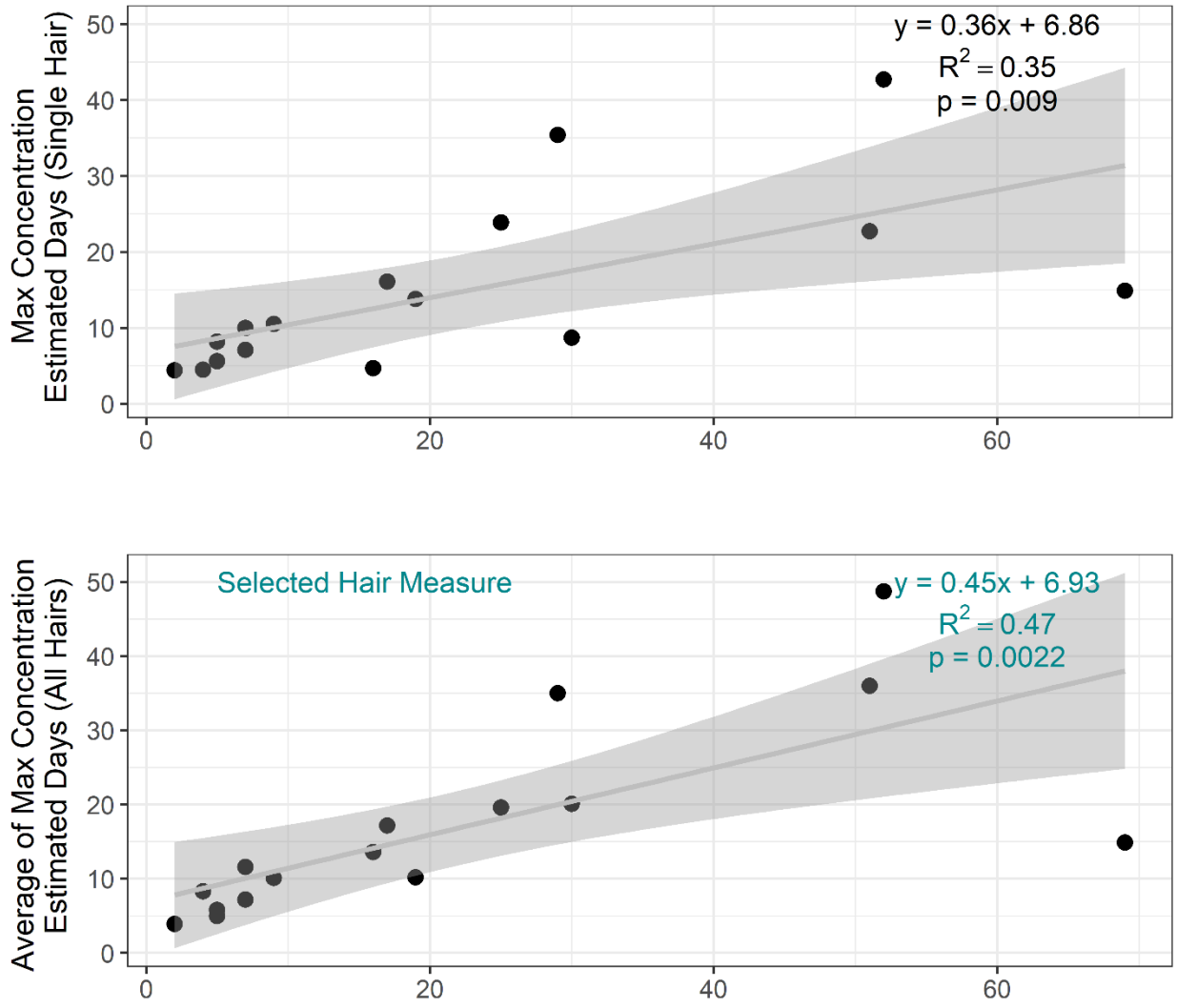

Figure 20. Regressions between actual days and estimated days between injection and death

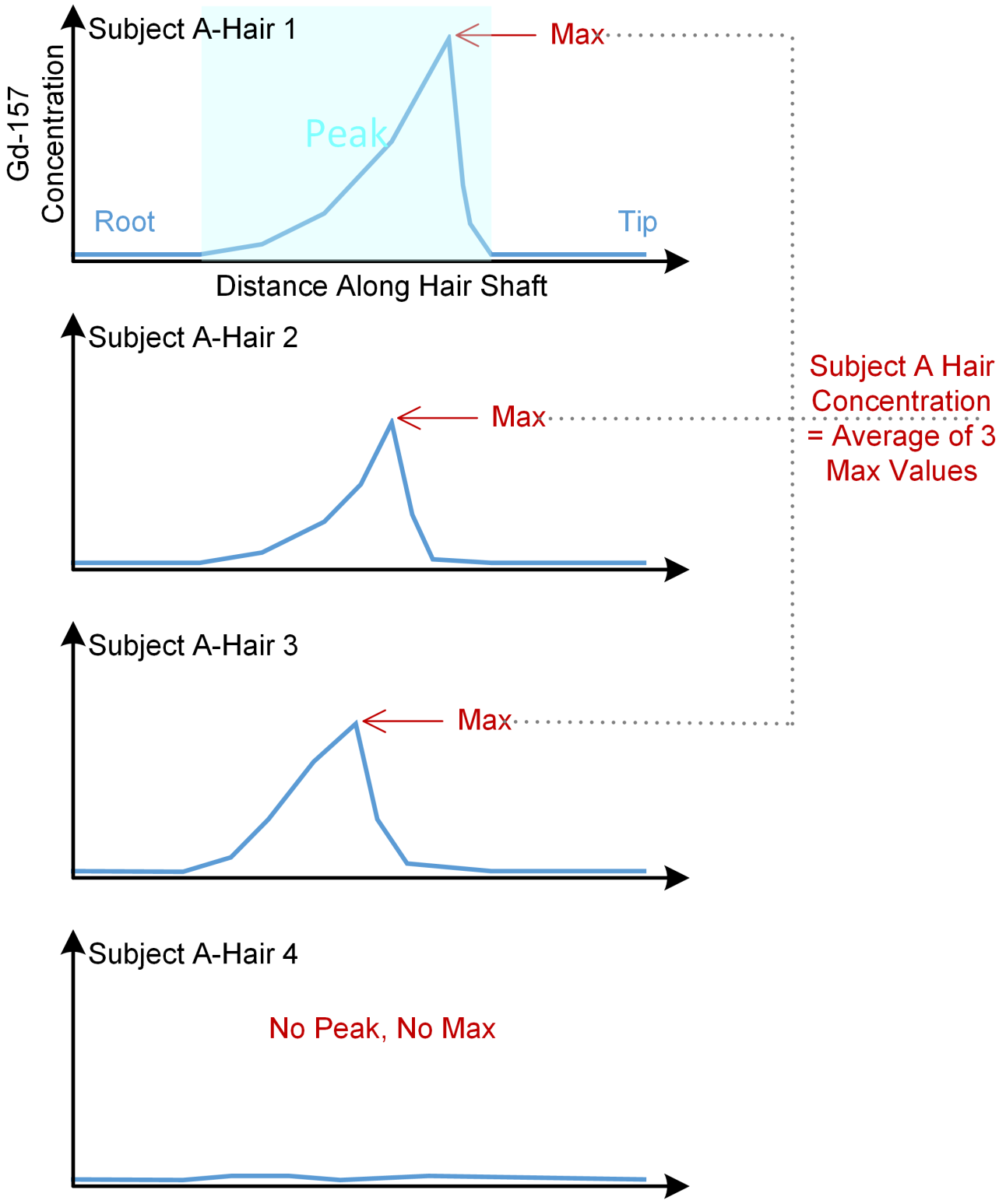

Figure 21. Visualization of method to calculate the selected hair concentration measure for each subject

Appendix D—Internal Standard Assessment

Previous studies have used sulfur (^{32}S and ^{34}S) and carbon (^{13}C) as internal standards since they are part of the keratinized hair matrix. The use of an internal standard is reported to help adjust for variability in laser ablation or instrument drift over time (Kumtabtim et al. 2011). In a review of 20 papers reporting the use of LA-ICP-MS on hair samples, four used ^{13}C as an internal standard (Bartkus et al. 2011; Byrne et al. 2010; Steely et al. 2007; Steely et al. 2005), four used ^{32}S as an internal standard (Rodushkin and Axelsson 2003; Sela et al. 2007; Steely et al. 2007; Steely et al. 2005), ten used ^{34}S as an internal standard (Cheajesadagul et al. 2011; Dressler et al. 2010; Eastman et al. 2013; Kumtabtim et al. 2011; Legrand et al. 2004; Legrand et al. 2007; Luo et al. 2017; Noel et al. 2015; Pozebon et al. 2008; Steely et al. 2007), and one used an unspecified sulfur isotope (Stadlbauer et al. 2005).[1]

At the University of Washington Environmental Health lab where samples were analyzed for this research, the ICP-MS instrument (Agilent 7900) is equipped with a quadrupole mass analyzer. One of the limitations in using this particular instrument is that it sequentially measures each isotope (Thomas 2001) instead of acquiring data for all target isotopes simultaneously (e.g., time of flight mass analyzer; Thomas 2002). Additionally, new material from the hair continues to be ablated in a line scan and sent to the ICP-MS for analysis, rather than a bulk introduction like that from a solution in regular ICP-MS analysis. The result is that although each 0.515 sec interval reports cps data for all selected isotopes, the results are not necessarily obtained from the same section of the ablated hair. Using an internal standard as noted above may not be entirely appropriate because the target isotope(s) may be normalized using data from a different section of the hair shaft.

The variability between the gadolinium raw signal (cps), sulfur-normalized signal (^{34}S), and rolling averages (centered on five values, cps) was compared to assess which method effectively reduced data variability. A subset of the hairs analyzed in September 2018 and January 2019 were included in this analysis; this included 35 hairs from six subjects. A section of each hair scan was identified that was outside of any elevated peak concentrations and included in the comparison. Overall, the rolling average results showed the smallest coefficient of variation (CV) values. Figure 22 displays raw, sulfur-normalized, and rolling average CVs for non-peak sections of 35 hairs. In 97% of hairs analyzed (34/35 hairs) the rolling average method achieved the lowest CV for gadolinium. Further, the results with the sulfur-normalized values had higher CVs than the raw data indicating that this increased variability in the data.

[1] Two studies looked at more than one isotope as an internal standard: Steely et al. (2005) used ^{13}C and ^{32}S, and Steely et al. (2007) used all three.

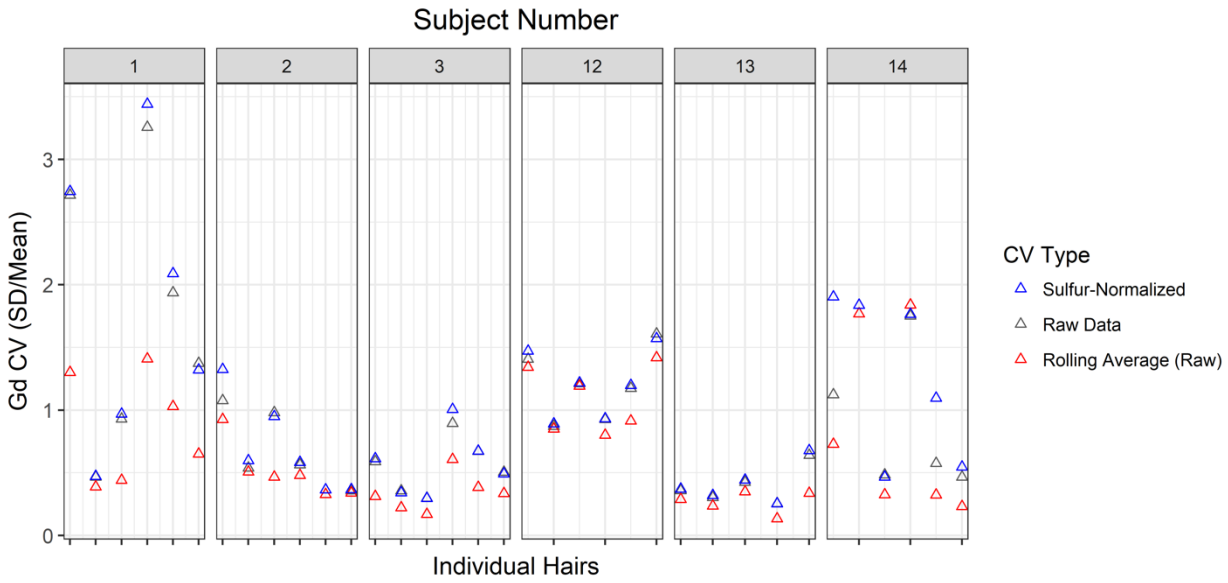

Figure 22. CV comparison

In a previously published review of LA-ICP-MS state-of-the-science in 2015, it was noted that an internal standard and analyte of interest must be homogenously distributed within the sample material (Limbeck et al. 2015). While sulfur is incorporated throughout the hair shaft matrix, gadolinium is not. Based on the above analyses, the known limitations of the mass analyzer, and the available guidance on internal standard use, the rolling average method was selected as the data processing step used for this research.

Appendix E—Stability

The analyses presented below assess instrument stability, material heterogeneity, and systematic instrument drift for an individual scan, scans completed on a given day, and all scans completed throughout the multi-month study. The materials included here are the hair samples themselves and the NIST SRM glass pellet. Additionally, other studies utilizing LA-ICP-MS to analyze hair were compiled to determine whether the stability observed in this study was comparable to other studies to date.

Sulfur in Hair

To assess the potential for drift in instrument response, ^{34}S results were reviewed. The raw responses (cps) were compared to the scan time (in seconds) using linear regression. These slopes were compared across days and between subjects to investigate potential similarities or sources of variability.

Data for 159 hairs from 18 subjects collected over the course of 12 days was reviewed for ^{34}S. The ^{34}S results for hair ranged from 1,259,000 to 7,624,000 cps (average 5,294,000 cps). The CVs for each hair fell between 0.051 and 0.35 (average 0.16). There were 100 hairs with a positive slope and 59 hairs with a negative slope.

The absolute value of the slopes ranged from 4.68 to 79,805 cps/sec. To put these values into context, the slope was divided by the average value of the line scan (in cps) and multiplied by 100 to derive a percentage. Although 79,805 may seem like a large number, it is only 1.5% of the average cps value for that line scan and representing a very small change over the length of the hair. The largest magnitude slope (reported above) was the only line scan with a slope:average cps percentage over 1%. Figure 23a shows the line scan for the hair with the largest ^{34}S slope, and Figure 23b shows the line scan for the hair with the smallest ^{34}S slope. Average ^{34}S cps results for each hair ranged from approximately 1.2 million to 7.6 million.

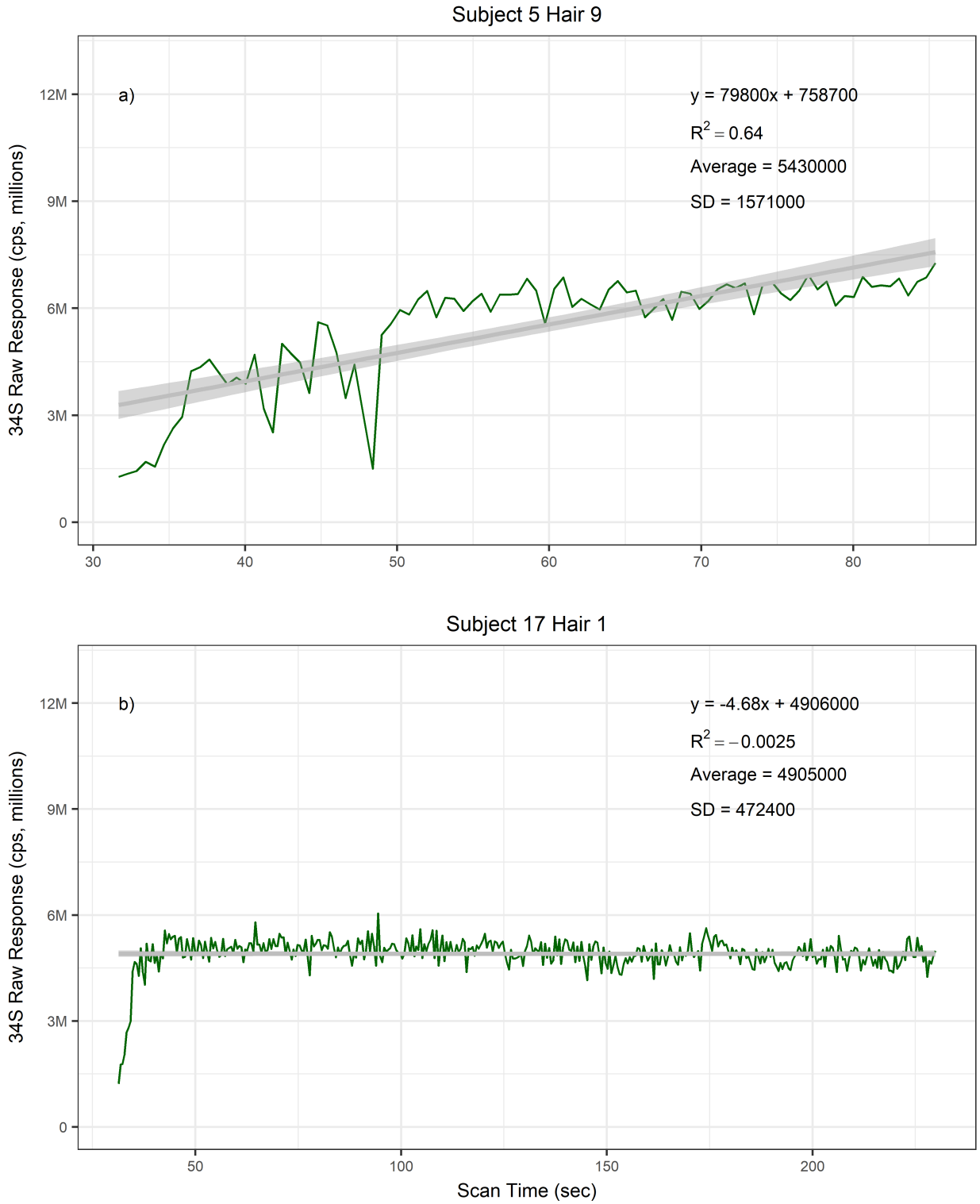

Figure 23. Raw ^{34}S response in hair line scans with a) largest slope (absolute value), and b) smallest slope (absolute value)

All days had both positive and negative slopes for sulfur, except for August 9th and 13th (two samples analyzed on each day), which had only negative slopes. The samples from subjects 14 and 17 had negative slopes, and the samples from subjects 5, 7, 9, and 18 had positive slopes. The remaining subjects had hair samples with both positive and negative sulfur slopes. Table 13 and Table 14 show summaries by analysis date and subject number respectively.

Table 13. Sulfur slope by analysis date

Analysis Date	Hairs Analyzed (N)	Positive (N)	Negative (N)
04/02/2018	3	1	2
04/03/2018	4	1	3
04/04/2018	3	1	2
04/05/2018	3	2	1
08/09/2018	2	0	2
08/13/2018	2	0	2
09/14/2018	5	3	2
09/17/2018	13	10	3
01/31/2019	29	8	21
07/25/2019	30	24	6
07/26/2019	55	45	10
08/05/2019	10	5	5
Total	159	100	59

Table 14. Sulfur slope by subject number

Subject No	Hairs Analyzed (N))	Positive (N)	Negative (N)
Subject 1	11	5	6
Subject 2	11	7	4
Subject 3	11	6	5
Subject 4	10	8	2
Subject 5	10	10	0
Subject 6	10	6	4
Subject 7	10	10	0
Subject 8	4	1	3
Subject 9	10	10	0
Subject 10	9	6	3
Subject 11	10	5	5
Subject 12	6	4	2
Subject 13	5	4	1
Subject 14	18	0	18
Subject 15	10	9	1
Subject 16	10	7	3
Subject 17	2	0	2
Subject 18	2	2	0
Total	159	100	59

The summary by subject (Table 14) could be indicative of minor temporal changes in instrument response (i.e., drift). Alternatively, the observed temporal changes in the sulfur response within a hair could reflect real changes in sulfur content within the hair due to behavioral or physiological influences (e.g., hygiene practices, changes in health status, changes in nutrition over time, or some other biological control mechanism). No known study has evaluated changes in hair sulfur content over time. A 2016 study (Lin et al. 2016) determined that the direction of LA-ICP-MS drift (i.e., positive v. negative slope) may change, particularly during analysis that includes large mass ranges.

There also appeared to be a correlation between analyzed hair length and the overall slope of the ^{34}S line scan for each hair. Figure 24 compares the hair shaft length to the magnitude of the slope of the line. The plot shows that analyzing shorter hair lengths may identify trends over the short-term for an individual and the variability in hair shaft composition, but may not be indicative of the stability of the laser. This is also exemplified in Figure 23 where we see the shorter hair (a) analyzed has a much larger slope than the longer hair (b). Hairs representative of longer periods of growth illustrate a stable ^{34}S signal with minimal positive or negative line slope. The greater

variability in shorter hair lengths suggests that the slope of the sulfur trend within the hair may not necessarily be representative of instrument drift, but may reflect heterogeneity of the hair matrix.

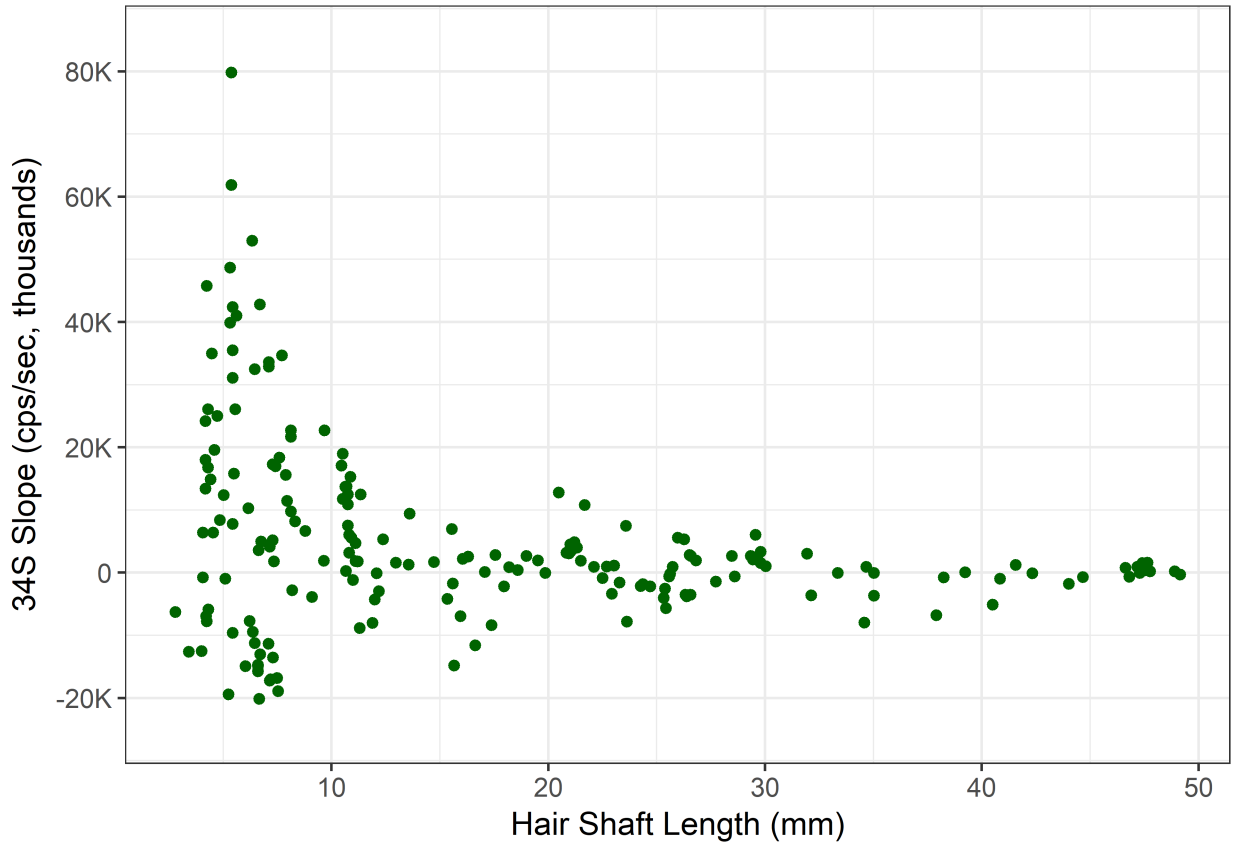

Figure 24. Comparison of analyzed hair shaft length to ^{34}S slopes

The above summaries focus on changes in response within individual hairs. An alternative approach to assess ^{34}S variability is to compare the distribution of slopes for different hairs from an individual subject analyzed on a single day (see Figure 25). Generally, the slopes remained within a limited range, but hairs analyzed on July 25, 2019 showed greater variability between average slopes. A review of the data revealed that subjects 4, 5, and 7 have hair samples that were relatively short, and as noted above this shorter hair length was associated with greater variability.

In any case, days on which analysis proceeded for extended periods of time numerous calibration curves were generated so that changes in instrument response over the course of a day could be corrected.

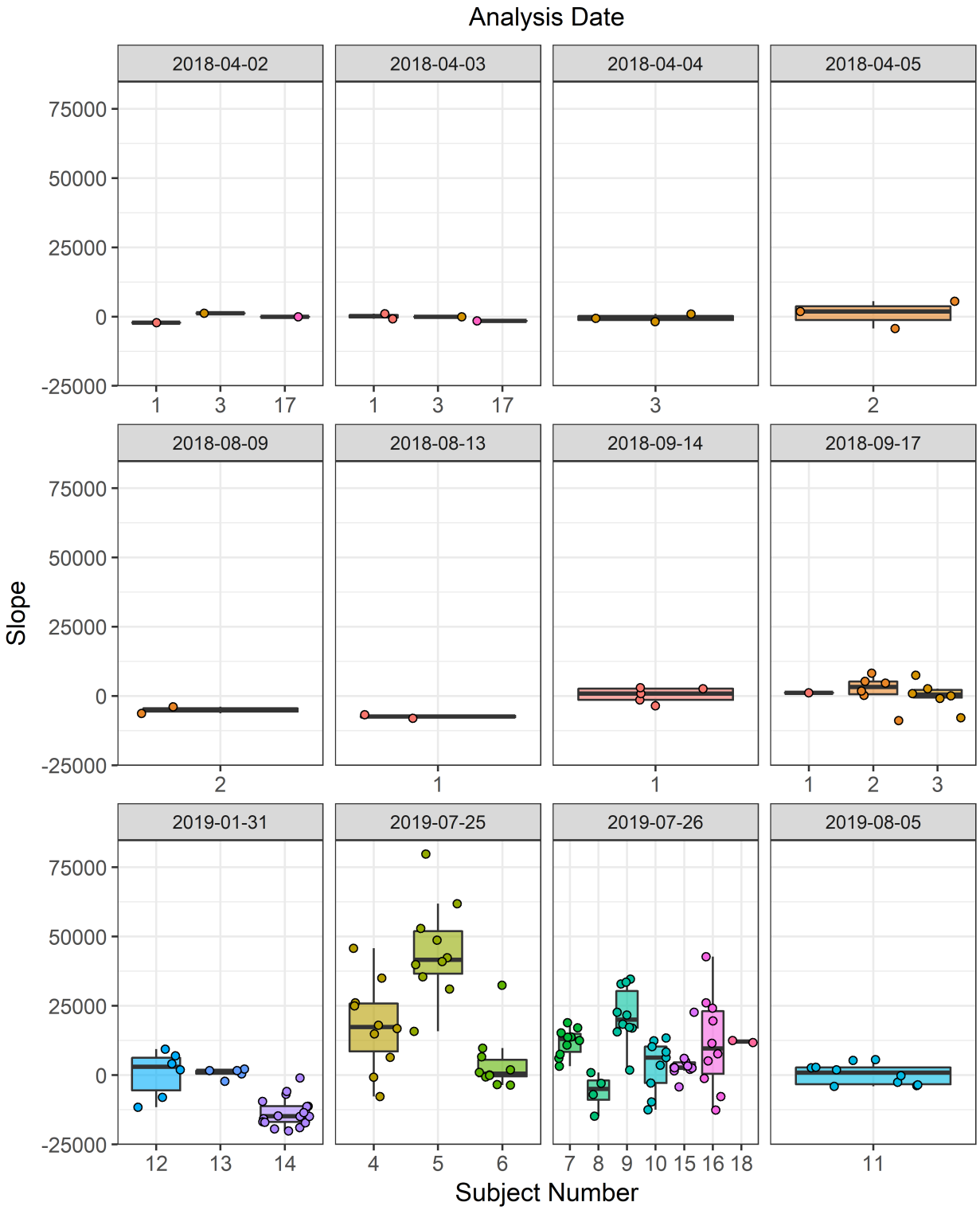

Figure 25. Line scan slopes for ^{34}S results by analysis date and subject

Gadolinium in SRM

Though the SRM (NIST 612 glass disc) utilized throughout this study was a different material from the hair samples, it was incorporated into batch analyses to assess stability of the LA-ICP-MS system without the influence of the sample material heterogeneity. Throughout the 12 days on which samples were analyzed, the SRM was analyzed 37 times, 1–7 times per day. Line scan averages for ^{157}Gd ranged from 435,700 to 1,051,000 cps (average 770,700 cps). The average responses were normally distributed around 770,000 cps (Figure 26). The CVs for each scan fell between 0.072 and 0.14 (average 0.11).

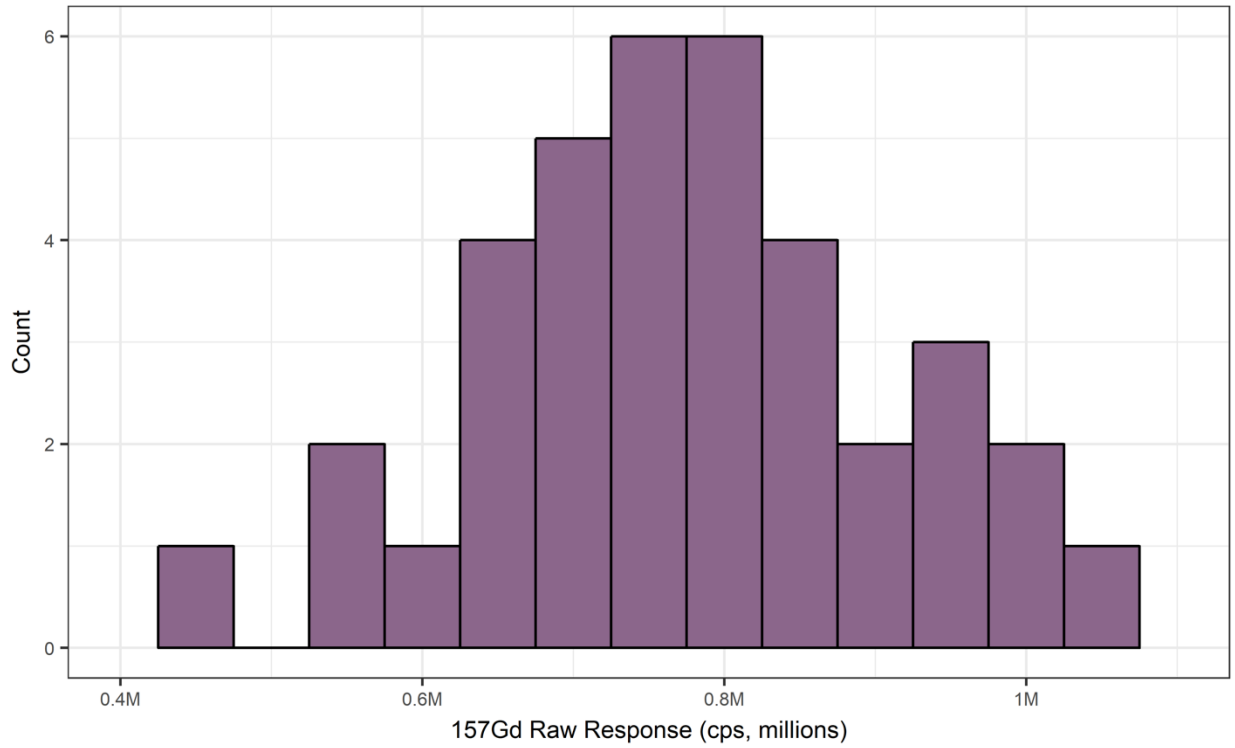

Figure 26. Distribution of average ^{157}Gd raw response for SRM analyses

Comparison of average raw ^{157}Gd results by day revealed what appeared to be a cyclical pattern of increase, decrease, and increase over the course of the analysis period (see Figure 27). The days on which samples were analyzed were not spaced evenly and in some cases months passed between analysis days. A summary of the average line scans and standard deviations is presented in Table 15.

Table 15. Summary of NIST results by sample

Analysis Date	Sample ID	Average ^{157}Gd Response (cps)	SD of ^{157}Gd Response (cps)
4/2/2018	180402_NIST 612-1	708000	68100
4/2/2018	180402_NIST 612-2	558500	62000
4/3/2018	180403_NIST 612-1	781100	83800
4/3/2018	180403_NIST 612-2	681100	75400
4/3/2018	180403_NIST 612-3	631100	62700
4/4/2018	180404_NIST 612-1	739400	85300
4/4/2018	180404_NIST 612-2	734700	89500
4/4/2018	180404_NIST 612-3	736700	77600
4/5/2018	180405_NIST 612-1	876400	118000
4/5/2018	180405_NIST 612-2	842900	115000
4/5/2018	180405_NIST 612-3	696900	97700
8/9/2018	180809_NIST 612-1	977900	130000
8/9/2018	180809_NIST 612-2	811600	91100
8/13/2018	180813_NIST 612-1	987100	124000
8/13/2018	180813_NIST 612-2	934900	120000
9/14/2018	180914_NIST 612-1	668100	72100
9/17/2018	180917_NIST 612-1	674900	77300
9/17/2018	180917_NIST 612-2	910700	113000
9/17/2018	180917_NIST 612-3	582500	51000
1/31/2019	190131_NIST 612-1	776700	77200
1/31/2019	190131_NIST 612-2	561200	59600
1/31/2019	190131_NIST 612-3	435700	59600
7/25/2019	190725_NIST 612-1	848000	60800
7/25/2019	190725_NIST 612-2	765200	82800
7/25/2019	190725_NIST 612-3	760900	71600
7/25/2019	190725_NIST 612-4	633600	69000
7/25/2019	190725_NIST 612-5	732500	93400
7/25/2019	190725_NIST 612-6	677400	67700
7/26/2019	190726_NIST 612-1	956300	73600
7/26/2019	190726_NIST 612-3	821100	78600
7/26/2019	190726_NIST 612-4	833800	90500
7/26/2019	190726_NIST 612-5	818000	74100
7/26/2019	190726_NIST 612-6	853800	107000
7/26/2019	190726_NIST 612-7	723500	72500
7/26/2019	190726_NIST 612-8	780600	84100
8/5/2019	190805_NIST 612-1	1051000	98000
8/5/2019	190805_NIST 612-2	952100	116000

The variability in raw response observed in this analysis could be partially due to inhomogeneity within the SRM, since each line scan occurred at a different location on the disc. Inhomogeneity of NIST 612 has been detailed in previous publications (Eggins and Shelley 2002; Jochum et al. 2011). However, the cause of the underlying cyclical pattern is not known at this time.

Similar to the sulfur slope analysis, the slopes of the SRM line scans for ^{157}Gd were reviewed and showed both positive and negative trends. Of the 37 line scans, 15 had positive slopes and 22 had negative slopes. The negative slopes were primarily limited to the pre-July 2019 samples, with more recent samples showing mostly positive slopes (Figure 27). On July 25th, before samples were analyzed, the tubing system in the laser, which transports material from the chamber to the ICP-MS was replaced after white particulates were identified within the tubes. Example plots of the largest and smallest (absolute value) slopes are provide in Figure 28a and Figure 28b respectively. Relative to the average line scan value (cps), the slopes are a small proportion (0.0058–0.62%) of the average value and represent minimal change over the course of the scan, similar to the ^{34}S results reported above.

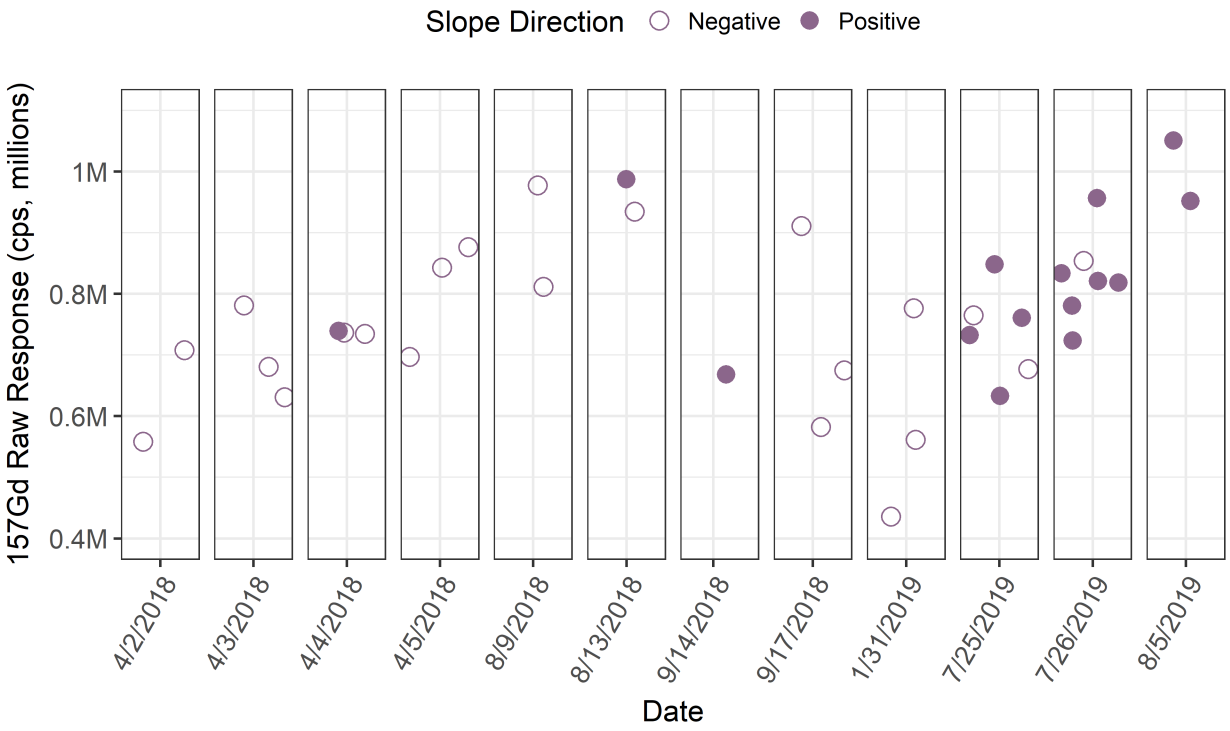

Figure 27. SRM average ^{157}Gd raw response by analysis day

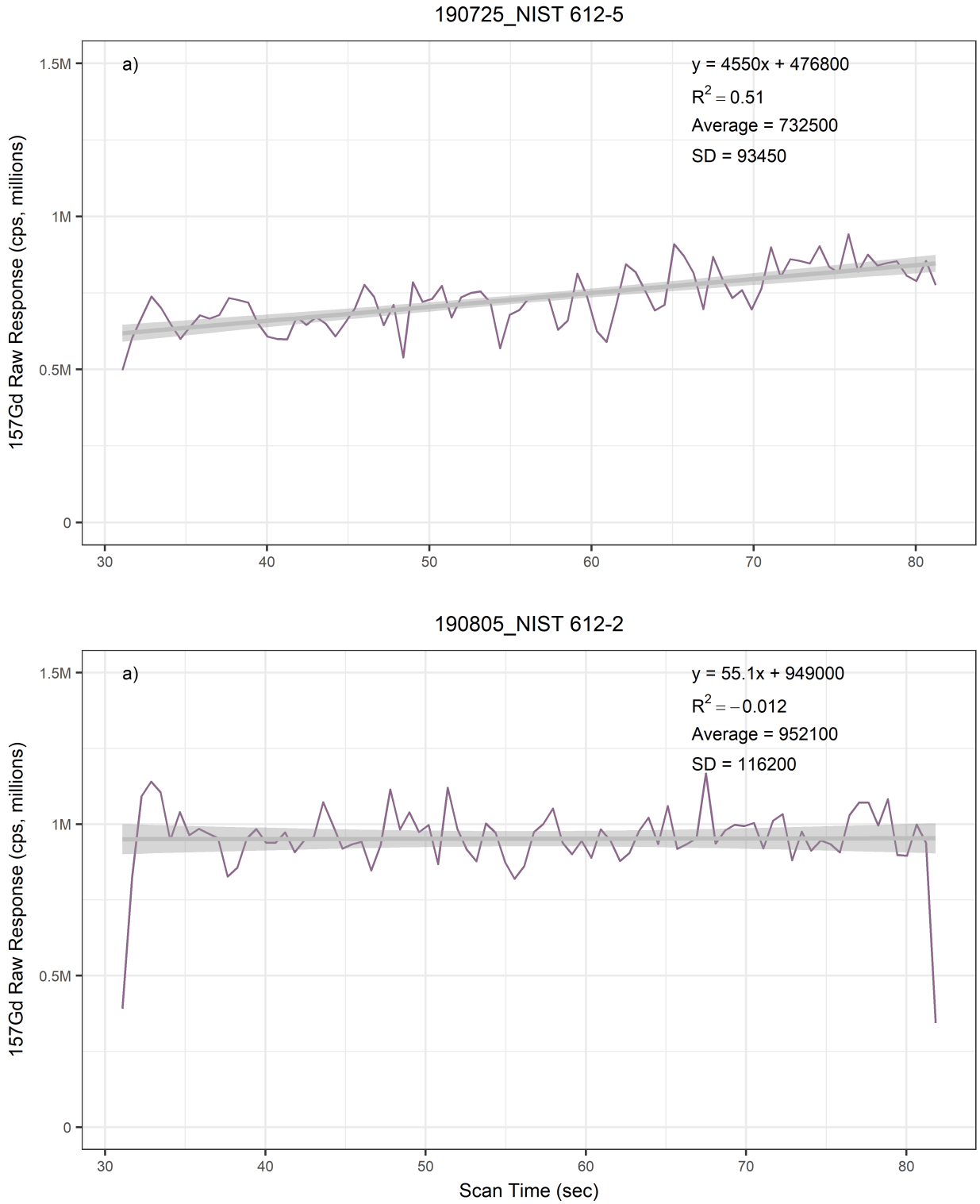

Figure 28. Raw ^{157}Gd response in hair line scans with a) largest slope (absolute value), and b) smallest slope (absolute value)

Comparison to Other Studies

Eleven studies utilizing LA-ICP-MS for analysis of human hair that reported CVs or data sufficient to calculate CVs (i.e., mean and standard deviation) were identified in a literature review. The studies were conducted from 1994 to 2017 and analyzed one or more isotopes. CVs ranged from 0.012 to 1.2 and average CVs were between 0.13 and 0.50. These studies are summarized in Table 16.

Table 16. Literature review CV summary

Study	Element(s)	CV			
		Value	Min	Mean	Max
Bartkus et al. 2011	Pb		0.023	0.27	0.67
Cheajesadagul et al. 2011	Pb		0.14	0.27	0.39
Dressler et al. 2010	Ag, Al, Ba, Bi, Cd, Co, Cr, Cu, Fe, Hg, I, K, Li, Na, Mg, Mn, Mo, Ni, Pb, Sr, Tl, U, V, Zn		0.2	0.5	1.2
Durrant and Ward 1994	Al, Ba, Ca, Cr, Cu, Hg, K, Mg, Mn, Ni, P, Pb, Sr, Zn		0.2		0.4
Legrand et al. 2004	Hg	0.06			
Legrand et al. 2007	Hg		0.07	0.18	0.4
Luo et al. 2017	As, Pb		0.06	0.19	0.3
Pozebon et al. 2008	Pt		0.15		0.22
Rodushkin and Axelsson 2003	Ag, Al, As, Au, B, Ba, Bi, Br, Be, Ca, Cd, Ce, Cl, Co, Cr, Cs, Cu, Fe, Ga, Hf, Hg, I, K, La, Li, Mg, Mn, Mo, Na, Nb, Ni, P, Pb, Pt, Rb, Re, Sb, Sc, Se, Si, Sn, Sr, Ta, Te, Th, Ti, Tl, U, V, W, Y, Zn, Zr				0.2
Sela et al. 2007	Cu, Cr, Fe, Pb, U, Zn		0.012	0.13	0.5
Stadlbauer et al. 2005	Hg, S		0.07		0.09
This study	Gd, S		0.05	0.13	0.35

Note: values reported for this study are taken from the ^{34}S results for hair samples and ^{157}Gd from the SRM samples.

The CVs observed in the sulfur, SRM, and calibrants (see preceding sections) were generally in the same range as those reported by the other studies. This indicates that the data derived from this exhibited similar variability to data published by other researchers

Appendix F—Calibrants

Due to instrument response variability between days, and even over the course of several hours, calibration gels were analyzed in full generally once or twice per day. There were two days (April 3 and 4, 2018) where calibration gels were not analyzed. All calibrants were analyzed twice on January 31, 2019 and July 25, 2019. Four analysis days included one or more individual calibrant line scans incorporated throughout the batch runs to assess calibrant consistency.

Fourteen calibration curves (0–10 µg/g) were generated throughout the 12 days on which sample analysis occurred and 10 individual calibration gel samples were analyzed on four days. Two of the calibration curves (numbers 11 and 12 from July 26, 2019) were acquired using incorrect laser parameters and have been excluded. Curve 14 is the same data as curve 13, but it includes calibrant level 25 µg/g to accommodate two subjects that had higher levels of ^{157}Gd. This last issue resulted in curve numbering 1–15 despite there being 14 "unique" curves. The response for the zero-level gel calibrant was subtracted from all calibrants within a given curve before calculating concentrations to adjust the baseline. Calibration curves were all unweighted.

For the calibrants analyzed as part of the calibration curves, 81% of samples showed good precision with CVs below 0.1. Only 4% had CVs above 0.25, and all of these were the zero-level gels (see Table 17). CVs for the zero-level gels were calculated based on the average line scan and line scan standard deviation before setting the average value to zero to generate the calibration curves. All calibration curves showed good linearity with r-squared values above 0.98.

Regarding accuracy, 55/85 (65%) calibrant line scans had a percent error below 25%, 18 had a percent error above 25%, and the remaining 12 calibrant line scans did not have a calculated percent error because the expected concentration was 0 µg/g (i.e. zero in denominator for statistic). The calibrants with percent error above 25% were restricted to the lower concentrations (Table 18).

After samples were analyzed, it was noticed that at least one of the gels (the 0.1 µg/g standard) had become partially disconnected from the double stick tape resulting in distortion of the surface contour (i.e., it no longer laid flat). This can prevent the laser from focusing properly on the material. This may have happened to other gels and may have contributed to elevated percent errors.

Table 17. Calibrant CV precision

CV Range	Calibrant Concentration (µg/g)								Total
	0	0.05	0.1	0.5	1	5	10	25	
< 0.05	0	0	5	7	11	10	12	1	46
0.05–0.1	0	9	7	5	1	1	0	0	23
0.1–0.25	9	3	0	0	0	1	0	0	13
> 0.25	3	0	0	0	0	0	0	0	3
Total	12	12	12	12	12	12	12	1	85

Table 18. Calibrant accuracy

Percent Error	Calibrant Concentration (µg/g)								Total
	0	0.05	0.1	0.5	1	5	10	25	
< 5	0	1	0	6	8	8	12	1	36
5–10	0	1	1	4	0	0	0	0	6
10–25	0	0	4	1	4	4	0	0	13
25–50	0	4	3	0	0	0	0	0	7
> 50	0	6	4	1	0	0	0	0	11
NA	12	0	0	0	0	0	0	0	12
Total	12	12	12	12	12	12	12	1	85

Calibration slopes ranged from 6,393 to 12,334 cps/sec (average 8,582 cps/sec; SD 2,933 cps/sec) and calibration curves from the same analysis day had slopes that varied by approximately 1,500 cps/sec between the first and second curve. Table 19 summarizes calibration curve statistics and Figure 29 shows the plotted curves (except for curves 11, 12, and 14 for the reasons previously detailed).

Table 19. Calibration curve summary

Curve No.	Analysis Date	Curve Range (µg/g)	Adjusted R-Squared	Slope (cps/µg/g)
1	04/02/2018	0–10	0.989	10,140
2	04/05/2018	0–10	0.991	8,862
3	08/09/2018	0–10	0.990	11,660
4	08/13/2018	0–10	0.995	12,330
5	09/14/2018	0–10	1.000	9,581
6	09/17/2018	0–10	0.999	10,510
7	01/31/2019	0–10	1.000	7,706
8	01/31/2019	0–10	0.996	6,394
9	07/25/2019	0–10	1.000	9,085
10	07/25/2019	0–10	1.000	7,789
13	07/26/2019	0–10	1.000	8,706
14	07/26/2019	0–25	0.998	9,622
15	08/05/2019	0–10	1.000	11,360

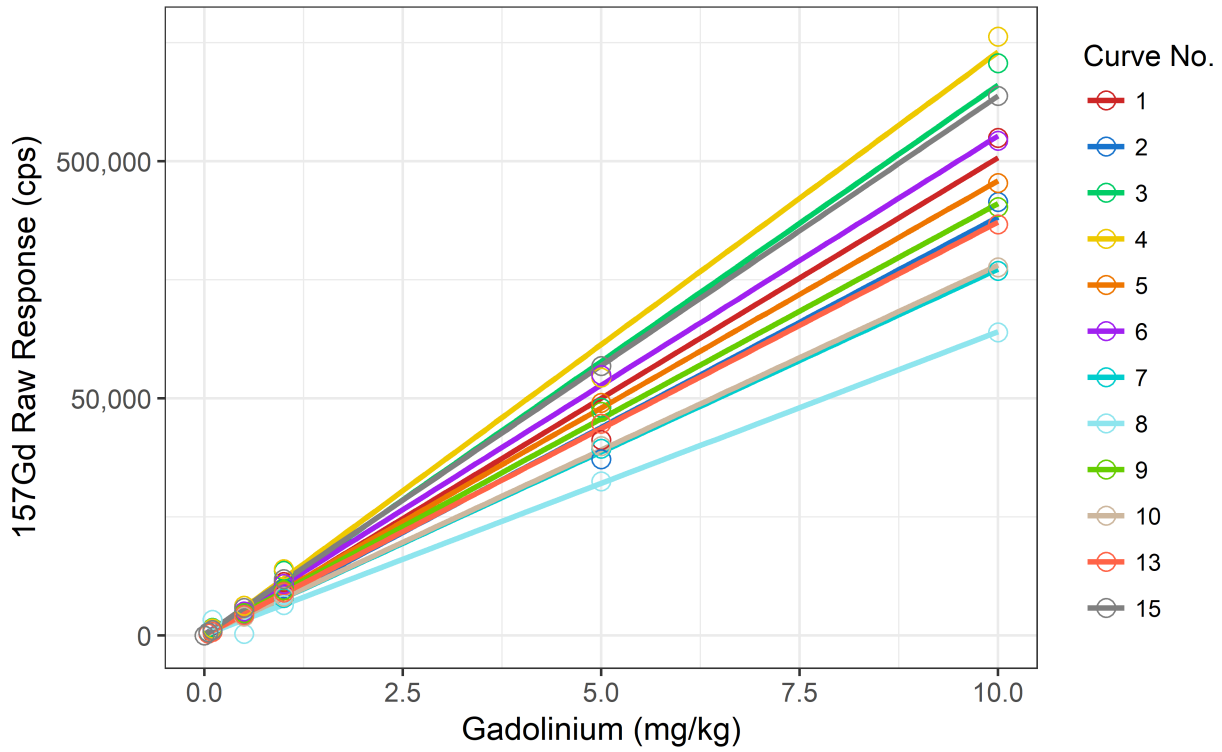

Figure 29. Calibration curve plots

For the individual calibrant line scans, the concentration was calculated from the line scan average and compared to the target concentration. Response averages were adjusted for baseline by subtracting the response for the zero-level gel calibrant in the corresponding calibration curve. Percent error values were 8.6–124% with the highest percentage from the 0.05 µg/g standard (lowest value above zero). The elevated percent error is due to limited instrument sensitivity at these low concentrations. Percent errors were not calculated for the 0 µg/g standard. A summary of the calculated concentrations for the individual calibrant line scans and percent error is provided in Table 20. A disconnected gel calibrant (detailed above) may have caused the elevated percent error (44%) in sample ID 190726_Gel STD 1-TEST1.

Table 20. Individual calibrant summary

Sample ID	Analysis Date	Target Conc. (µg/g)	^{157}Gd Raw Response Avg (cps)	^{157}Gd Raw Response SD (cps)	^{157}Gd Conc. (µg/g)	% Error in Gd Accuracy
180404_Gel STD 0	04/04/2018	0	29	18	0.048	
180404_Gel STD 0.05	04/04/2018	0.05	601	40	0.11	124
180404_Gel STD 0.5-1	04/04/2018	0.5	5124	167	0.62	25
180404_Gel STD 0.5-2	04/04/2018	0.5	4819	154	0.59	18
180405_Gel STD 0	04/05/2018	0	26	19	0.047	
180405_Gel STD 0.5	04/05/2018	0.5	5240	162	0.64	27
190725_Gel STD 5-TEST1	07/25/2019	5	41791	1100	4.6	8.6
190726_Gel STD 1-TEST1	07/26/2019	1	12732	331	1.4	44
190726_Gel STD 1-TEST2	07/26/2019	1	10854	474	1.2	23
190726_Gel STD 5-TEST3	07/26/2019	5	40124	801	4.6	8.1

Generally, calibration curves showed good linearity and calibrants had relatively low CVs and percent errors. However, some issues with the gel mounting methodology would benefit from improvement to prevent detachment from the double stick tape substrate. Additionally, quantification in low concentrations is challenging due to sensitivity limitations. Increasing the material ablated through wider path width or greater ablation depth may improve this limitation.

Appendix G—Development of Study Plans to Evaluate the Feasibility of Using Zinc to Quantify Hair Growth Rates in Humans

Introduction

Zinc is an essential trace element required for human growth, development, and maintenance of functions (ATSDR 2005; Rink 2011). This element is integrated into thousands of proteins, hundreds of enzymes, and is utilized in biological signaling events in the human body (Rink 2011). Zinc levels in the skin (primarily the epidermis) are the third highest (behind skeletal muscles and bone) in the human body at 6% of total body zinc compared to other organ systems. Skin concentrations in adult males (70 kg) have been found at 32 µg/g, with hair concentrations at 150 mg/kg (both expressed in wet weight) (Mills 1989).

Zinc levels in food generally range from 2 µg/g to 29 µg/g and humans ingest 5.2–16.2 mg/day through food or water sources (ATSDR 2005). Recommended dietary allowance for adults is 8 mg/day for women and 14 mg/day for men (IOM 2001). Tolerable upper intake level (UL) for adults is 40 mg/day (IOM 2001).

The target study subject numbers for the oral dosing and shampoo arms were derived from reviewing published literature assessing LA-ICP-MS use on human hair analysis. Eleven LA-ICP-MS analysis of hair studies between 2003 and 2014 recruited 1–24 people with an average of 5 participants among the studies (Bartkus et al. 2011; Dressler et al. 2010; Eastman et al. 2013; Israelsson and Pettersson 2014; Kumtabtim et al. 2011; Luo et al. 2017; Pozebon et al. 2008; Rodushkin and Axelsson 2003; Santamaria-Fernandez et al. 2009; Sela et al. 2007; Stadlbauer et al. 2005). Since we expect no more than 10% loss to follow-up, the study size was increased from five to six.

In humans, 80–90% of scalp hair is in anagen phase, 1–3% is in catagen phase, and 4–20% are in telogen phase (Lebeau et al. 2011; Robertson 1999). Since anagen phase lasts 2–6 years we expect a relatively small proportion of hairs to transition from growth to resting during the brief study periods outlined below (four weeks for the oral dosing and three weeks for the shampoo trial). At each sampling event, the number hairs recommended for collection from each participant is 30.

The objectives for these studies is to evaluate the feasibility of using an oral dose of zinc or zinc shampoo to quantify hair growth rates in humans.

Oral Zinc Dosing

Clinical trials with children have used a 20 mg/day dose as an antidiarrheal measure (Dutta et al. 2011; Larson et al. 2010; Malik et al. 2013); this is near two times the UL for children (ages 1–3

years UL = 7 mg/day; ages 4–8 years UL = 12 mg/day) (IOM 2001). Trials on adults, some with pre-existing conditions such as type 2 diabetes, have used a 40 mg/day dose (the UL for zinc) (Chu et al. 2015). Evidence suggests that individuals with type 2 diabetes may have a disruption in zinc metabolism (Chu et al. 2015). Studies using doses as high as 225 to 450 mg of zinc induced vomiting in subjects, and doses from 50 to 150 mg resulted in gastrointestinal distress (IOM 2001). The Institute of Medicine (IOM) publication on dietary reference intake (DRI) values states that dosages over the UL should not be discouraged provided the subjects are informed of potential toxicity and monitored for symptoms.

Study subjects: six people; male or female; adult ages 18 to 60 (no evidence that increased age affects zinc absorption; IOM 2001).

Exclusion criteria:

- Known zinc deficiency status.
- Type 2 diabetes
- Pregnant women
- Currently taking a zinc supplement (including homeopathic medications for colds that contain zinc).
- Positive autoimmune disease status.
- No hair on scalp.
- Currently use zinc shampoos or conditioners (zinc pyrithione; e.g., DHS, some Head and Shoulders products, Denorex, some Selsun Blue products).
- Currently taking tetracycline antibiotics or penicillamine (zinc may reduce absorption of these drugs; NIH 2016).
- Currently taking thiazidine diuretics (may reduce absorption of zinc; NIH 2016).
- Using denture adhesives that contain zinc.
- Have eaten oysters in the last month (oysters contain 74 mg zinc per 3 ounces; NIH 2018).
- Consume alcohol on a daily basis (ethanol consumption reduces zinc absorption; NIH 2018).

Potential participants will respond to questions over the phone as part of the screening process to determine eligibility.

Participants will receive 60 mg zinc as zinc gluconate (Nature’s Bounty 30 mg zinc as zinc gluconate, 2 supplements per dose). The National Institute of Health (NIH) indicates that there are several types of dietary zinc supplements (e.g., zinc gluconate, zinc sulfate and zinc acetate), but that it is not clear if one form is better than another (NIH 2016). The dosage recommended for this study is below dosages used in studies that resulted in more severe adverse outcomes. Participants will receive two doses of 60 mg zinc supplementation; once after enrollment, and again at two weeks.

Participants will be discouraged from eating one hour before, and one hour after taking the zinc supplement. Research shows inhibition of zinc absorption if the zinc (or its source) is consumed simultaneously with phytate (aka phytic acid; present in seeds, grains, and legumes), high levels

of calcium (e.g., >1,300 mg), or iron (IOM 2001; Rink 2011). Additionally, phytate and calcium together have a stronger effect on the inhibition of zinc absorption (IOM 2001; Rink 2011).

Thirty hair samples will be collected (i.e., plucked) from the scalps of the participants two weeks after the second dosing event. Two weeks after the second dosing gives the hair sufficient time to grow; other studies have used the assumption that it takes two weeks for a hair to reach the surface of the scalp (Lebeau et al. 2011). Hairs will be stored in ziplock plastic bags within the lab prior to preparation and analysis.

Zinc Shampoo Use

Research on exogenous contamination of hair shafts indicates that sweat and sebaceous gland secretions may provide physical or chemical pathways that allow trace minerals to bind to the hair (Combs et al. 1982). Cosmetic products, such as shampoos, are a potential source of exogenous mineral contributions (Dawber 1996). It is unclear whether the zinc from the shampoo will be integrated into the hair shaft and/or remain on the surface of the hair shaft.

Study subjects: six people; male or female; adult ages 18 to 60.

Exclusion criteria:

- Currently taking a zinc supplement (including homeopathic medications for colds that contain zinc).
- No hair on scalp.
- Currently use zinc shampoos or conditioners (zinc pyrithione; e.g., DHS, some Head and Shoulders products, Denorex, some Selsun Blue products).
- Using denture adhesives that contain zinc.
- Have eaten oysters in the last month (oysters contain 74 mg zinc per 3 ounces [NIH18A]).

Potential participants will be asked to fill out a questionnaire to determine their eligibility for inclusion in the study.

Participants will use Free & Clear Medicated Anti-Dandruff Shampoo (contains 2% pyrithione zinc) during week one, Free & Clear Hair Shampoo for Sensitive Skin (zinc-free formulation) during week two, and the zinc-containing shampoo again during week three. The Free & Clear Hair Conditioner for Sensitive Skin (zinc-free) will be provided for use as desired.

Thirty hairs will be harvested after the week of first zinc shampoo use, two days after ceasing the zinc shampoo use, one week after ceasing the zinc shampoo use, and at the end of the third week after the zinc shampoo is used for the second time. This is a total of four hair harvesting events for a total of 120 hairs from each participant. Figure 30 shows the timeline of UW visits,

shampoo use, and hair harvesting. Hairs will be stored in ziplock plastic bags within the lab prior to preparation and analysis.

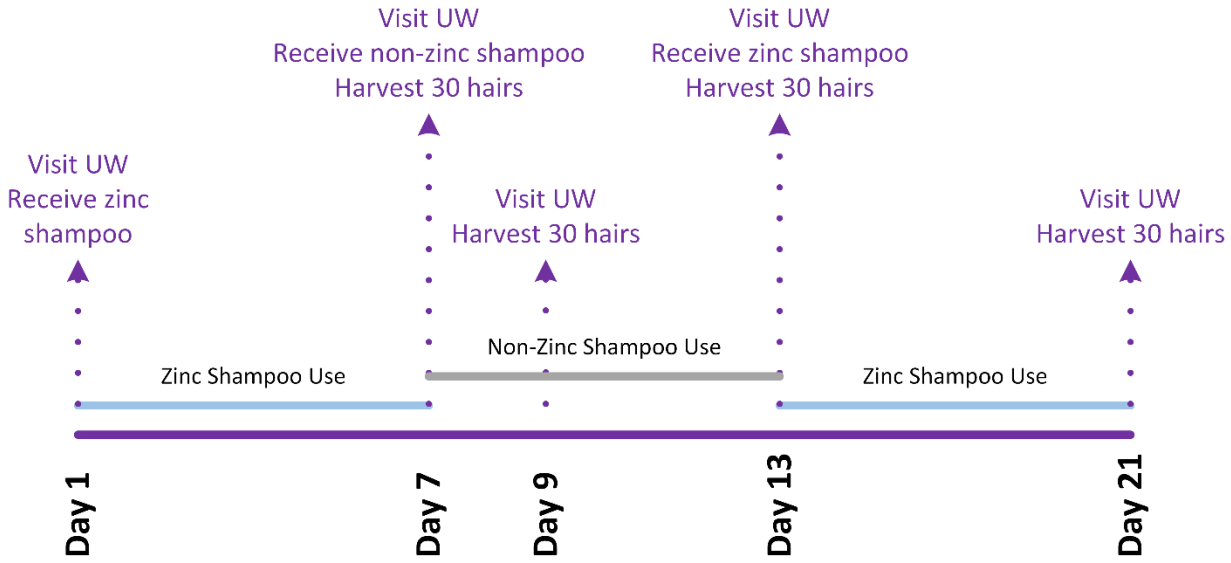

Figure 30. Proposed zinc shampoo study timeline

References

Agilent Technologies. 2004. Introduction to laser ablation ICP-MS for the analysis of forensic samples. www.agilent.com/chem.

Alonso, L., and E. Fuchs. 2006. The hair cycle. J Cell Sci 119:391–393.

ATSDR. 2003. Analysis of hair samples: how do hair sampling results relate to environmental exposure? Agency for the Toxic Substances and Disease Registry.

ATSDR. 2005. Toxicological profile for zinc. Agency for the Toxic Substances and Disease Registry. Atlanta, GA. 352 pp.

ATSDR. 2007. Toxicological profile for arsenic. Agency for the Toxic Substances and Disease Registry. Atlanta, GA. 559 pp.

ATSDR. 2012a. Toxicological profile for cadmium. Agency for the Toxic Substances and Disease Registry. Atlanta, GA. 487 pp.

ATSDR. 2012b. Toxicological profile for manganese. Agency for the Toxic Substances and Disease Registry. Atlanta, GA. 556 pp.

Bader, M., M. C. Dietz, A. Ihrig, and G. Triebig. 1999. Biomonitoring of manganese in blood, urine and axillary hair following low-dose exposure during the manufacture of dry cell batteries. Int Arch Occup Environ Health 72(8):521–527.

Baker, M. G., B. Stover, C. D. Simpson, L. Sheppard, and N. S. Seixas. 2016. Using exposure windows to explore an elusive biomarker: blood manganese. Intl Arch Occ Environ Health 89(4):679–687.

Bartkus, L., D. Amarasiriwardena, B. Arriaza, D. Bellis, and J. Yañez. 2011. Exploring lead exposure in ancient Chilean mummies using a single strand of hair by laser ablation-inductively coupled plasma-mass spectrometry (LA-ICP-MS). Microchem J 98(2):267–274.

Becker, J. S., M. Zoriy, A. Matusch, B. Wu, D. Salber, C. Palm, and J. S. Becker. 2010. Bioimaging of metals by laser ablation inductively coupled plasma mass spectrometry (LA-ICP-MS). Mass Spectrom Rev 29(1):156–175.

Berry, J. E. 2015. Trace metal analysis by laser ablation-inductively coupled plasma-mass spectrometry and x-ray K-edge densitometry of forensic samples. Chemistry Department, Iowa State University. 170 pp.

Bohme, S., H. J. Stark, D. Kuhnel, and T. Reemtsma. 2015. Exploring LA-ICP-MS as a quantitative imaging technique to study nanoparticle uptake in *Daphnia magna* and zebrafish (*Danio rerio*) embryos. Anal Bioanal Chem 407:5477–5485.

Boyken, J., T. Frenzel, J. Lohrke, G. Jost, and H. Pietsch. 2018. Gadolinium accumulation in the deep cerebellar nuclei and globus pallidus after exposure to linear but not macrocyclic gadolinium-based contrast agents in a retrospective pig study with high similarity to clinical conditions. Invest Radiol.

Brady, F. O. 1991. Induction of metallothionein in rats. pp. 559-567. In: Methods in enzymology; metallobiochemistry part B, metallothionein and related molecules. Academic Press.

Buffoli, B., F. Rinaldi, M. Labanca, E. Sorbellini, A. Trink, E. Guanziroli, R. Rezzani, and L. F. Rodella. 2014. The human hair: from anatomy to physiology. Intl J Dermatol 53(3):331–341.

Byrne, S., D. Amarasiriwardena, B. Bandak, L. Bartkus, J. Kane, J. Jones, J. Yañez, B. Arriaza, and L. Cornejo. 2010. Were Chinchorros exposed to arsenic? Arsenic determination in Chinchorro mummies' hair by laser ablation inductively coupled plasma-mass spectrometry (LA-ICP-MS). Microchem J 94(1):28–35.

Cheajesadagul, P., W. Wananukul, A. Siripinyanond, and J. Shiowatana. 2011. Metal doped keratin film standard for LA-ICP-MS determination of lead in hair samples. J Anal At Spectrom 26(3):493–498.

Chu, A., M. Foster, D. Hancock, K. Bell-Anderson, P. Petocz, and S. Samman. 2015. TNF-[alpha] gene expression is increased following zinc supplementation in type 2 diabetes mellitus. Genes Nutr 10(1):1–10.

Cihan, B. Y., S. Sozen, and S. O. Yildirim. 2011. Trace elements and heavy metals in hair of stage III breast cancer patients. Biol Trace Elem Res 144(1-3):360–379.

Combs, D. K., R. D. Goodrich, and J. C. Meiske. 1982. Mineral concentrations in hair as indicators of mineral status: a review. J Animal Sci 54(2):391–398.

Dawber, R. 1996. Hair: its structure and response to cosmetic preparations. Clinics Dermatol 14(1):105–112.

Dressler, V. L., D. Pozebon, M. F. Mesko, A. Matusch, U. Kumtabtim, B. Wu, and J. Sabine Becker. 2010. Biomonitoring of essential and toxic metals in single hair using on-line solution-based calibration in laser ablation inductively coupled plasma mass spectrometry. Talanta 82(5):1770–1777.

Durrant, S. F., and N. I. Ward. 1994. Laser ablation-inductively coupled plasma-mass spectrometry (LA-ICP-MS) for the multielemental analysis of biological materials: a feasibility study. Food Chemistry 49(3):317–323.

Dutta, P., U. Mitra, S. Dutta, T. N. Naik, K. Rajendran, and M. K. Chatterjee. 2011. Zinc, vitamin A, and micronutrient supplementation in children with diarrhea: a randomized controlled clinical trial of combination therapy versus monotherapy. J Pediatrics 159(4):633–637.

Duverger, O., and M. I. Morasso. 2009. Epidermal patterning and induction of different hair types during mouse embryonic development. Birth Defects Res Part C 87(3):263–272.

Eastman, R. R., T. P. Jursa, C. Benedetti, R. G. Lucchini, and D. R. Smith. 2013. Hair as a biomarker of environmental manganese exposure. Environ Sci Technol 47(3):1629–1637.

Eggins, S. M., and J. M. G. Shelley. 2002. Compositional heterogeneity in NIST SRM 610-617 glasses. Geostds Newsletter 26(3):269–286.

EMA. 2017. Gadolinium-containing contrast agents. EMA's final opinion confirms restrictions on use of linear gadolinium agents in body scans. https://www.ema.europa.eu/en/medicines/human/referrals/gadolinium-co. Accessed on May 1, 2019. Last updated on November 23, 2017. European Medicines Agency.

Engstrom, A. K., J. M. Snyder, N. Maeda, and Z. Xia. 2017. Gene-environment interaction between lead and apolipoprotein E4 causes cognitive behavior deficits in mice. Molec Degen Accepted January 2017.

ERG. 2001. Summary report - hair analysis panel discussion: exploring the state of the science (June 12-13, 2001). Prepared for the Agency for Toxic Substances and Disease Registry, Division of Health Assessment and Consultation and Division of Health Education and Promotion, Atlanta, GA. Eastern Research Group. Lexington, MA.

ESI. No Date. NWR213 specifications summary. Elemental Scientific Lasers LLC, Bozeman, MT.

FDA. 2017a. Medical imaging drugs advisory committee meeting: gadolinium retention after gadolinium based contrast magnetic resonance imaging in patients with normal renal function (September 8, 2017). U.S. Food and Drug Administration. 138 pp.

FDA. 2017b. FDA drug safety communication: FDA identifies no harmful effects to date with brain retention of gadolinium-based contrast agents for MRIs; review to continue. https://www.fda.gov/drugs/drug-safety-and-availability/fda-drug-safety-communication-fda-identifies-no-harmful-effects-date-brain-retention-gadolinium. Accessed on May 1, 2019. Last updated on May 22, 2017. U.S. Food and Drug Administration.

Ferré-Huguet, N., M. Nadal, M. Schuhmacher, and J. L. Domingo. 2009. Monitoring metals in blood and hair of the population living near a hazardous waste incinerator: temporal trend. Biol Trace Elem Res 128(3):191–199.

Garofalo, J.-M., S. P. Black, and L. B. Martin. 2016. Laparotomic approach for collecting serial hepatic biopsies in rats (*Rattus norvegicus*) and mice (*Mus musculus*). JAALAS 55(3):324-330.

Geyfman, M., M. V. Plikus, E. Treffeisen, B. Andersen, and R. Paus. 2015. Resting no more: re-defining telogen, the maintenance stage of the hair growth cycle. Biol Rev Cambridge Philos Soc 90(4):1179–1196.

Ginat, D. T., and S. P. Meyers. 2012. Intracranial lesions with high signal intensity on T1-weighted MR images: differential diagnosis. RadioGraphics 32(2):499–516.

Glaven, J. A., R. E. Gandley, and B. A. Fowler. 1991. Biological indicators of cadmium exposure. pp. 592-599. In: Methods in enzymology; metallobiochemistry part B, metallothionein and related molecules. Academic Press.

Goulle, J. P., L. Mahieu, J. Castermant, N. Neveu, L. Bonneau, G. Laine, D. Bouige, and C. Lacroix. 2005. Metal and metalloid multi-elementary ICP-MS validation in whole blood, plasma, urine and hair. Reference values. Forensic Sci Int 153(1):39–44.

Goyer, R., M. Golub, H. Choudhury, M. Hughes, E. Kenyon, and M. Stifelman. 2004. Issue paper on the human health effects of metals. Submitted to U.S. Environmental Protection Agency, Risk Assessment Forum. ERG. Lexington, MA. 49 pp.

Hare, D., C. Austin, and P. Doble. 2012. Quantification strategies for elemental imaging of biological samples using laser ablation-inductively coupled plasma-mass spectrometry. Analyst 137(7):1527–1537.

IAEA. 1993. The significance of hair mineral analysis as a means for assessing internal body burdens of environmental pollutants. NAHRES-18. International Atomic Energy Agency. Vienna, Austria. 310 pp.

IOM. 2001. Dietary reference intakes for vitamin A, vitamin K, arsenic, boron, chromium, copper, iodine, iron, manganese, molybdenum, nickel, silicon, vanadium, and zinc. Institute of Medicine, Food and Nutrition Board. National Academies Press, Washington, D.C.

Israelsson, A., and H. Pettersson. 2014. Measurements of (234)U and (238)U in hair, urine, and drinking water among drilled bedrock well water users for the evaluation of hair as a biomonitor of uranium intake. Health Phys 107(2):143–149.

Jochum, K. P., U. Weis, B. Stoll, D. Kuzmin, Q. Yang, I. Raczek, D. E. Jacob, A. Stracke, K. Birbaum, D. A. Frick, D. Günther, and J. Enzweiler. 2011. Determination of reference values for NIST SRM 610–617 glasses following ISO guidelines. Geostds Geoanal Res 35(4):397–429.

Kanda, T., T. Fukusato, M. Matsuda, K. Toyoda, H. Oba, J. Kotoku, T. Haruyama, K. Kitajima, and S. Furui. 2015. Gadolinium-based contrast agent accumulates in the brain even in subjects without severe renal dysfunction: evaluation of autopsy brain specimens with inductively coupled plasma mass spectroscopy. Radiology 276(1):228–232.

Kanda, T., K. Ishii, H. Kawaguchi, K. Kitajima, and D. Takenaka. 2014. High signal intensity in the dentate nucleus and globus pallidus on unenhanced T1-weighted MR images: relationship with increasing cumulative dose of a gadolinium-based contrast material. Radiology 270(3):834–841.

Kempson, I. M., W. M. Skinner, and K. P. Kirkbride. 2007. The occurrence and incorporation of copper and zinc in hair and their potential role as bioindicators: a review. J Toxicol Environ Health, Part B 10(8):611–622.

Kintz, P., and M. Villain. 2005. Hair in forensic toxicology with a special focus on drug-facilitated crimes. In: Hair in toxicology, an important bio-monitor. D. J. Tobin, editor. RSC Publishing, Cambridge, England.

Klaassen, C. D., J. Liu, and B. A. Diwan. 2009. Metallothionein protection of cadmium toxicity. Toxicol Appl Pharma 238(3):215-220.

Kollmer, W. E. 1982. The significance of Cd in hair: influence of the level of intake and the external contamination in the rat. Sci Tot Environ 25(1):41–51.

Kumtabtim, U., A. Matusch, S. U. Dani, A. Siripinyanond, and J. S. Becker. 2011. Biomonitoring for arsenic, toxic and essential metals in single hair strands by laser ablation inductively coupled plasma mass spectrometry. Intl J Mass Spectrom 307(1-3):185–191.

Larson, C. P., D. Nasrin, A. Saha, M. I. Chowdhury, and F. Qadri. 2010. The added benefit of zinc supplementation after zinc treatment of acute childhood diarrhoea: a randomized, double-blind field trial. Trop Med Intl Health 15(6):754–761.

Layne, K. A., P. I. Dargan, J. R. H. Archer, and D. M. Wood. 2018. Gadolinium deposition and the potential for toxicological sequelae - a literature review of issues surrounding gadolinium-based contrast agents. Br J Clin Pharmacol.

Lebeau, M. A., M. A. Montgomery, and J. D. Brewer. 2011. The role of variations in growth rate and sample collection on interpreting results of segmental analyses of hair. Forensic Science International 210(1):110–116.

Lee, W. J., H. W. Cha, H. J. Lim, S.-J. Lee, and D. W. Kim. 2012. The effect of sebocytes cultured from nevus sebaceus on hair growth. Exper Dermatol 21(10):796-798.

Legrand, M., R. Lam, M. Jensen-Fontaine, E. D. Salin, and H. Man Chan. 2004. Direct detection of mercury in single human hair strands by laser ablation inductively coupled plasma mass spectrometry (LA-ICP-MS). J Anal At Spectrom 19(10):1287–1288.

Legrand, M., R. Lam, C. J. S. Passos, D. Mergler, E. D. Salin, and H. M. Chan. 2007. Analysis of mercury in sequential micrometer segments of single hair strands of fish-eaters. Environ Sci Technol 41:593–598.

Limbeck, A., P. Galler, M. Bonta, G. Bauer, W. Nischkauer, and F. Vanhaecke. 2015. Recent advances in quantitative LA-ICP-MS analysis: challenges and solutions in the life sciences and environmental chemistry. Anal Bioanal Chem 407(22):6593–6617.

Lin, J., Y. Liu, Y. Yang, and Z. Hu. 2016. Calibration and correction of LA-ICP-MS and LA-MC-ICP-MS analyses for element contents and isotopic ratios. Solid Earth Sci 1(1):5–27.

Lum, T.-S., Y.-K. Tsoi, P. Y.-K. Yue, and K. S.-Y. Leung. 2016. Therapeutic drug monitoring using LA-ICP-MS: initial studies with metallodrugs in mouse whiskers. Microchem J 127:94–101.

Luo, R., X. Su, W. Xu, S. Zhang, X. Zhuo, and D. Ma. 2017. Determination of arsenic and lead in single hair strands by laser ablation inductively coupled plasma mass spectrometry. Sci Rep 7(1):3426.

Malik, A., D. K. Taneja, N. Devasenapathy, and K. Rajeshwari. 2013. Short-course prophylactic zinc supplementation for diarrhea morbidity in infants of 6 to 11 months. Pediatrics 132(1):e46.

McDonald, R. J., D. Levine, J. Weinreb, E. Kanal, M. S. Davenport, J. H. Ellis, P. M. Jacobs, R. E. Lenkinski, K. R. Maravilla, M. R. Prince, H. A. Rowley, M. F. Tweedle, and H. Y. Kressel. 2018. Gadolinium retention: a research roadmap from the 2018 NIH/ACR/RSNA workshop on gadolinium chelates. Radiology 289(2):517–534.

McDonald, R. J., J. S. McDonald, D. Dai, D. Schroeder, M. E. Jentoft, D. L. Murray, R. Kadirvel, L. J. Eckel, and D. F. Kallmes. 2017. Comparison of gadolinium concentrations within multiple rat organs after intravenous administration of linear versus macrocyclic gadolinium chelates. Radiology 285(2):536–545.

McDonald, R. J., J. S. McDonald, D. F. Kallmes, M. E. Jentoft, D. L. Murray, K. R. Thielen, E. E. Williamson, and L. J. Eckel. 2015. Intracranial gadolinium deposition after contrast-enhanced MR imaging. Radiology 275(3):772–782.

Mikulewicz, M., K. Chojnacka, T. Gedrange, and H. Górecki. 2013. Reference values of elements in human hair: a systematic review. Environ Toxicol Pharmacol 36(3):1077–1086.

Mills, C. F. 1989. Zinc in human biology. Springer-Verlag, Berlin, Germany.

Murata, N., L. F. Gonzalez-Cuyar, K. Murata, C. Fligner, R. Dills, D. Hippe, and K. R. Maravilla. 2016. Macrocyclic and other non-group 1 gadolinium contrast agents deposit low levels of gadolinium in brain and bone tissue: preliminary results from 9 patients with normal renal function. Invest Radiol 51(7):447–453.

NIH. 2016. Zinc, fact sheet for consumers. p. 2. National Institutes of Health, Office of Dietary Supplements.

NIH. 2018. Zinc, fact sheet for health professionals. https://ods.od.nih.gov/factsheets/Zinc-HealthProfessional/. Accessed on June 13, 2018. Last updated on March 2, 2018. National Institutes of Health.

NKF. 2019. Estimated glomerular filtration rate (eGFR). https://www.kidney.org/atoz/content/gfr. Accessed on October 22, 2019. National Kidney Foundation.

Noel, M., J. R. Christensen, J. Spence, and C. T. Robbins. 2015. Using laser ablation inductively coupled plasma mass spectrometry (LA-ICP-MS) to characterize copper, zinc and mercury along grizzly bear hair providing estimate of diet. Sci Total Environ 529:1–9.

NRC. 2006. Human biomonitoring for environmental chemicals. National Research Council. National Academies Press, Washington, D.C.

OSHA. 2010. OSHA celebrates 40 years of accomplishments in the workplace. Occupational Safety and Health Administration.

OSHA. 2016. National Emphasis Program - primary metal industries (directive number CPL 03-00-018). Occupational Safety and Health Administration.

Plikus, M. V., and C.-M. Chuong. 2008. Complex hair cycle domain patterns and regenerative hair waves in living rodents. J invest Derm 128(5):1071–1080.

Plikus, M. V., J. A. Mayer, D. de la Cruz, R. E. Baker, P. K. Maini, R. Maxson, and C. M. Chuong. 2008. Cyclic dermal BMP signalling regulates stem cell activation during hair regeneration. Nature 451(7176):340–344.

Pozebon, D., V. L. Dressler, A. Matusch, and J. S. Becker. 2008. Monitoring of platinum in a single hair by laser ablation inductively coupled plasma mass spectrometry (LA-ICP-MS) after cisplatin treatment for cancer. Intl J Mass Spectrom 272(1):57–62.

Pozebon, D., G. L. Scheffler, and V. L. Dressler. 2017. Elemental hair analysis: a review of procedures and applications. Analytica Chimica Acta 992:1–23.

Reiss, B. 2016. Hair as a biomarker for manganese exposure among welders. Department of Environmental and Occupational Health Sciences, University of Washington. 111 pp.

Reiss, B., C. D. Simpson, M. G. Baker, B. Stover, L. Sheppard, and N. S. Seixas. 2016. Hair manganese as an exposure biomarker among welders. Ann Occup Hyg 60(2):139–149.

Rink, L. 2011. Zinc in human health. IOS Press, Amsterdam, Netherlands. 592 pp.

Robbins, C. R. 2002. Chemical and physical behavior of human hair. Fourth Edition. Springer, New York, NY.

Robbins, C. R. 2012a. Chemical and physical behavior of human hair. Fifth Edition. Springer, New York, NY.

Robbins, C. R. 2012b. Chemical composition of different hair types. In: Chemical and physical behavior of human hair. Springer, New York, NY.

Robertson, J. 1999. Forensic examination of human hair. Taylor & Francis, London, England.

Rodushkin, I., and M. D. Axelsson. 2003. Application of double focusing sector field ICP-MS for multielemental characterization of human hair and nails. Part III. Direct analysis by laser ablation. Sci Total Environ 305(1-3):23–39.

Rogosnitzky, M., and S. Branch. 2016. Gadolinium-based contrast agent toxicity: a review of known and proposed mechanisms. Biometals 29(3):365–376.

Saint Olive Baque, C., J. Zhou, W. Gu, C. Collaudin, S. Kravtchenko, J. Y. Kempf, and D. Saint-Leger. 2012. Relationships between hair growth rate and morphological parameters of human straight hair: a same law above ethnical origins? Intl J Cosmetic Sci 34(2):111-116.

Saitoh, M., M. Uzuka, and M. Sakamoto. 1970. Human Hair Cycle. J invest Derm 54(1):65-81.

Sanborn, M., and K. Telmer. 2003. The spatial resolution of LA-ICP-MS line scans across heterogeneous materials such as fish otoliths and zoned minerals. J Anal At Spectrom 18(10):1231–1237.

Santamaria-Fernandez, R., J. Giner Martinez-Sierra, J. M. Marchante-Gayon, J. I. Garcia-Alonso, and R. Hearn. 2009. Measurement of longitudinal sulfur isotopic variations by laser ablation MC-ICP-MS in single human hair strands. Anal Bioanal Chem 394(1):225–233.

Saussereau, E., C. Lacroix, A. Cattaneo, L. Mahieu, and J. P. Goulle. 2008. Hair and fingernail gadolinium ICP-MS contents in an overdose case associated with nephrogenic systemic fibrosis. Forensic Sci Int 176(1):54–57.

Scheff, J. D., R. R. Almon, D. C. DuBois, W. J. Jusko, and I. P. Androulakis. 2011. Assessment of pharmacologic area under the curve when baselines are variable. Pharma Res 28(5):1081-1089.

Sela, H., Z. Karpas, M. Zoriy, C. Pickhardt, and J. S. Becker. 2007. Biomonitoring of hair samples by laser ablation inductively coupled plasma mass spectrometry (LA-ICP-MS). Intl J Mass Spectrom 261(2-3):199–207.

Semelka, R. C., J. Ramalho, A. Vakharia, M. AlObaidy, L. M. Burke, M. Jay, and M. Ramalho. 2016. Gadolinium deposition disease: initial description of a disease that has been around for a while. Magn Reson Imaging 34(10):1383–1390.

Sinclair, D. J., L. P. J. Kinsley, and M. T. McCulloch. 1998. High resolution analysis of trace elements in corals y laser ablation ICP-MS. Geochim Cosmo Acta 62(11):1889–1901.

Stadlbauer, C., T. Prohaska, C. Reiter, A. Knaus, and G. Stingeder. 2005. Time-resolved monitoring of heavy-metal intoxication in single hair by laser ablation ICP-DRCMS. Anal Bioanal Chem 383(3):500–508.

Stanford. No Date. Simpson's rule and integration. https://web.stanford.edu/sisl/MO-unit4-pdfs/4.2simpsonintegrals.pdf. Accessed on November 5, 2019. Stanford University.

Steely, S., D. Amarasiriwardena, J. Jones, and J. Yañez. 2007. A rapid approach for assessment of arsenic exposure by elemental analysis of single strand of hair using laser ablation-inductively coupled plasma-mass spectrometry. Microchem J 86(2):235–240.

Steely, S., D. Amarasiriwardena, and J. Yanez. 2005. Laser ablation-inductively coupled plasma-mass spectrometry (LA-ICP-MS): a rapid method for elemental analysis of hair. Abstr Pap Am Chem S 229:U390–U390.

Thomas, R. 2001. A beginner's guide to ICP-MS; part VI: the mass analyzer. Spectroscopy 16(10):44–48.

Thomas, R. 2002. A beginner's guide to ICP-MS; part VIII: mass analyzers: time-of-flight technology. Spectroscopy 17(1):36–41.

Tobin, D. J. 2012. Hair in toxicology: an important bio-marker. The Royal Society of Chemistry, Cambridge, England. 355 pp.

Tzung, T., C. Yang, Y. Huang, and F. Kao. 2009. Colorimetry provides a rapid objective measurement of de novo hair growth rate in mice. Skin Research and Technology 15(4):459–463.

Urso, R., P. Blardi, and G. Giorgi. 2002. A short introduction to pharmacokinetics. Euro Rev Med Pharma Sci 6(2-3):33-44.

Vallee, B. L. 1991. Introduction to metallothionein. pp. 3-7. In: Methods in enzymology; metallobiochemistry part B, metallothionein and related molecules. Academic Press.

Wang, B., L. Yan, W. Huo, Q. Lu, Z. Cheng, J. Zhang, and Z. Li. 2017. Rare earth elements and hypertension risk among housewives: a pilot study in Shanxi Province, China. Environ Pollut 220(Pt B):837–842.

Wilkins, D. G., A. Mizuno, C. R. Borges, M. H. Slawson, and D. E. Rollins. 2003. Ofloxacin as a reference marker in hair of various colors. J Anal Toxicol 27(3):149-155.

Williams, C. R., J. W. MacDonald, T. K. Bammler, M. H. Paulsen, C. D. Simpson, and E. P. Gallagher. 2016. Cadmium exposure differentially alters odorant-driven behaviors and expression of olfactory receptors in juvenile coho salmon (*Oncorhynchus kisutch*). Toxicol Sci 154(2):267–277.

Young, J. R., J. Qiao, I. Orosz, N. Salamon, M. A. Franke, H. J. Kim, and W. B. Pope. 2018. Gadolinium deposition within the paediatric brain: no increased intrinsic T1-weighted signal intensity within the dentate nucleus following the administration of a minimum of four doses of the macrocyclic agent gadobutrol. Eur Radiol.

Zota, A. R., A. M. Riederer, A. S. Ettinger, L. A. Schaider, J. P. Shine, C. J. Amarasiriwardena, R. O. Wright, and J. D. Spengler. 2016. Associations between metals in residential environmental media and exposure biomarkers over time in infants living near a mining-impacted site. J Expo Sci Environ Epidemiol 26(5):510–519.